

Interferon signaling in chronic hepatitis C: Mechanisms and implications for therapy

Inauguraldissertation

zur
Erlangung der Würde eines Doktors der Philosophie
vorgelegt der
Philosophisch-Naturwissenschaftlichen Fakultät
der Universität Basel

von

Magdalena Sarasin-Filipowicz

aus Riehen, Basel-Stadt

Basel, Mai 2008

Genehmigt von der Philosophisch-Naturwissenschaftlichen Fakultät der Universität Basel
auf Antrag von

Dissertationsleiter: Prof. Dr. M. H. Heim

Koreferent: Prof. Dr. E. Palmer

Fakultätsverantwortlicher: Prof. Dr. H.-P. Hauri

Basel, den 20.05.2008

Prof. Dr. H.-P. Hauri
Dekan Phil.-Naturwissenschaftliche Fakultät

Content

	Page
Acknowledgements	1
Summary	2
Abbreviations	4
1. Introduction	7
1.1 Hepatitis C virus (HCV) infection	
1.1.1 HCV epidemiology	7
1.1.2 Model systems in HCV research	8
1.1.3 Structure of HCV	9
1.1.4 Pathogenesis	11
1.1.5 Clinical manifestations	12
1.1.6 Treatment of hepatitis C	14
1.2 Interferon-alpha (IFN α) signaling	
1.2.1 The IFN cytokine family and the IFN receptors	17
1.2.2 Antiviral effects of IFN α	17
1.2.3 Jak-STAT signal transduction pathway	18
1.2.4 IFN α as a trigger of the Jak-STAT pathway	20
1.2.5 Negative regulation of IFN α signal transduction	22
1.2.6 Clinical relevance of disrupted Jak-STAT signaling	24
1.2.7 Role of phosphatase PP2A in interference with Jak-STAT signaling	24
1.2.8 IFN signaling in HCV infection	26
1.3 Viral sensory pathways	
1.3.1 Pattern recognition receptors (PRRs)	27
1.3.2 Cytoplasmic PRRs	27
1.3.3 Toll-like receptors (TLRs)	29
1.3.4 HCV interference with viral sensory pathways	30
2. Aims of the PhD-thesis project	32
3. Materials and methods	33

4. Results	35
4.1 Interferon signaling and treatment outcome in chronic hepatitis C Proc Natl Acad Sci USA 2008, May 13; 105(19):7034-7039	35
- PNAS Article	37
- PNAS Supporting Information	43
4.2 Cardif cleavage in chronic hepatitis C and correlation with ISG induction	67
4.2.1 Cardif is cleaved in human HCV infected liver and cleavage occurs more often in patients infected with genotypes 2 and 3	67
4.2.2 Expression of full-length Cardif correlates with ISG pre-activation in the liver	69
4.2.3 Activation of STAT1 in hepatocytes correlates with levels of ISG mRNAs in the liver of patients with chronic hepatitis C	70
4.3 Interferon alpha induces long-lasting refractoriness of Jak-STAT signaling in the mouse liver through induction of USP18/UBP43 (Manuscript in preparation, 2008)	71
- Abstract	74
- Introduction	75
- Materials and methods	78
- Results	82
- Discussion	87
- References	90
- Figures	93
5. Discussion	102
5.1 Interferon regulated gene expression in the liver determines response to treatment in chronic hepatitis C	102
5.2 Correlation of HCV genotype with ISG pre-activation in the liver and involvement of viral sensory pathways in inducing type I IFNs	104
5.3 Refractoriness of IFN α signaling in the mouse liver	106
5.4 Outlook: The role of miRNAs in liver disease and IFN signalling	108
5.5 Concluding remarks	109
References	111
Curriculum Vitae	123

Acknowledgements

I thank Markus Heim for giving me the opportunity to carry out my PhD thesis in the Laboratory of Hepatology at the Department of Biomedicine, University Hospital Basel. I am grateful for his competent supervision, his enthusiasm, his constant encouragement and friendship. It was a pleasure for me to work in the warm and friendly atmosphere of his laboratory.

My special thanks go to François Duong for all his efforts, advices and patience in teaching me. I appreciated his excellent and honest comments in the daily supervision and enjoyed learning from him. Our friendship and good mood has made long working days pass very quickly!

I wish to thank all members of Markus Heim's laboratory: Verena Christen, Christine Bernsmeier, David Semela, Michael Dill, Shanshan Lin, Vijay Shanker and Silvia Ketterer. I could always count on their help and advise. I want to thank Xueya Wang, a former member of the Hepatology Laboratory, for our fruitful collaboration on the "refractoriness of IFN α signaling in the mouse liver" project.

Thank you, Othella, for the beautiful hours I was allowed to spend with you: Your dancing classes energize me...

Last but not least, I thank my family, my husband Yves and my friends for their support and patience. I am grateful to my parents for having given me the opportunity of an excellent education at the University of Basel and for having introduced me to the world of science.

Summary

Hepatitis C virus (HCV) infection is a major cause of chronic liver disease worldwide and can lead to liver cirrhosis and hepatocellular carcinoma. The current standard therapy of chronic hepatitis C (CHC) consists of a combination of pegylated interferon alpha (pegIFN α) and ribavirin. However, sustained viral clearance is achieved in only 50-60% of patients. The underlying mechanism of failure of pegIFN α based therapy remains unknown and no molecular or genetic markers have been identified that could predict the treatment outcome. The overall aim of the study described in this thesis is to understand the molecular basis for failure of IFN α based therapies in patients with CHC. The study has focused on the IFN-induced Jak-STAT (janus kinase-signal transducer and activator of transcription) signaling pathway. To address the molecular basis of treatment response to IFN therapy, three experimental approaches have been employed.

The first approach involved the analysis of IFN α signaling and expression of interferon stimulated genes (ISGs) in liver biopsies and peripheral blood mononuclear cells (PBMCs) of HCV patients undergoing pegIFN α treatment. Paired liver biopsies and PBMCs from 16 patients were collected before and 4 hours after the first injection of pegIFN α , and were subjected to analysis of global gene expression using Affymetrix arrays. Further, activation of the IFN-induced Jak-STAT signaling pathway was analyzed by immunoblotting, immunohistochemistry and gel shift assays. The correlation of these biochemical and molecular data with the clinical response to treatment demonstrated that in the liver of patients with a rapid response pegIFN α induced a strong upregulation of ISGs, whereas in patients that did not respond to therapy, induction of IFN-dependent gene expression was impaired. Surprisingly, the non-responders had maximally induced ISG expression already before treatment with pegIFN α . Furthermore, the analyses of STAT1 phosphorylation, nuclear localization and DNA binding confirmed that the endogenous IFN signaling pathway in non-responders is pre-activated and refractory to further stimulation. In contrast to liver samples, ISG expression in PBMCs was stimulated by pegIFN α in both responders and non-responders, indicating that PBMCs are not a good surrogate marker for IFN α responses in the liver and that chronic HCV infection has strong local effects on the IFN system in liver. Our findings support an interesting concept that activation of the endogenous IFN system in CHC not only is ineffective in clearing the infection, but may also impede the response to therapy, most likely by inducing a refractory state of the IFN signaling pathway in the liver.

In the second approach we addressed the mechanisms underlying the pre-activation of the endogenous IFN system in a defined group of HCV patients (future non-responders). For this purpose, we analyzed ISG expression by quantitative RT-PCR and nuclear localization of STAT1 by immunohistochemistry in a cohort of 112 patients with CHC. By subdividing this cohort according to the HCV genotype (GT), we discovered that patients infected with HCV GT 1 and 4 more often show hepatic ISG preactivation than GT 2 and 3 patients, thus providing an explanation for the poor response to IFN therapy seen in GT 1/4 patients. We analyzed the possible involvement of viral sensory pathways in type I IFN production and ISG upregulation. Previously, the viral HCV NS3-4A protease was shown to interfere with viral sensory pathways by cleaving and thereby inactivating an important adaptor molecule, Cardif. We therefore assessed Cardif cleavage in liver biopsies of HCV patients and found that cleavage more often occurred in patients infected with HCV GTs 2 and 3. Our findings support a concept that the success of the virus in preventing the induction of the endogenous IFN system in the livers of these patients would, however, come at the cost of being more susceptible to IFN α therapies as is the case with GT 2/3 patients.

In the third approach we designed an experimental model to study the molecular basis of refractoriness of IFN signaling *in vivo*. Previously, cell culture experiments demonstrated a long lasting desensitization period, which followed the initial activation of the IFN α signaling pathway. In the approach used here, we established a mouse model in which continuous presence of IFN α *in vivo* was achieved by multiple subcutaneous injections, mimicking the constitutively high serum levels achieved by pegIFN α in patients. Interestingly, this resulted in refractoriness of IFN α signaling. Activation of STAT1 and STAT2, but not STAT3, in the mouse liver was desensitized by continuous IFN α stimulation. To elucidate the mechanism of this refractoriness, the role of negative regulators of the Jak-STAT signaling pathway was investigated. IFN signaling remained refractory in mice deficient in suppressor of cytokine signaling (SOCS) 3 and persisting refractoriness was also observed in mice deficient in IL-10, a strong inducer of SOCS3. Ubiquitin specific peptidase 18 (USP18/UBP43) was recently identified as novel negative regulator of IFN α signal transduction. Interestingly, refractoriness could be overcome in USP18/UBP43 knockout mice. These data strongly indicate that UBP43 is the decisive factor in inducing a refractory state in the IFN α signaling pathway *in vivo*.

Abbreviations

aa	amino acids
ALAT	alanine aminotransferase
Alb	albumine
arg	arginine
ASAT	aspartate aminotransferase
CARD	caspase-recruitment domain
CBP	CREB binding protein
CD	cluster of differentiation
cDNA	complementary DNA
CHC	chronic hepatitis C
CREB	cAMP response element binding protein
DMA	dimethyl arginine
dsRNA	double stranded RNA
EGF	Epidermal growth factor
eIF2 α	eukaryotic initiation factor 2 alpha
EMSA	Electrophoretic mobility shift assay
EoTR	end of treatment response
ER	Endoplasmic reticulum
EVR	early virological response
FERM	band 4.1, ezrin, radixin, moesin
GAS	Gamma activated sequence
GT	genotype
HA	Haemagglutinin
HAV	Hepatitis A virus
HBV	Hepatitis B virus
HCC	Hepatocellular carcinoma
HCV	Hepatitis C virus
HCV _{cc}	cell-culture derived HCV
hIFN α	Human interferon alpha
HIV	Human immunodeficiency virus
Huh7	Human hepatoma cell line
HVR	Hypervariable region
IFN	Interferon
IFNAR	Interferon alpha/beta receptor
IFNGR	Interferon gamma receptor
IKK	inhibitor of NF- κ B kinase
IL	Interleukin
IRAK	IL-1 receptor-associated kinase
IRES	Internal ribosomal entry site
IRF	interferon regulatory factor
IRG	Interferon-regulated gene
ISDR	IFN sensitivity-determining region
ISG	Interferon-stimulated gene
ISGF3	Interferon-stimulated gene factor 3
ISRE	Interferon-stimulated response element
Jak	Janus kinase

JFH	Japanese fulminant hepatitis
JH	Jak homology
kDa	kilo Dalton
LCMV	Lymphocytic Choriomeningitis Virus
LDL	Low density lipoprotein
LDLR	LDL-receptor
LRR	Leucine-rich repeat
Mda5	Melanoma differentiation associated gene 5
MHC	Major histocompatibility complex
mIFN- α	Mouse interferon alpha
miRNA	Micro RNA
MTA	5'-methyl-thioadenosine
NF- κ B	nuclear factor kappa B
NK	Natural killer (cell)
NOD	nucleotide oligomerization domain
NS	non-structural (protein)
NTPase	Nucleoside triphosphatase
OA	Ocadaic acid
OAS	2'-5' oligoadenylate synthetase
ORF	Open reading frame
PAMPs	Pathogen-associated molecular patterns
PBMCs	peripheral blood mononuclear cells
PCR	Polymerase chain reaction
pDCs	plasmacytoid dendritic cells
pegIFN α	Pegylated interferon alpha
PIAS	Protein inhibitors of activated STATs
PKR	Protein kinase R
PNR	primary non-response
PPase	Protein phosphatase
PP2A	Protein phosphatase 2A
PPMT	Prenylated-protein carboxyl methyltransferase
PRMT-1	Protein arginine methyltransferase
PRR	pattern recognition receptor
PTPA	PTPase activator
PTPase	Phosphotyrosyl phosphatase
RdRp	RNA-dependent RNA-polymerase
RIG-I	Retinoic-acid inducible gene-I
RLH	RIG-I-like helicase
RNAi	RNA interference
RVR	rapid virological response
SAME	S-adenosyl-methionine
SCID	Severe combined immunodeficiency
SHP	SH2-containing phosphatase
SH2	<i>src</i> homology 2
SIE	Serum inducible element
SOCS	Suppressor of cytokine signalling
ser	serine
SR-B1	scavenger receptor class B type 1
src	Rous sarcoma
ssRNA	single stranded RNA

STAT	Signal transducer and activator of transcription
SVR	Sustained virological response
TBK-1	TANK-binding kinase 1
TC-PTP	T cell protein tyrosine phosphatase
TH	T helper (cell)
thr	threonine
TIR	Toll/IL-1 receptor homology
TLR	Toll-like receptor
TNF	tumor necrosis factor
TRAF	TNF-receptor associated factor
TRIF	TIR domain containing adaptor inducing IFN β
tyr	tyrosine
USP18/UBP43	ubiquitin-specific peptidase 18
UTR	Untranslated region
VSV	vesicular stomatitis virus
wt	wildtype

1. Introduction

1.1 Hepatitis C virus infection

1.1.1 HCV epidemiology

Hepatitis C virus (HCV) is the cause for chronic hepatitis C (CHC), a liver disease previously called non-A non-B hepatitis. CHC can lead to liver cirrhosis and hepatocellular carcinoma (HCC). An estimated 170 million people worldwide, approximately 3% of the global population, are infected with HCV (reviewed in (1)). Since a protective vaccine against HCV does not yet exist and the therapeutic options remain limited, the number of patients presenting with long-term complications of CHC, including liver cancer, is expected to increase further over the next 20 years (2).

As HCV was discovered only in 1989 (3), blood transfusions represented the highest risk factor for HCV infection before 1990. The establishment of an efficient blood-screening system has then drastically decreased the incidence of post-transfusion hepatitis in developed countries (4). Blood-screening measures based on the detection of HCV antibodies carry a residual risk resulting from a delay of approximately 12 weeks between a possible infection and the generation of antibodies. This diagnostic gap after primary HCV infection can be decreased by more sensitive screening methods based on polymerase chain reaction (PCR) of HCV-RNA (5). New cases of HCV infection continue to occur mainly as a result of injection drug use. Maternal-fetal transmission is a rare event and mainly seen in mothers who are co-infected with HIV-1 (6). Current guidelines for pregnant women recommend normal childbirth and breast-feeding, both associated with only minimal risk of HCV transmission. Likewise, the sexual transmission of HCV is infrequent but its risk increases upon co-infection with HIV-1 (7). Nosocomial transmission of the virus is possible and includes needle-stick injuries among health care workers, infection during surgery, colonoscopy or dialysis. In one third of cases, however, the transmission route of the disease remains unclear.

1.1.2 Model systems in HCV research

HCV was first identified in an infected chimpanzee by expression cloning of RNA isolated from its serum and screening with human serum from a non-A non-B hepatitis patient (3). Soon after, an assay for HCV antibody detection was developed (8). Subsequently, it was demonstrated that intrahepatic injection of RNA transcripts from HCV cDNA clones into chimpanzees resulted in viral replication and the development of hepatitis (9, 10). The chimpanzee (*Pan troglodytes*) remains the only suitable animal model for studying HCV infection *in vivo*, although not widely applicable due to ethical and economical concerns. So far, no suitable small animal model of HCV infection has been developed, and moreover an efficient system for HCV replication in cell culture is available only since 1999. Lack of these models has hampered both research on HCV function and the development of therapeutic measures for HCV infection. In 1999, an HCV subgenomic replicon system in human hepatoma derived Huh7 cells was established (11), which however did not allow production of infectious virions. It was only in 2005 when an *in vitro* model of HCV replication that reproduces the full viral lifecycle (12, 13), including production of infectious virus, in permissive Huh7 cells was developed. Wakita and colleagues transfected an HCV genotype (GT) 2a clone isolated from a Japanese patient with fulminant hepatitis C, designated JFH-1 (for Japanese fulminant hepatitis), into Huh7 cells leading to production of virus (designated HCVcc for cell-culture-derived HCV) that was infectious for naïve Huh7 cells. The group of Charles M. Rice used a viral genome of a chimaeric HCV GT 2a sequence termed FL-J6/JFH that showed robust replication with production of 10^5 infectious units/ml and this replication could be inhibited by interferon-alpha ($IFN\alpha$) and several HCV-specific antiviral compounds.

Owing to the development of the infectious system, there is rapid progress in understanding previously unexplored steps of the HCV lifecycle including viral entry, genome packaging, virion assembly, maturation and release. For instance, Evans and colleagues have recently identified Claudin-1, a tight junction component highly expressed in the liver, as co-receptor required for HCV entry (14).

Transgenic mice carrying cDNA covering the entire coding region of the HCV genome have been generated, but in this model replication of the virus does not take place (15, 16). In 2001 the first murine model suitable for studying the human HCV *in vivo* has been established by transplanting normal human hepatocytes into SCID (severe combined

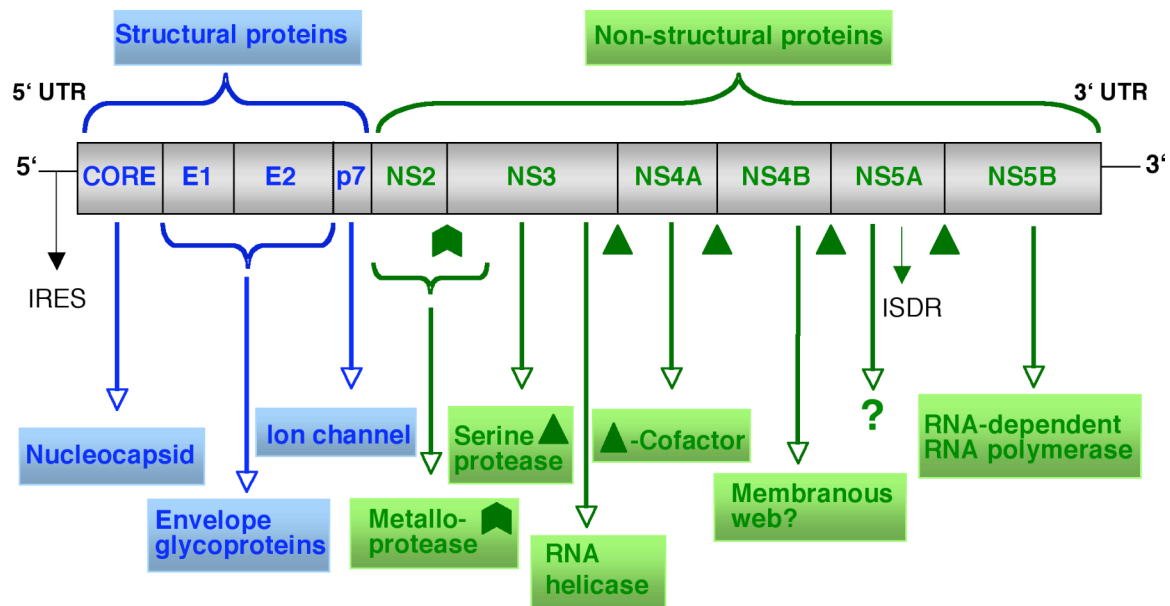
immunodeficiency) mice. These mice developed prolonged HCV infections after inoculation with infected human serum (17). The SCID/albumin (Alb)-urokinase plasminogen activator mouse model might therefore become a useful tool for investigating an *in vivo* efficacy of anti-HCV drugs.

1.1.3 Structure of HCV

HCV is a positive-stranded RNA virus and is classified in the *Hepacivirus* genus within the family of *flaviviruses* (reviewed in (18)). Based on electron microscopy studies, HCV particles are approximately 55 nm in diameter (19). Six distinct but related genotypes (GTs) of HCV have been documented (20). In Western Europe and the United States GTs 1a and 1b are most common, followed by GTs 2 and 3. The GTs 4, 5 and 6 are hardly ever found in these countries but are common in other areas such as Egypt or South Africa. The six major GTs differ by up to 35% in their sequence.

The genome of HCV is approximately 9.6 kb long and contains a single large open reading frame (ORF) that encodes a polyprotein of slightly more than 3000 amino acids (aa) (reviewed in (21)). This precursor protein is processed by a combination of host- and virus-encoded proteases into at least 10 individual proteins, representing both structural and non-structural components of HCV. Structural proteins (Core, E1 and E2), which form the viral envelope, are located at the N-terminus, while non-structural proteins involved in viral replication (NS2-NS5b) occupy the rest of the polyprotein (*Scheme 1*).

The core protein is considered to form a nucleocapsid, while E1/E2 are glycoproteins integrated into the lipid envelope and are likely to be responsible for the binding and entry of the virus to target cells (22). These structural components are followed by p7, a polypeptide reported to form an ion channel (23). Mutation of two conserved basic residues, previously shown to be important for the ion channel activity of p7 *in vitro*, drastically impaired infectious virus production (24). The proteins mentioned above are cleaved by host signal peptidases (25), while the proteins located downstream of p7 are processed by autocatalytic mechanisms.



Scheme 1. Structure of the HCV-genome.

Core, envelope (E) proteins, p7, non-structural (NS) proteins, IFN-sensitivity determining region (ISDR), untranslated region (UTR), internal ribosomal entry site (IRES). See text for further details.

The major part of the NS2 protein and the N-terminal part of the NS3 protein form a viral metalloprotease (NS2-3 protease) that cleaves at the NS2/3 junction. The cleavage of the remaining non-structural proteins is catalyzed by a serine protease (NS3-4A protease) that is a part of the NS3 protein (26). In addition, the C-terminal portion of NS3 contains sequences for a nucleoside triphosphatase (NTPase) and RNA helicases that are considered to regulate the replication of viral RNA (27). The NS4A polypeptide acts as a cofactor for the NS3 serine protease. All HCV proteins are associated to intracellular membranes. The processing of the polyprotein occurs at the endoplasmic reticulum (ER). Moreover, it is currently hypothesized that the formation of the membrane-associated viral replication complex occurs at altered cellular membranes possibly derived from the ER. NS4B was reported to induce the formation of these so-called membranous webs (28, 29).

The phosphorylation state of NS5A affects HCV-RNA replication (30, 31) and current evidence indicates that NS5A might function as a molecular switch between viral replication and assembly. Further, it has been reported that a mutation in the C-terminal part of NS5A increases the sensitivity to IFN α , used as the main antiviral drug (see chapter 1.1.6). Therefore this region is termed the IFN sensitivity-determining region (ISDR) (32). NS5A interacts with the IFN-induced protein kinase PKR via the ISDR and inhibits PKR activity, leading to a decrease of the IFN-mediated response to viral infection (33, 34). NS5B is the

key component in HCV replication since it contains a domain acting as RNA-dependent RNA-polymerase (RdRp) (35).

The highly conserved untranslated regions (UTRs) are required for viral replication. The 5' UTR contains an internal ribosomal entry site (IRES) that can initiate translation of the viral polyprotein in a cap-independent manner. It was recently reported that the liver-specific micro-RNA miR-122 base-pairs to the 5'-UTR of the genomic RNA of HCV and positively regulates replication of HCV-RNA *in vitro* (36). The 3' UTR of HCV is divided into three regions, two of which have been shown to be required for virus *in vivo* replication (37).

1.1.4 Pathogenesis

Hepatocytes and, possibly, B-lymphocytes as well as dendritic cells are the natural targets of HCV. CD81 is considered to function as a cell surface receptor recognized by the E2 protein of the virus (38). CD81 may not be sufficient for viral entry (39) and it has been postulated that additional roles are played by the low-density-lipoproteins receptor (LDLR) binding an unknown component of the viral envelope (40) and the scavenger receptor class B type I (SR-BI) (41). The LDLR is an attractive candidate receptor because HCV can be associated to LDLs (reviewed in (42)). Claudin-1 was recently identified as co-receptor required at a late stage of HCV entry (14).

Viral replication is extremely efficient and is catalyzed by the C-terminal RNA-polymerase. The HCV half-life is estimated as only a few hours with a production of as much as 10^{12} virions per day (43). Since the RdRp lacks a "proofreading" function, this results in a high diversity of transcripts and generation of multiple HCV-quasispecies within an infected person. This diversity poses major difficulties in HCV therapy and provides a strong rationale for the development and implementation of antiviral combination treatments in analogy to therapies used in HIV infection.

The immune system is known to play an important role in the development of hepatitis. T lymphocytes can be found within the infected hepatic parenchyma and it has been suggested that they are mobilized to control and possibly eliminate the virus. However, the result of their presence in the liver is a collateral damage through the secretion of inflammatory cytokines (44). Inflammation may also be related to clearance of HCV infected cells by activated cytotoxic T cells (45).

Viral proteins may influence proliferation of infected host cells. The most important pathogenic function has been documented for HCV core protein (46). Its effects include activation of the ras/raf kinase pathway (47), the transcription factor NFκB and modulation of apoptosis by suppressing the activation of caspase 8 (48). In addition, core protein may have a transforming ability in cooperation with ras oncogene and epidermal growth factor EGF receptor signaling (49). In addition, an interaction of core protein with lipid droplets might affect lipid metabolism, contributing to the development of liver steatosis, which is often seen in patients infected with HCV genotype 3 (50). The envelope protein E2 was shown to interfere with PKR function, while NS3 protein can interact with tumor suppressor p53 and has, similarly to NS4B, a cell transforming ability (45). Several proteins involved in viral pathogenesis are potential targets for the development of virus-specific inhibitors. These drug targets include the HCV NS2-3 and NS3-4A proteases (51), HCV helicases (52) and the NS5B RdRp as well as the IRES, the p7 polypeptide and the CD81 receptor (1).

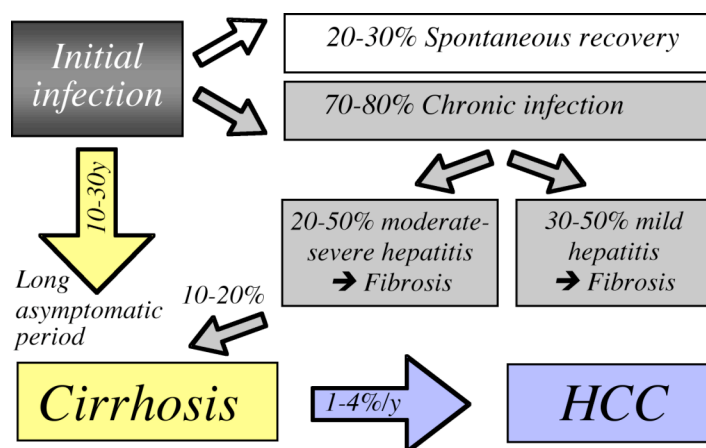
1.1.5 Clinical manifestations

The course of disease varies widely among infected persons. HCV infection is hardly ever diagnosed during the acute phase. The majority of persons have either none or only mild and unspecific symptoms after exposure to HCV. Nevertheless, clinical manifestations of acute hepatitis consisting of jaundice, malaise and nausea can occur in some patients, usually within 7 to 8 weeks after infection (1).

Progression to chronic disease occurs in about 70-80% of infected persons, whereas 20-30% show spontaneous recovery (*Scheme 2*). The early stage of chronic infection is typically characterized by a prolonged asymptomatic period. Spontaneous clearance of viremia, once chronic infection has been established, is rare. Most chronic infections will lead to hepatitis and to some degree of fibrosis. 10-20% of those infected chronically develop liver cirrhosis. At this stage of the disease the risk of developing hepatocellular carcinoma (HCC) is 1-4% per year (53).

Factors that increase the risk of clinical disease progression include alcohol intake, co-infection with hepatitis B virus (HBV) (54) or HIV-1 (55), male sex and older age at infection. In this high-risk group, cirrhosis can develop within 20 years or less after infection.

In contrary, low risk patients often do not have progressive liver disease until 30 or more years after infection. In HCV-infected patients a superinfection with hepatitis A virus (HAV) can lead to acute or even fulminant hepatitis (56).



Scheme 2. Disease progression.

In addition to hepatic disease, HCV infection is associated with important extrahepatic manifestations. As mentioned above the virus may target B cells, and indeed a number of B cell-mediated disorders are associated with HCV infection. For example, HCV is the major cause of essential mixed cryoglobulinemia. Cryoglobulins can be found in about 50 % of HCV patients, but only 10-15% develop a symptomatic disease consisting of weakness, arthralgia and purpura (57, 58). Since cryoglobulins accumulate in kidney, membranoproliferative glomerulonephritis can occur as a serious complication (59). A higher incidence of B cell non-Hodgkin's lymphoma (60), Sjögren's syndrome (61), autoimmune thyroiditis, idiopathic pulmonary fibrosis and dermatologic manifestations like Lichen planus and porphyria cutanea tarda in association with HCV infection has been observed (62). The pathogenic link between HCV infection and these disorders has been suggested on the basis of the frequently positive response to antiviral therapy. On the other hand, antiviral treatment with IFN has been suggested to be responsible for the induction of autoimmune thyroiditis since discontinuation of therapy can ameliorate this condition (63).

1.1.6 Treatment of hepatitis C

Since HCV infection is rarely diagnosed during the acute phase, data regarding the need for treatment of acute hepatitis are very limited. Some patients with acute symptomatic infection

show a spontaneous clearance suggesting that their treatment would have been unnecessary. However, recent studies indicate that early treatment with IFN α may be beneficial (64, 65).

All patients with chronic HCV infection (defined as infection persisting over more than six months with positive HCV-antibody and HCV-RNA detectable in the serum) are candidates for therapy, but the risks and benefits of treatment have to be evaluated individually because of the typically slow course of natural infection and the high occurrence of treatment side effects. Therapy is recommended for patients with persistently elevated transaminase levels (alanine aminotransferase ALAT and aspartate aminotransferase ASAT), documented viral replication (HCV-RNA positivity in the serum), and fibrosis documented by liver histology (Metavir fibrosis stage $F \geq 2$ out of maximally 4). Patients with normal ALAT levels and no or little histological signs of inflammation and fibrosis have an excellent prognosis without therapy (1).

Until 2001, the treatment of HCV infection consisted of IFN α in combination with the nucleoside analogue ribavirin. This combination therapy led to a sustained virologic response in 35-40% of patients (66). IFN α was administered subcutaneously (3 million units three times a week) and ribavirin was given orally twice a day (1000-1200 mg/day, depending on body weight). The serum concentrations of this unmodified IFN α (with an elimination half-life of 4 to 10 hours) declined below pharmacologically active levels in the second half of each 48 hour dosing interval (67, 68).

The introduction of a polyethylene glycol modified form of IFN α , called pegylated IFN α (pegIFN α), has resulted in a greater than 50% sustained response rate, if combined with ribavirin (69, 70). This combination has proven particularly efficient in the treatment of patients with poor prognosis due to infection with genotype 1, high baseline levels of HCV-RNA or cirrhosis (Metavir staging F4). PegIFN α has an extended half-life compared to IFN α and therefore can be administered only once a week. There are currently two pegIFN α isoforms used for the treatment of CHC: pegIFN α 2a (Pegasys®, administered in a dose of 180 μ g/week) and pegIFN α 2b (PegIntron®, given in a dose of 1.5 μ g/kg body weight). Pegasys is a 40kDa molecule with a half-life of 60-80 hours and PegIntron is a 15kDa molecule with a half-life of 40 hours. Despite these differences in half-life, both drugs are injected once a week. Hence, Pegasys is still found at high concentrations after 7 days before the injection of the next dosage, whereas PegIntron concentrations decrease to nearly baseline values during the weekly dosing interval. It is not clear whether these pharmacokinetic differences are relevant for the efficacy of therapy and it is assumed that both drugs are

equally effective. It is also unknown if the pharmacokinetic differences have an impact on the IFN α signaling and IFN α effector systems in the liver. Moreover, the reasons for an improved efficacy of pegIFN α compared to unmodified IFN α are not known, but it is assumed that the constantly high serum concentrations achieved with pegIFN α provide for un-interrupted antiviral activity through persistent stimulation of the IFN signaling pathway.

The most frequent side effects of IFN α -based therapy consist of influenza-like symptoms (40-85%), digestive dysfunction, depression (5-10%), thyroid dysfunction (5-10%), thrombocytopenia and neutropenia (*Table 1*). The concomitant use of ribavirin can lead to hemolysis with consecutive anemia in 30% of patients (71).

Frequency of side effects	Interferon alpha	Ribavirin
>30%	Influenza-like symptoms -Headache, Fatigue -Fever -Myalgia, Rigors Thrombocytopenia Induction of autoantibodies	Hemolysis Nausea Abdominal pain
1-30%	Anorexia Diarrhea, Abdominal pain Depression, Insomnia Emotional lability, Irritability Dermatological problems Thyroid dysfunction Leukocytopenia Induction of autoimmune disease	Anemia Nasal congestion Cough, Laryngitis Pruritus
<1%	Polyneuropathy, Optic neuritis Diabetes mellitus, Retinopathy Paranoia or suicidal ideation Cardiotoxicity, Seizures	Gout

Table 1. Side effects of HCV therapy (modified from [1]).

Over the last years, HCV associated end-stage liver disease has become the most frequent cause for liver transplantation in Switzerland, Europe and the US (72). Transplantation is the only treatment option for patients with uncompensated cirrhosis or early stages of HCC. Although infection of the graft is inevitable, the survival rate does not differ from the one of patients with other common indications for liver transplantation.

Because of extreme sequence variability within the HCV genome, development of an effective vaccine against HCV infection has proven to be very difficult. Promising

approaches have been developed in chimpanzees: sera raised against HVR1, the most variable region of the HCV genome (located within the sequence encoding the E2 protein), protected against HCV infection (73). Other approaches to HCV vaccination include use of various attenuated viral vectors to enhance priming of immune responses to multiple HCV gene products expressed by the vector (74). The chimpanzee challenge model (in which animals are being inoculated with HCV after vaccination) is used to explore efficacy and safety of the candidate vaccines.

Knowledge of the HCV GT is important because it helps to predict the outcome of antiviral therapy and influences the choice of the therapeutic regimen (75). Better responses are associated with GTs 2 and 3 than with 1 and 4. Treatment duration is 48 weeks for GTs 1 and 4, and 24 weeks for GTs 2 and 3 (70). For GTs 2 and 3, even a 12-week treatment regimen was shown to be effective in patients who achieved a rapid virological response (RVR) (76). The cause for these differential responses to treatment is currently unknown. Other factors associated with non-response to treatment are high baseline viral load as well as high fibrosis stage, old age, male gender, African American race, obesity, alcohol intake and changes in the host immune response, e.g. high interleukin-8 (IL-8) and IL-10 serum levels (77). The number of NS5A/ISDR mutations have also been shown to be relevant to the outcome of anti-HCV therapy (78). The current definitions of treatment response are based on the viral load (*Table 2*).

<p><i>Rapid Virological Response (RVR)</i> = Negative HCV-RNA in week 4 of treatment</p> <p><i>Early Virological Response (EVR)</i> = HCV-RNA reduction > 2 log after 12 treatment weeks</p> <p><i>Primary Non-Response (PNR)</i> = less than 2 log decrease of viral titer after 12 weeks</p> <p><i>End of Treatment Response (EoTR)</i> = no detectable serum HCV-RNA at end of treatment</p> <p><i>End of Treatment Non-Response</i> = detectable serum HCV-RNA at end of treatment</p> <p><i>Sustained Virological Response (SVR)</i> = undetectable HCV-RNA 6 months after end of treatment</p> <p><i>Relapse</i> = detectable HCV-RNA in serum at any time after having achieved EoTR</p>
--

Table 2. Treatment outcome classification according to generally accepted terminology.

1.2 IFN α -signaling

1.2.1 The IFN cytokine family and the IFN receptors

Interferons are a heterogeneous group of cytokines that play an important role in mediating antiviral and antiproliferative responses and in modulating immune reactions. They are classified into two types, type I consisting of IFN α , IFN-beta (IFN β) and IFN-omega (IFN ω) and type II with IFN-gamma (IFN γ) as the only member (79). So far twelve different IFN α s have been characterized. Plasmacytoid dendritic cells (pDCs) are known to have an extraordinary capacity to produce type I IFNs (80). All type I IFNs bind to the same interferon alpha/beta receptor (IFNAR) that consists of two chains, IFNAR1 and IFNAR2. IFN γ is produced by T lymphocytes and natural killer (NK) cells (81). It binds to the IFN γ receptor (IFNGR) consisting of two subunits, IFNGR1 and IFNGR2 (82). Upon binding to these receptors, both type I and type II IFNs exert their effects by activating the Jak/STAT signal transduction pathway (see chapter 1.2.3).

1.2.2 Antiviral effects of IFN α

IFN α has multiple antiviral effects, based on both direct antiviral actions and modulation of the host immune response. The induction of antiviral mechanisms consists of transcriptional activation of interferon stimulated genes (ISGs) encoding proteins such as double-stranded RNA (dsRNA) activated protein kinase PKR, 2'-5' oligoadenylate synthetase (OAS) and Mx proteins (79).

PKR plays a role in the control of transcription and translation (83). In response to IFN, PKR becomes upregulated and subsequently activated by binding viral dsRNA and autophosphorylation. The best-characterized substrate of PKR is eIF2 α , the α subunit of eukaryotic initiation factor. Its phosphorylation results in inhibition of translation of both viral and cellular proteins, explaining the antiviral and antiproliferative effect of IFN. Two HCV proteins are known to interact with PKR: NS5A via the ISDR and E2 via a region identical to the phosphorylation sites of PKR and eIF2 α (84). These interactions lead to an inhibition of PKR activity and therefore may contribute to HCV mediated IFN α resistance. The OAS activates a multienzyme pathway leading to the cleavage of viral and cellular

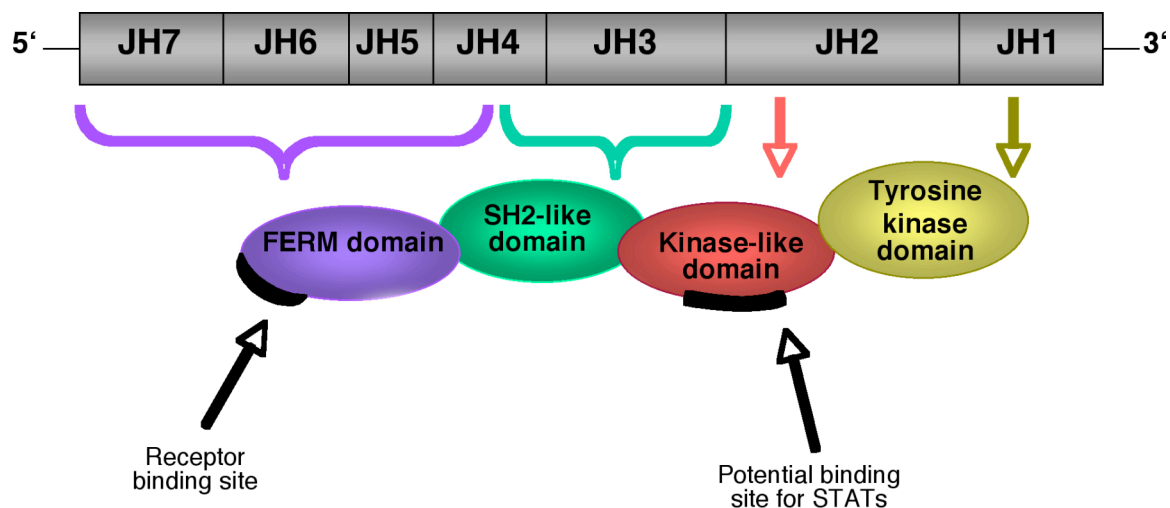
single-stranded RNAs (ssRNAs) by RNase L (85). RNase L was recently shown to play an important role in positive feedback mechanisms enhancing the innate immune system by generation of small RNA cleavage products from self-RNA (86). Mx proteins are IFN-inducible GTPases that interfere with replication of negative-stranded RNA viruses such as influenza (87).

Besides these direct antiviral actions, IFN α may exert its therapeutic effect by enhancing the immune response against infected hepatocytes and against the virus itself. An important immunomodulatory effect of IFN α is mediated through activation of NK cells that non-specifically recognize and lyse infected cells. An additional pathway may involve killing of infected cells by cytotoxic T lymphocytes, activity of which is increased in patients receiving IFN α treatment (88). This is supported by an IFN induced upregulation of MHC class I expression. Furthermore, IFN α can promote T helper cell 1 (TH1) responses including a positive feedback through enhancing expression of other IFN genes like that of IFN γ (89).

1.2.3 Jak-STAT signal transduction pathway

A large number of extracellular signaling proteins including polypeptide hormones, cytokines, growth factors and interleukins are using the Jak/STAT pathway for intracellular signal transduction, which results in transcriptional activation of target genes (90).

Jaks (Janus kinases) are cytoplasmic tyrosine kinases containing two tandem tyrosine kinase domains. There are four identified mammalian Jak family members (Jak1, Jak2, Jak3 and Tyk2) with molecular weights of approximately 120-140 kDa. Except for Jak3, found mainly in cells of myelocytic and lymphocytic lineages, the other three Jak members are ubiquitously expressed. Jaks contain seven conserved domains called JH1 to JH7 (Jak homology) (*Scheme 3*). JH1 is the tyrosine kinase domain at the carboxy-terminus and JH2 is a catalytically inactive kinase-like domain that might have a regulatory function and is considered to be a potential binding site for STATs (91). JH3-JH7 are located at the N-terminus and important for specific receptor recognition and association. JH3 and JH4 possess structural features of a potential SH2 (*src* homology 2)-like domain (92). Part of JH4 and the JH5 to JH7 region was renamed FERM domain and is able to bind the cytoplasmic tail of transmembrane receptors (93).

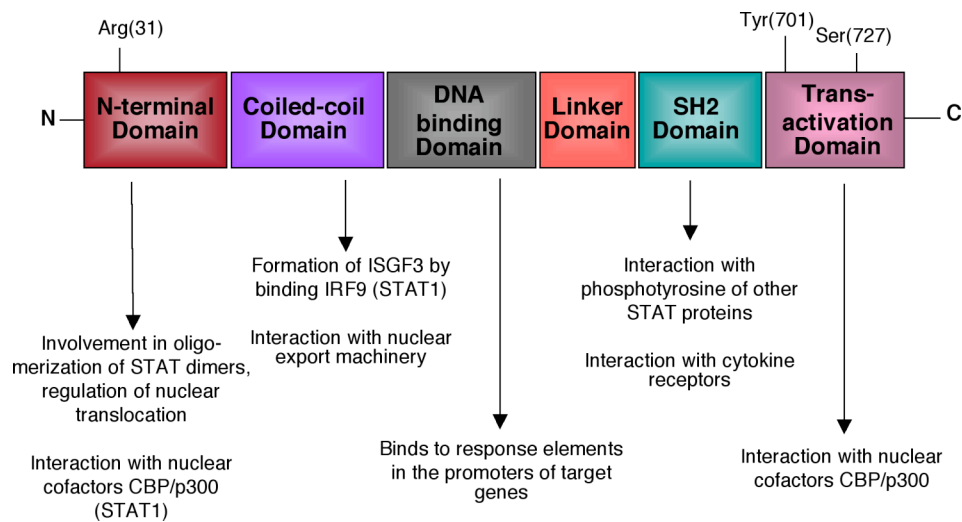


Scheme 3. Structure of Janus kinases (Jaks).

Jak homology (JH) regions, *src*-homology 2 (SH2), FERM (band 4.1/ ezrin/ radixin/ moesin), Signal Transducer and Activator of Transcription (STAT).

STATs (Signal Transducers and Activators of Transcription) act as both signalling molecules and transcription factors. They shuttle between cytoplasm and nucleus. In non-stimulated cells STATs are predominantly located in the cytoplasm, whereas upon stimulation they are able to enter the nucleus where they stimulate transcription by binding to promoter response elements. So far, seven mammalian STATs have been identified (STAT1-4, STAT5a, STAT5b and STAT6). STAT4 is mainly expressed in thymus and testes, whereas the remaining STAT proteins are ubiquitous (reviewed in (90, 94)). In *Scheme 4*, the functional domains of STAT proteins are described.

The C-terminus is the autonomously functioning transcriptional activation domain containing tyrosine and serine residues that become phosphorylated upon activation. The potent transcriptional activators CBP and p300 interact with this domain (95). The SH2 domain binds to the phosphotyrosine of a homo- or heterotypic STAT leading to the formation of dimers (96). The SH2 domain is also able to interact with cytokine receptors that have become tyrosine-phosphorylated upon ligand binding (97). The DNA binding domain has the structure of an immunoglobulin variable fold and is responsible for STAT-DNA binding. The coiled-coil domain interacts with IRF9, a component of the interferon-stimulated gene factor 3 (ISGF3). The N-terminal domain acts as a protein-protein interaction domain and has been implicated in the regulation of dephosphorylation of STAT1 on tyrosine 701, the interaction with CBP/p300 and the regulation of nuclear translocation (98).



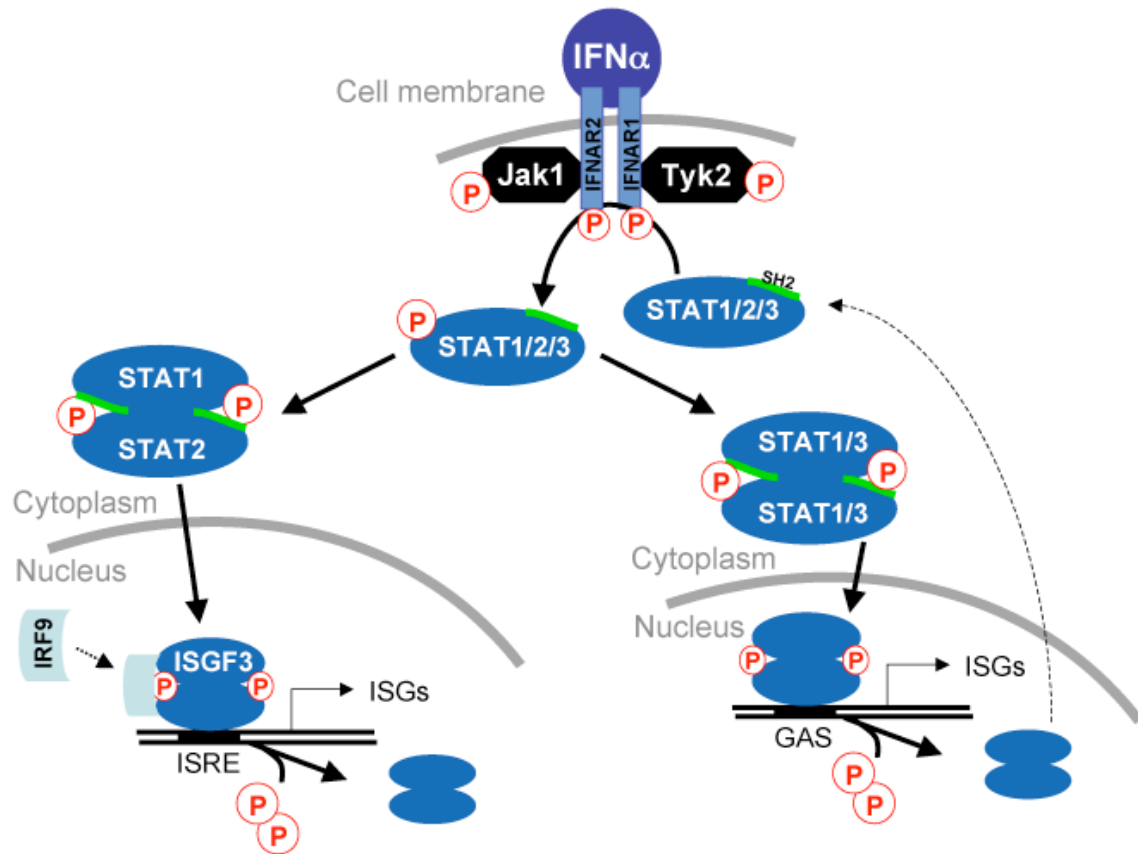
Scheme 4. Structure of Signal Transducers and Activators of Transcription (STATs). Interferon-stimulated gene factor 3 (ISGF3), nuclear cofactor CBP.

Cytokine receptors possess no intrinsic catalytic activity, and therefore depend on Jaks that are permanently associated to their cytoplasmic tails. Homodimeric and heteromeric receptors activate different combinations of Jaks. After having trans-phosphorylated each other, the Jaks proceed to phosphorylate the receptor subunit(s). Subsequently, STATs are brought to the proximity of the Jaks by binding to the receptor phosphotyrosine through their SH2 domain (97). After their phosphorylation, STATs are able to form homo- or heterodimers by mutual SH2-phosphotyrosine interactions. As dimers, they are able to translocate into the nucleus and to act as transcription factors. An alternative model of STATs pre-existing as dimers, and their activation leading to a conformational change, was recently proposed by Mao and colleagues (99).

1.2.4 IFN α as a trigger of the Jak-STAT pathway

Binding of IFN α leads to the crosslinking of the receptor chains IFNAR1 and IFNAR2. Activated Jak1 and Tyk2 proceed to phosphorylate STAT1, STAT2 and STAT3 (97, 100). The activated STATs dissociate from the receptor and translocate to the nucleus where they act as transcription factors binding to specific regions in the promoters of IFN regulated genes (IRGs) (101). As shown in *Scheme 5*, there are two distinct pathways leading to transcription of IFN α target genes. The first involves the formation of STAT1-STAT2 heterodimers, which translocate to the nucleus and there, after combining with IFN-

regulatory factor (IRF)-9, form the IFN stimulated gene factor 3 (ISGF3). ISGF3 binds to the interferon-stimulated response element (ISRE) within the promoters of ISGs (90, 102). IFN α also activates homo- and heterodimers of STAT1 and STAT3, which bind to gamma-activated sequence (GAS) response elements in the nucleus (103).



Scheme 5. IFN α induced Jak/STAT signaling.

Interferon- α (IFN α) binds to the IFN α receptor (IFNAR1/2) leading to dimerization of the receptor chains. Activated (i.e. phosphorylated) Janus kinases (Jak1/Tyk2) phosphorylate IFNAR1/2, the Signal Transducers and Activators of Transcription (STAT1/2/3) become activated at the receptor-kinase complex and form either the interferon-stimulated gene factor 3 (ISGF3) which binds to interferon-stimulated response element (ISRE) or the STAT1/3 homo- and hetero-dimers which bind to γ -activated sequence (GAS). These signaling cascades ultimately result in the transcription of interferon-stimulated genes (ISGs). Finally, STATs are dephosphorylated in the nucleus and exported into the cytoplasm.

Besides inducing transcription of antiviral ISGs, IFN α can also upregulate genes involved in signaling, including STAT1, STAT2, IRF-9 and IFN α itself (104). This effect results in a positive feedback loop in the IFN α dependent Jak/STAT pathway.

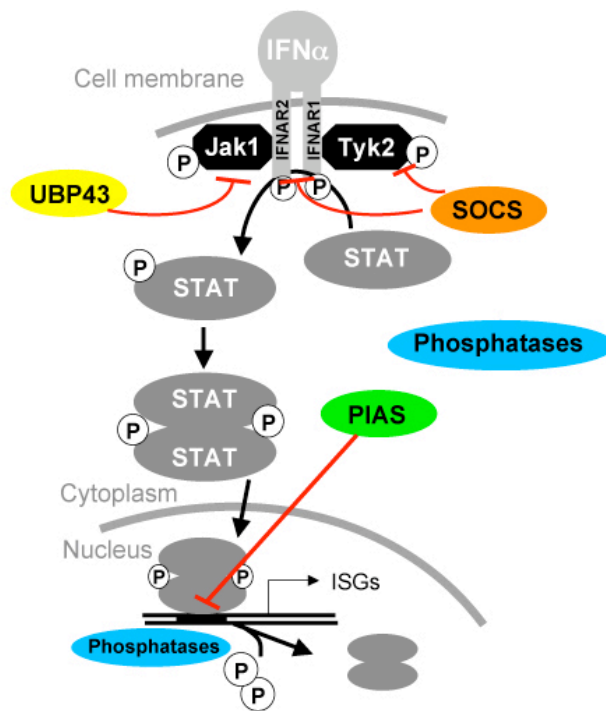
STAT1 activity is regulated by tyrosine phosphorylation (tyr-701), which is essential for dimer formation, nuclear translocation and DNA-binding. Serine phosphorylation (ser-

727) is not essential but required for STAT1 to achieve its full transcriptional activity (105-107). STAT activity in cytokine-treated cells is regulated by degradation and active shut-off mechanisms of which dephosphorylation plays the most important role. Dephosphorylation of STAT1 is catalyzed by several phosphatases (see chapter 1.2.5). Besides tyrosine and serine phosphorylation, STAT1 undergoes an additional posttranslational modification. The methylation of an arginine residue (arg-31) by protein arginine methyl-transferase (PRMT-1) is also required for transcriptional activation of STAT1 (108). Inhibition of PRMT-1 and, consequently, absence of arginine methylation leads to an increased association of the inhibitory protein PIAS1 with phosphorylated STAT1 dimers. Importantly, this interaction results in an impaired binding of STAT1 to response elements in the promoters of target genes. Abnormally elevated levels of 5'-methyl-thioadenosine (MTA), an inhibitor of PRMT-1, have been found in certain cancer cells and might be responsible for the lack of IFN α responsiveness observed in many malignancies.

1.2.5 Negative regulation of IFN α signal transduction

Negative regulation of cytokine signaling is crucial to control signal transduction cascades and prevent side effects as well as tumor transformation. For example, constitutively activated STATs were found in many hematological malignancies (109).

The activation of the Jak/STAT pathway is tightly controlled by several negative regulatory mechanisms acting at different levels of the signaling cascade. The Suppressors of Cytokine Signaling (SOCS) prevent STAT activation by inhibiting Jaks or preventing STAT binding to the receptor (110). Further downstream, the protein inhibitor of activated STAT (PIAS) binds to hypomethylated STAT dimers and inhibits STAT-DNA interaction (108, 111, 112). STATs are deactivated by the 45kDa isoform of nuclear phosphatase TC-PTP, followed by nuclear export (113) (114) (115). Further, an involvement of SH2-containing phosphatases 1 and 2 (SHP-1 and -2) (116) (117) is postulated. Previous work in our laboratory has demonstrated a role of protein phosphatase 2A (PP2A) in inhibiting the Jak/STAT pathway at the level of STAT-DNA interactions (118) (see chapter 1.2.7).



Scheme 6. Negative regulation of IFN α induced Jak/STAT signaling.

Ubiquitin-specific peptidase 18 (USP18/UBP43); Suppressor of cytokine signaling (SOCS); Protein inhibitor of activated STAT (PIAS).

There is evidence that all these proteins negatively regulate IFN α signaling (*Scheme 6*). For example, PIAS1 and PIAS3 associate with STAT1 and STAT3, respectively (111, 119). Members of the SOCS family (SOCS1 and SOCS3) prevent phosphorylation and activation of IFN α induced STATs by inhibiting the IFN receptor associated Jak kinases or preventing STATs from binding to the cytoplasmic tails of the IFNAR. PIAS deficient mice show increased protection against viral and microbial infection consistent with a negative regulatory function of PIAS1 on a subset of type I IFN responsive genes (120). Mice with SOCS1 deletion die during the neonatal period due to severe hepatotoxicity and multiorgan inflammation (121) and SOCS3 deficient mice die in mid-gestation due to placental insufficiency (122). Recently, ubiquitin specific peptidase 18 (USP18/UBP43) has been described as negative regulator in type I IFN signaling. USP18/UBP43 was originally identified as a protease cleaving ubiquitin-like modifier ISG15 from target proteins, but was recently found to play a negative regulatory role independently of its ISG-deconjugating ability (123, 124). USP18/UBP43 was reported to inhibit the activation of Jak1 by interfering with its interaction with IFNAR2 (125). USP18/UBP43 is induced by IFN α (126, 127) and provides a negative feedback loop that restricts IFN α signals. UBP43 deficient mice show a severe phenotype characterized by brain cell injury, poly-(I:C) hypersensitivity, and

premature death (128, 129). Interestingly, they are resistant to otherwise fatal cerebral infections with LCMV and VSV (130). USP18/UBP43 is elevated in livers of future non-responders to pegIFN α therapy (131). Moreover, USP18/UBP43 silencing in cells with a replicating chimeric HCV genome results in deregulation of STAT1 signaling and potentiation of IFNs ability to inhibit HCV-RNA replication (132).

1.2.6 Clinical relevance of disrupted Jak-STAT signaling

Interference of HCV proteins with the IFN-induced antiviral effector system (such as PKR) represents one mechanism of viral escape. Another strategy is based on the disruption of IFN α signaling. Indeed, decreased levels of IFN α receptor in the liver have been reported in HCV patients (133). Likewise, expression of the entire HCV ORF in cell lines impaired the formation of ISGF3 and its subsequent DNA binding (134). In melanoma cell lines resistant to IFN α treatment, multiple defects in Jak/STAT signaling have been described. Examples are the lack of a functional Tyk2 or lack of tyrosine phosphorylation of STAT1 and STAT3 (135).

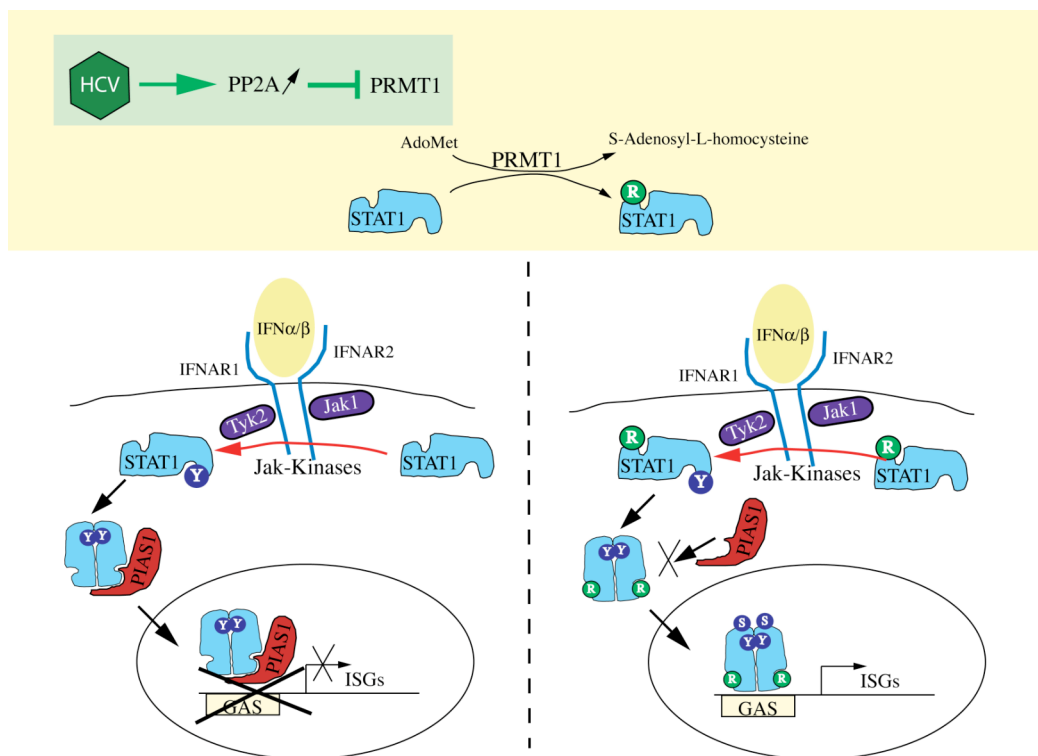
Mice deficient for components of the Jak/STAT signaling pathway have underlined the importance of a functional signal transduction. STAT1 deficient mice do not show any developmental defects, but are unresponsive to IFNs resulting in a high susceptibility to viral infections (136). Interestingly, STAT1 is activated by many ligands but seems to be essential only for IFN signaling. STAT3 deficiency in mice is lethal during embryonic development. Therefore, in order to study STAT3 function, mice with tissue specific deficiency in STAT3 have been generated using the Cre recombinase/loxP recombination system (137, 138).

SCID, severe combined immunodeficiency, is an example of a human disease associated with defects in the Jak/STAT signaling pathway caused by Jak3 or IL-2 receptor mutations. Likewise, human myeloproliferative disorders carry mutations in Jak2 (139).

1.2.7 Role of PP2A in interference with Jak-STAT signaling

Previous studies in our laboratory demonstrated that expression of HCV proteins in human osteosarcoma cell lines or in liver cells of transgenic mice inhibits IFN α induced intracellular signaling through the Jak/STAT pathway at the level of STAT-DNA interactions (16, 134).

Further experiments demonstrated that expression of HCV proteins in livers of mice and liver biopsies of patients with CHC induces an upregulation of the catalytic subunit of protein phosphatase 2A (PP2A) (118). This effect may serve as a mechanism of interference with the Jak/STAT signaling pathway and lead to an impaired response to IFN α in HCV infected cells. The overexpression of the catalytic subunit of PP2A in human hepatoma derived Huh7 cells resulted in reduced activity of PRMT-1 (140), hypomethylation of STAT1, increased STAT1 association with the inhibitory protein PIAS1 and, consequently, inhibition of STAT1 binding to DNA. *Scheme 7* summarizes our current model of HCV interference with IFN α induced Jak-STAT signaling. Interestingly, the PP2A induced inactivation of PRMT-1, and resulting hypomethylation of STAT1, can be reversed *in vitro* by the addition of the methyl-group donor S-adenosyl-methionine (SAME) (140). Based on these data, a clinical pilot study with 30 patients receiving pegIFN α , Ribavirin and SAME has been initiated at the Gastroenterology and Hepatology Department of the University Hospital Basel.



Scheme 7. Inhibition of IFN α induced Jak/STAT signaling by Hepatitis C virus

CHC induces an upregulation of the catalytic subunit of protein phosphatase 2A (PP2Ac). PP2Ac inhibits the enzymatic activity of protein arginine methyltransferase 1 (PRMT-1) resulting in decreased methylation of STAT1. Hypomethylated STAT1 associates with the inhibitory protein PIAS1 (protein inhibitor of activated STAT1) leading to inhibition of STAT1-DNA binding and, therefore, reduced transcriptional activation of IFN target genes.

1.2.8 IFN signaling in HCV infection

Over the last years, there is accumulating evidence that the endogenous IFN system is activated to various degrees in patients with CHC. Yu et al. (141) and MacQuillan et al. (142) found an upregulation of a number of ISGs in liver biopsies from HCV patients. There was a considerable variation of the extent of the upregulation of ISGs between patients. Chen et al (131) performed expression profiling with gene arrays on liver biopsy specimens taken before therapy comparing gene expression levels of 15 non-responders, 16 responders and 20 normal liver biopsies. Surprisingly non-responders showed high baseline expression of ISGs, whereas responders to therapy (and those who relapsed) more closely resembled healthy controls. These findings suggest that non-responders have an upregulated and largely ineffective IFN response, suggesting little benefit from administration of exogenous IFN α . The mechanisms responsible for a preactivated IFN system in the liver observed in a subgroup of HCV patients remain unknown.

Similarly to humans, the analysis of intrahepatic gene expression during chronic HCV infection in chimpanzees revealed upregulation of many ISGs (143). Interestingly, the single HCV GT 3-infected animal analyzed exhibited reduced levels of ISG expression when compared to the GT 1-infected chimpanzees. Strong IFN responses have also been demonstrated in the livers of acutely HCV infected chimpanzees (144). Recently, Lanford et al reported a lack of response to exogenous IFN α in chimpanzees chronically infected with HCV (145). Data obtained from uninfected chimpanzees revealed remarkable tissue-specificity of the transcriptional response to IFN α when comparing liver and peripheral blood mononuclear cells (PBMCs) (146).

1.3 Viral sensory pathways

1.3.1 Pattern recognition receptors (PRRs)

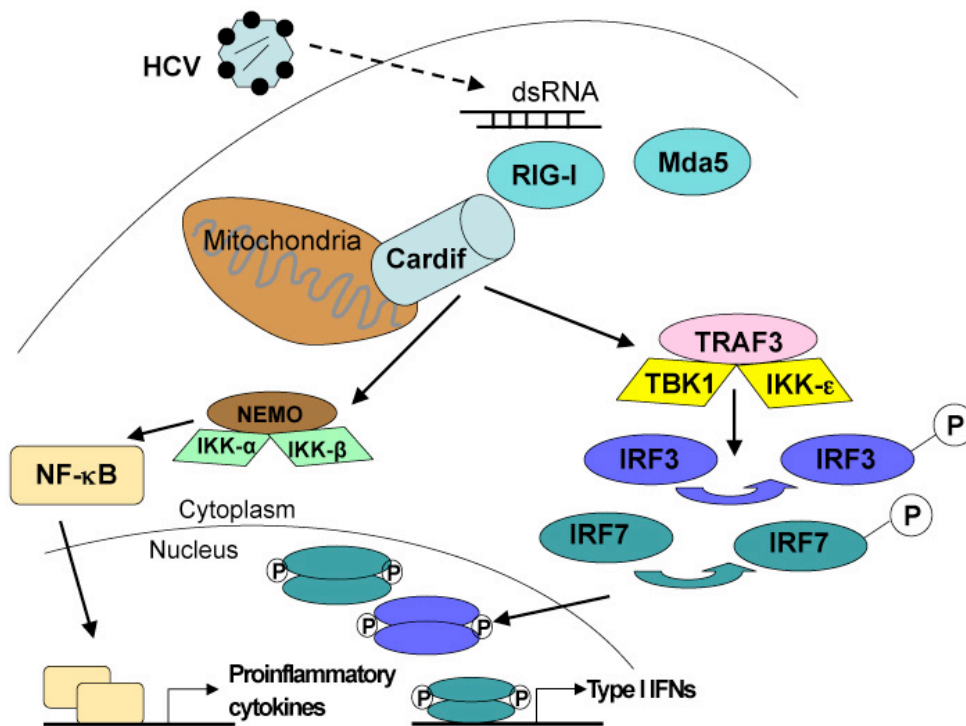
Pattern recognition receptors (PRRs) are part of the innate immune response. They recognize distinct components of microorganisms, the so-called pathogen-associated molecular patterns (PAMPs), and transmit signals through a variety of pathways finally leading to the activation of immune cells and various anti-microbial effector systems. These include type I interferon responses or the production of proinflammatory cytokines (reviewed in (147, 148)). Different classes of PRRs have been described to date, including the membrane-bound Toll-like receptors (TLRs) and cytoplasmic receptors comprising retinoic-acid-inducible gene-I (RIG-I)-like helicases (RLHs) and nucleotide-oligomerization domain leucine-rich repeat (NOD-LRR) proteins. The different PRRs recognize specific PAMPs and, as a consequence, activate distinct anti-pathogenic responses. PRRs are highly conserved among species, they are germ-line encoded and constitutively expressed in host cells. The current knowledge on PRRs indicates that the innate immune response has specific features arguing against the earlier concept of innate immunity being entirely unspecific.

1.3.2 Cytoplasmic PRRs

Cytoplasmic receptors like the RLHs and NOD-LRR proteins recognize microorganisms that have invaded the cytoplasm of host cells. NOD-LRR proteins comprise a C-terminal LRR, a central nucleotide binding domain and a N-terminal signaling domain (149). NOD1 and NOD2 are members of the NOD-LRR family and involved in intracellular sensing of bacterial products. RLHs consist of a C-terminal DexD/H box helicase domain (responsible for dsRNA binding) and of N-terminal caspase-recruitment domains (CARDs) (150). RLH-mediated signaling is triggered by dsRNA and results in transcriptional induction of IFN α and IFN β , which are crucial for mounting the defense against viral infection. RIG-I (also known as Ddx58) and Melanoma differentiation associated gene-5 (Mda5, also known as Ifih1 or helicard), representing two RLH family members, were shown to respond differently to RNA viruses (151). This can be illustrated by the response to influenza virus, which was highly pronounced in Mda5 deficient mice, while absent in RIG-I deficient cells. It was

recently shown, that the RIG-I pathway is also stimulated by 5'-triphosphate ssRNA (152, 153).

In 2005 an important adaptor protein for RLH signaling, Cardif/IPS-1/VISA/MAVS (154-157), was identified by 4 independent research groups. Cardif deficient mice fail to produce type I IFNs in response to infection with RNA viruses (158, 159). Cardif is associated to the outer mitochondrial membrane and contains a protein-binding CARD-domain through which it associates with RIG-I. This interaction ultimately, upon activation of a kinase complex, results in the phosphorylation of the interferon-regulatory factors (IRF)-3 and IRF-7 (*Scheme 8*).



Scheme 8. Sensing of viral dsRNA by cytoplasmic RIG-I-like helicases (RLHs)

Retinoic-acid-inducible gene-I (RIG-I) senses viral dsRNA and interacts with the adaptor protein Cardif. This results in the activation of two kinase complexes: (i) TRAF3 adaptor protein and TBK1/IKK-ε kinases with resulting activation of IRF-3 and IRF-7 and transcriptional induction of type I IFNs; (ii) NEMO adaptor and IKK-α/IKK-β kinases with resulting activation of nuclear factor kappa B (NF-κB) and transcription of proinflammatory cytokines.

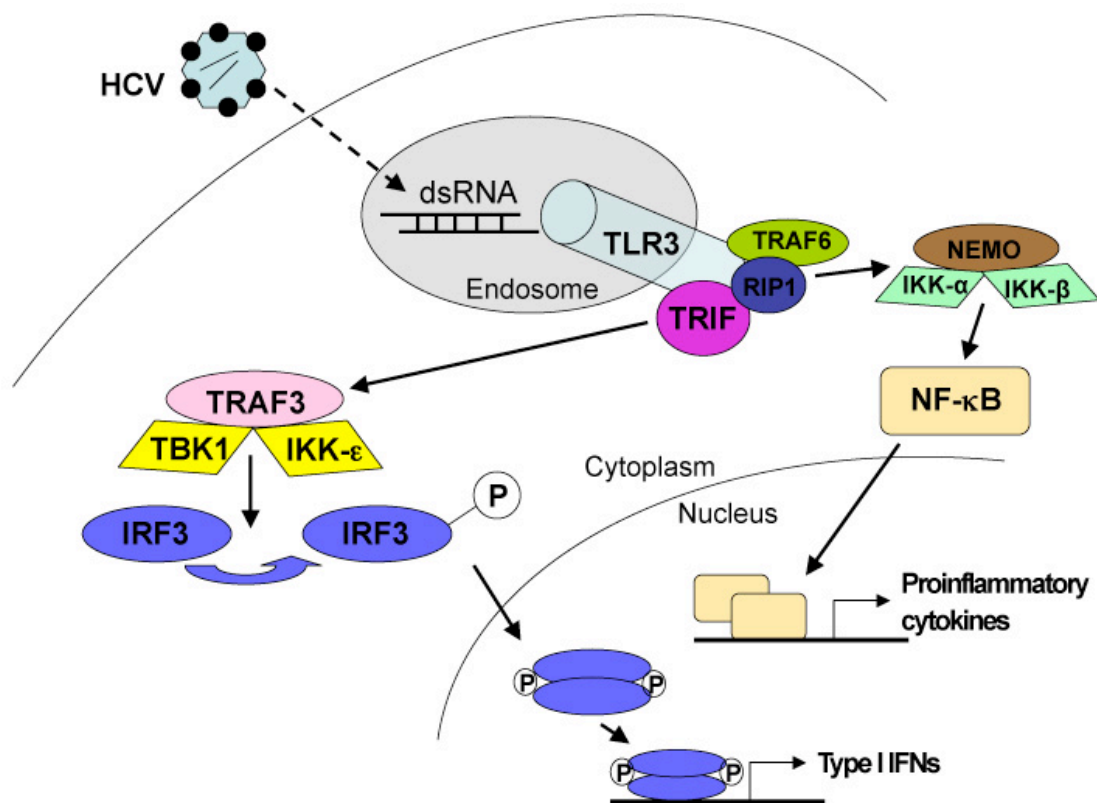
IRF-3 and IRF-7, normally present in the cytoplasm, dimerize upon phosphorylation and translocate to the nucleus where they induce the transcription of type I IFNs. Cells lacking IRF-3 therefore have a severely impaired IFN α and IFN β production (160). Using mice deficient in the IRF-7 gene, IRF-7 was also shown to be crucial for type I IFN induction via the virus-activated RLH pathway (161). In the past years, further molecules involved in

IRF activation have been described: TANK-binding kinase 1 (TBK-1) and IKK- ϵ , both members of the inhibitor of NF- κ B kinase (IKK) family (162, 163). Moreover, TNF-receptor associated factor (TRAF) 3 has been shown to associate to Cardif (164, 165) and to recruit and activate TBK-1/IKK- ϵ . RLHs also activate the transcription factor nuclear factor-kappa B (NF- κ B) through the adaptor NEMO and the kinases IKK- α and IKK- β . Interestingly, NEMO was recently reported to also be required for IRF-3 activation and thus functions as adaptor protein allowing RIG-I mediated activation of both the NF- κ B and IRF signaling pathways (166).

1.3.3 Toll-like receptors (TLRs)

TLRs were first discovered in 1988 in studies on fruit fly development (167). In murine studies it was later demonstrated that injection of endotoxin into mice with a defective TLR4 was not lethal in contrast to wildtype mice (168), indicating the involvement of TLRs in responses to pathogens. There are at least 10 human TLRs. TLRs are comprised of leucine-rich repeats (LRRs), a transmembrane domain, and a TIR (Toll/IL-1 receptor homology) domain. Bacterial components including lipoproteins and lipopolysaccharides are being recognized by TLR1, TLR2, TLR4, TLR5 and TLR6. In contrast, TLR3, TLR7 and TLR9, all localized on endosomes, are able to detect viral nucleic acids. TLR3 recognizes dsRNA (e.g. HCV-RNA), whereas TLR7 detects ssRNA (169, 170) and TLR9 interacts with unmethylated DNA with CpG motifs (171). TLR activation induces signaling cascades that mainly involve the key transcription factors NF- κ B and various IRFs.

As an example, the HCV-induced TLR3 signaling cascade is shown in *Scheme 9*. TLR3 is present in endosomes of DCs where it senses dsRNA and induces signaling via the adaptor protein TRIF (TIR domain containing adaptor inducing IFN β , also known as TICAM-1) (172). Further downstream, TRAF3 is responsible for the activation of the TBK-1/IKK- ϵ kinases and phosphorylation of IRF-3 (164, 165). Of note, the TLR3 and the RIG-I signaling pathways converge at this level. TLR3 also activates the transcription factor NF- κ B through TRAF6, the adaptors RIP-1 and NEMO and the kinases IKK α and IKK β . The role of TLR3 is controversial as TLR3 deficient mice were shown to be more resistant to infections with West Nile Virus (173).



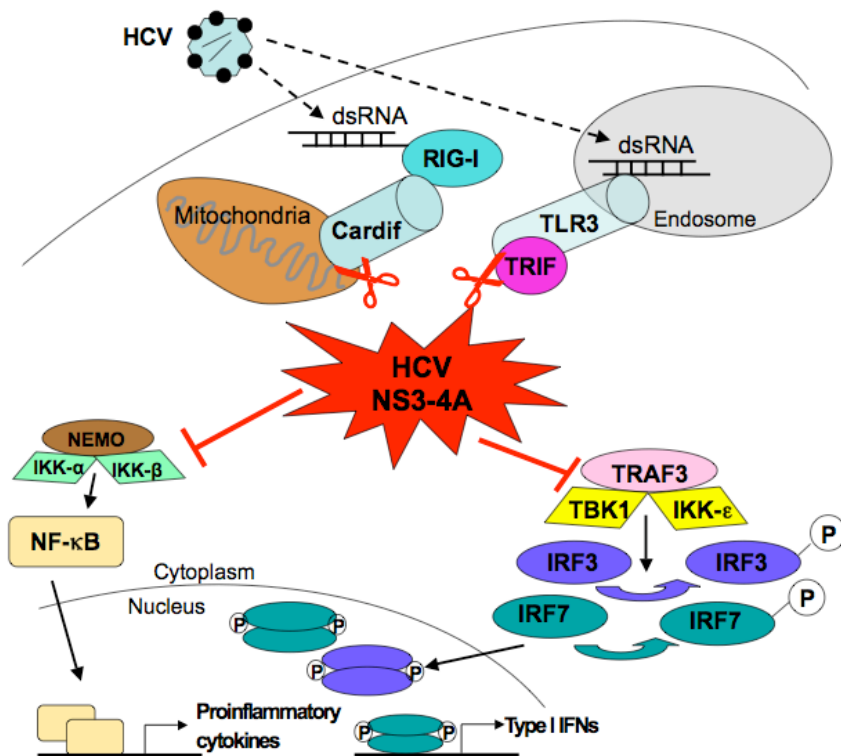
Scheme 9. TLR3 signaling pathway.

Toll-like receptor 3 (TLR3), localized on endosomes, recognizes viral dsRNA and activates adaptor proteins TRIF, TRAF, RIP-1 and NEMO. The kinases TBK1 and IKK-ε phosphorylate IFN regulatory factor (IRF)-3, whereas the IKK-α/IKK-β complex activates transcription factor NF-κB.

TLR7 and TLR9 are important for virus-induced type I IFN production in plasmacytoid DCs. Their signaling depends on MyD88 (a TIR domain containing adaptor protein). MyD88 recruits a complex consisting of IL-1 receptor-associated kinases (IRAK)-1 and IRAK-4, TRAF3, TRAF6, IKK-α and IRF-7 ultimately resulting in IRF-7 activation and IFN production.

1.3.4 HCV interference with viral sensory pathways

Many viruses, including influenza virus, have developed strategies to inhibit early signaling events that lead to IFN production in infected host cells (174). Similarly, HCV has not only evolved mechanisms that interfere with the downstream signaling pathway of IFNα, but also was shown to disrupt pathways leading to type I IFN production (*Scheme 10*).



Scheme 10. HCV NS3-4A interference with viral sensory pathways

The HCV NS3-4A protease cleaves the adaptor proteins Cardif and TRIF and thereby inactivates both the RIG-I and the TLR3 induced signaling pathways.

The HCV NS3-4A protease was reported to block phosphorylation and downstream effects of IRF-3 by an unknown mechanism (175). Importantly, Meylan et al. could show that the NS3-4A protease targets and inactivates Cardif (154). The cleavage site is located within the C-terminus of the Cardif protein. A cysteine to alanine mutation at position 508 (C508A) of Cardif resulted in complete resistance to cleavage by the viral protease. It remains unknown whether Cardif cleavage can be detected in patients infected with HCV and whether there exist HCV genotype-specific differences in the ability to cleave Cardif. Moreover, it remains unclear whether the ISG activation status of chronic HCV patients (with future non-responders to treatment showing a pre-activated endogenous IFN system in the liver) is dependent on the viral sensory pathways and therefore also on Cardif function.

The NS3-4A protease of HCV also counteracts TLR3 dependent pathways by targeting the adaptor protein TRIF for proteolytic cleavage (176). The site for this *in vitro* TRIF cleavage is cysteine 372. Of note, restoring Cardif and TRIF functions could explain antiviral efficacy of therapeutic compounds targeting the HCV NS3-4A protease through other mechanisms than only suppression of viral replication.

2. Aims of the PhD-thesis project

The current standard therapy for chronic hepatitis C (CHC) consists of a combination of a long-acting pegylated form of IFN α (pegIFN α) and ribavirin, both given for 6 to 12 months. It achieves a cure from HCV infection in only about half of the patients. The underlying mechanisms of failure of pegIFN α based therapy are unknown, mainly because the effects of IFN α in human liver have not been investigated due to difficulties in obtaining liver tissue from patients undergoing treatment. It is also not known how hepatocytes respond to the continuously high IFN α concentrations obtained with pegIFN α .

The aims of this PhD-thesis project were:

- I. To investigate IFN induced effects in the liver of CHC patients.

- II. To investigate the behavior of IFN signal transduction pathways in the liver during repeated or prolonged exposure to IFN α using mouse models.

3. Materials and methods

For main materials and methods, see the respective sections in the incorporated manuscripts (Sarasin-Filipowicz et al, PNAS *in press*, “IFN alpha signaling and the treatment outcome of chronic hepatitis C” and Sarasin-Filipowicz et al, manuscript in preparation, “Interferon alpha induces long-lasting refractoriness of Jak-STAT signaling in the mouse liver through induction of USP18/UBP43”). For additional materials and methods concerning results described in paragraph 4.2, see legends of the respective figures (Figures 4.2.A-D).

Described below is a summary of the methodological approaches used in the projects:

In a first approach, we collected paired liver biopsies from 16 patients with the aim to correlate the hepato-cellular response to pegIFN α with the clinical outcome of HCV treatment. The samples were obtained before treatment and 4 hours after the first injection of pegIFN α and IFN-induced gene expression with a special emphasis on Jak-STAT signaling was analyzed by Western blot, immunohistochemistry, Electrophoretic mobility shift assays (EMSAs) and Affymetrix microarrays. We also investigated IFN responsiveness of PBMCs obtained from the same patients in order to compare these findings with the effects induced in the HCV infected liver.

A second approach was used to investigate why certain HCV patients present an unexplained pre-activation of the endogenous IFN system in their liver. To elucidate the cause of this phenomenon, we analyzed a possible impact of different HCV genotypes on the pre-activation of ISGs (quantified by real-time RT-qPCR), using a collection of 112 pre-treatment liver biopsy samples from CHC patients. Moreover, we aimed at establishing a correlation of the observed ISG induction with the nuclear translocation of activated STAT1, as assessed by immunohistochemistry. Further, we investigated whether the ISG activation status of CHC patients is dependent on the viral sensory pathways in the liver. Towards this aim we used the pre-treatment liver biopsy samples to assess whether Cardif, an adaptor molecule known as a target of the NS3-4A HCV protease, is cleaved in patients infected with HCV and whether genotype-specific differences in Cardif cleavage exist. We assessed

Cardif protein and mRNA levels and correlated our findings with the clinical data of the patients.

In a third approach we established a mouse model with the aim to investigate whether a continuous presence of IFN α results in a permanent stimulation or, opposite, in a refractoriness of the IFN signaling pathway *in vivo*. We repeatedly injected wildtype mice with mouse IFN α and measured serum levels by ELISA. We assessed IFN α signaling in the mouse liver by Western blot for activated STATs, by EMSAs and by measuring target gene induction by Northern blot and RT-qPCR. A possible involvement of known negative regulators of IFN α -induced Jak-STAT signaling, including SOCS and UBP43, was investigated in knockout mice deficient in these molecules.

4. Results

4.1 Interferon signaling and treatment outcome in chronic hepatitis C

Sarasin-Filipowicz M. et al.

Proc Natl Acad Sci USA 2008, May 13; 105(19):7034-7039

	Page
- PNAS Article	37
- PNAS Supporting Information	43

Interferon signaling and treatment outcome in chronic hepatitis C

Magdalena Sarasin-Filipowicz*, Edward J. Oakeley†, Francois H. T. Duong*, Verena Christen*, Luigi Terracciano‡, Witold Filipowicz†, and Markus H. Heim*§¶

*Department of Biomedicine, University of Basel, CH-4031 Basel, Switzerland; †Friedrich Miescher Institute for Biomedical Research, CH-4002 Basel, Switzerland; ‡Institute for Pathology, University Hospital Basel, CH-4003 Basel, Switzerland; and §Division of Gastroenterology and Hepatology, University Hospital Basel, CH-4031 Basel, Switzerland

Edited by Charles M. Rice III, The Rockefeller University, New York, NY, and approved March 6, 2008 (received for review August 21, 2007)

Hepatitis C virus (HCV) infection is a major cause of chronic liver disease worldwide. The current standard therapy for chronic hepatitis C (CHC) consists of a combination of pegylated IFN alpha (pegIFN α) and ribavirin. It achieves a sustained viral clearance in only 50–60% of patients. To learn more about molecular mechanisms underlying treatment failure, we investigated IFN-induced signaling in paired liver biopsies collected from CHC patients before and after administration of pegIFN α . In patients with a rapid virological response to treatment, pegIFN α induced a strong up-regulation of IFN-stimulated genes (ISGs). As shown previously, nonresponders had high expression levels of ISGs before therapy. Analysis of posttreatment biopsies of these patients revealed that pegIFN α did not induce expression of ISGs above the pretreatment levels. In accordance with ISG expression data, phosphorylation, DNA binding, and nuclear localization of STAT1 indicated that the IFN signaling pathway in nonresponsive patients is preactivated and refractory to further stimulation. Some features characteristic of nonresponders were more accentuated in patients infected with HCV genotypes 1 and 4 compared with genotypes 2 and 3, providing a possible explanation for the poor response of the former group to therapy. Taken together with previous findings, our data support the concept that activation of the endogenous IFN system in CHC not only is ineffective in clearing the infection but also may impede the response to therapy, most likely by inducing a refractory state of the IFN signaling pathway.

Jak-STAT signaling | liver | viral hepatitis

Hepatitis C virus (HCV) infection is a major cause of chronic liver disease worldwide. An important and striking feature of hepatitis C is its tendency toward chronicity. In >70% of infected individuals, HCV establishes a persistent infection over decades that may lead to cirrhosis and hepatocellular carcinoma. An interesting hypothesis in HCV biology proposes that the viral NS3-4A protease not only processes the viral proteins but also cleaves and inactivates components of the intracellular sensory pathways, TRIF and Cardif, that detect viral infection and induce the transcriptional activation of type I IFN. Two RNA helicases, RIG-I and MDA5, identified as intracellular sensors of dsRNA, act through Cardif to induce IFN β production (1). The ability of HCV to inhibit the activation of the endogenous type I IFN system could underlie its success in establishing a chronic infection (2).

Type I IFNs not only are crucial factors in the innate immune system but also are the most important components of current therapies against CHC. The current standard therapy consists of pegylated IFN α (pegIFN α) and the antiviral agent ribavirin (3). The treatment achieves a sustained virological response (SVR) in \approx 55% of patients, with significant differences between genotypes (4). An SVR is defined as the loss of detectable HCV RNA during treatment and its continued absence for at least 6 months after stopping therapy. Studies of long-term followup on SVR patients demonstrate that this response is durable in >95% of patients. The probability of an SVR strongly depends on the

early response to treatment. Patients who do not show an early virological response (EVR), defined as a decline of the viral load by >2 log₁₀ after 12 weeks of therapy, are highly unlikely to develop an SVR (5–7). Patients with an EVR have a good chance of being cured, with 65% of them achieving SVR (5, 7). The prognosis is even better for patients who have a rapid virological response (RVR), defined as serum HCV RNA undetectable after 4 weeks of treatment. Over 85% of them will achieve SVR (6, 8). Unfortunately, <20% of patients with genotype 1 and \approx 60% of patients with genotypes 2 or 3 show an RVR (6, 8). The host factors that are important for an early response to therapy are currently unknown.

Type I IFNs achieve their potent antiviral effects through the regulation of hundreds of IFN-stimulated genes (ISGs). ISG-encoded proteins establish a general antiviral state within the cell (9). IFNs induce ISG transcription by activating the Jak-STAT pathway (10). Type I IFNs bind to the same cell surface receptor (IFNAR) and activate the receptor-associated tyrosine kinases Jak1 and Tyk2. The kinases then phosphorylate and activate STAT1 and STAT2. The activated STATs translocate to the nucleus, where they bind specific DNA elements in promoters of ISGs. Many ISGs have antiviral activity, but some are involved in other processes such as lipid metabolism, apoptosis, protein degradation, and inflammatory cell responses (11). HCV interferes with the IFN system probably at multiple levels. IFN-induced Jak-STAT signaling is inhibited in cells and transgenic mice that express HCV proteins (12, 13) and in liver biopsies of patients with CHC (14). *In vitro*, HCV proteins NS5A and E2 bind and inactivate protein kinase R, an important antiviral protein (15). However, the molecular mechanisms that are important for the response to pegIFN α in patients with CHC remain unknown.

The capacity of HCV to interfere with the IFN pathway at many different levels is a likely mechanism underlying HCV success to establish a chronic infection (2). However, quite paradoxically, in chimpanzees acutely or chronically infected with HCV, hundreds of ISGs are induced in the liver (16, 17). Nevertheless, despite the activation of the endogenous IFN system, the virus is not cleared from chronically infected animals (18). The results obtained with chimpanzees are difficult to extrapolate to humans, because there are important differences

Author contributions: M.S.-F., W.F., and M.H.H. designed research; M.S.-F., E.J.O., F.H.T.D., V.C., and M.H.H. performed research; M.S.-F., E.J.O., F.H.T.D., V.C., L.T., W.F., and M.H.H. analyzed data; and W.F. and M.H.H. wrote the paper.

The authors declare no conflict of interest.

This article is a PNAS Direct Submission.

Data deposition: The data reported in this paper have been deposited in the Gene Expression Omnibus (GEO) database, www.ncbi.nlm.nih.gov/geo (accession no. GSE 11190).

¶To whom correspondence should be addressed. E-mail: markus.heim@unibas.ch.

This article contains supporting information online at www.pnas.org/cgi/content/full/0707882105/DCSupplemental.

© 2008 by The National Academy of Sciences of the USA

Table 1. Study patient characteristics

Patient no.	4-week response	Sex	Age	HCV GT	Viral load, log ₁₀ international units/ml			12-week response	Follow-up	Metavir	Weight, kg
					Baseline	4	12				
					weeks	weeks	weeks				
1	RR	M	52	3a	7.14	Neg.	Neg.	EVR	SVR	A2/F2	75
2	RR	M	37	3a	4.90	Neg.	Neg.	EVR	SVR	A1/F2	73
3	RR	M	38	1a	6.91	Neg.	Neg.	EVR	EoTR	A2/F1	85
4	RR	M	33	2b	6.27	Neg.	Neg.	EVR	EoTR	A1/F2	57
5	RR	M	48	2b	6.67	Neg.	Neg.	EVR	SVR	A3/F4	110
6	RR	F	53	2a/c	4.95	Neg.	Neg.	EVR	SVR	A3/F3	74
7	RR	M	56	3	5.25	Neg.	Neg.	EVR	EoTR	A3/F4	61
8	RR	M	38	4	4.08	Neg.	Neg.	EVR	Ongoing	A2/F2	69
9	RR	F	50	1b	7.22	3.52	Neg.	EVR	Ongoing	A1/F2	47
10	RR	F	48	1	6.49	3.31	Neg.	EVR	Ongoing	A3/F4	60
11	Non-RR	F	54	3a	4.52	4.08	1.3	EVR	No EoTR	A3/F4	69
12	Non-RR	M	64	1b	6.24	4.83	3.46	EVR	No EoTR	A3/F4	74
13	Non-RR	M	49	4	6.91	5.87	5.22	PNR	-	A3/F4	102
14	Non-RR	M	56	1b	6.89	6.76	6.01	PNR	-	A2/F3	60
15	Non-RR	F	50	1a	7.11	6.58	6.35	PNR	-	A1/F2	77
16	Non-RR	F	47	1a	6.16	5.99	5.52	PNR	-	A2/F2	81

M, male; F, female; GT, genotype.

in the pathobiology of HCV infection between these species. Whereas most chimpanzees acutely infected with HCV clear the virus spontaneously, infections in humans mostly become chronic. However, chronically infected chimpanzees can rarely be cured with IFN, whereas more than half of patients with CHC are successfully treated (19).

Induction of ISGs was also found in pretreatment liver biopsies of many patients with CHC, again demonstrating that HCV infection can lead to activation of the endogenous IFN system (20). Notably, patients with preelevated expression of ISGs tended to respond poorly to therapy when compared with patients with low initial expression (20). The cause of this differential response to therapy is not understood. Are patients with elevated initial expression refractory to further stimulation of ISGs by exogenous IFN? Does the administration of IFN to patients with low initial ISG values lead to ISG expression levels exceeding those found in the other group, possibly explaining a success of therapy in low-ISG patients? Are there specific ISGs important for viral clearance that are not activated in nonresponders? To circumvent limitations in the procurement of liver biopsies, several groups have assessed whether peripheral blood mononuclear cells (PBMCs) could serve as a surrogate tissue to evaluate the response to IFN α (21–23). However, no conclusive data are available for humans, because a direct comparison of IFN-induced ISGs between liver and PBMCs has not been done.

To approach focal questions related to the pathophysiology of HCV infection, we investigated IFN-induced signaling and ISG expression in paired liver biopsies and PBMCs collected from patients with CHC before and after the first injection of peg-IFN α . We correlated the biochemical and molecular data with the response to treatment, and we compared the response to IFN α in liver and PBMCs.

Results

Patients and Response to Treatment. Sixteen patients included in this study, 6 women and 10 men, were treated with a weight-adjusted combination of s.c.-injected pegIFN α 2b once weekly and oral ribavirin twice daily. All had two liver biopsies, the pretreatment biopsy (B-1) and the second biopsy (B-2), obtained 4 h after the first injection of pegIFN α 2b. We have chosen to analyze gene expression 4 h after pegIFN α 2b injection, because

kinetics of the induction of ISGs by pegIFN α in liver of chimpanzees was maximal at this time and was followed by rapid down-regulation of many genes (22). We realize that we probably missed the up-regulation of some late-induced ISGs, but because of rapid down-regulation, we would have missed more ISGs when using later time points.

Seven of the patients were infected with HCV genotype (GT) 1, two with GT 4, four with GT 3, and three with GT 2. Eight patients who had negative serum HCV RNA after 4 weeks of treatment (RVR) and two patients with >3 log₁₀ drop of viral titer within the first 4 weeks were classified as rapid responders (RRs), whereas six patients showed a viral load reduction of <1.5 log₁₀ and were classified as non-RRs (Table 1).

Serum IFN α concentrations were below the limit of detection in all patients before treatment and, in accordance with previously published pharmacokinetic data (24), between 34 and 360 pg/ml in samples obtained at 4 h after the pegIFN α 2b injection (data not shown). There was no significant correlation between the virological response at week 4 and the serum IFN α concentration at 4 h postinjection.

IFN-Induced Regulation of Target Genes. Gene expression was analyzed with Affymetrix U133plus2.0 arrays in B-1 and B-2 samples and also in PBMCs isolated from blood obtained before (PBMC-1) and 4 h after the first pegIFN α 2b injection (PBMC-2). We identified 252 genes significantly [paired *t* test, *P* < 0.05, see [supporting information \(SI\) Materials and Methods](#)] changed >2-fold between B-1 and B-2 in >50% of the 10 RR biopsy samples, whereas only 36 genes passed the same criteria when analyzing the 6 non-RR patients (Fig. 1A). To compare the number of significantly regulated genes between RR and non-RR patients in groups with an equal number of patients, 15 groups of 6 patients randomly selected from the 10 RR patients were generated. In each group, the genes significantly (*P* < 0.05 or *P* < 0.01, paired *t* test) changed in >50% of patients were identified and counted. In liver biopsies of the 15 RR groups, the mean number (\pm SD) of regulated genes was 178.6 (\pm 58.8) and 225.9 (\pm 61.5) at significance levels *P* < 0.01 and *P* < 0.05, respectively. In the non-RR group, there were 23 and 36 genes significantly regulated at *P* < 0.01 and *P* < 0.05, respectively. The

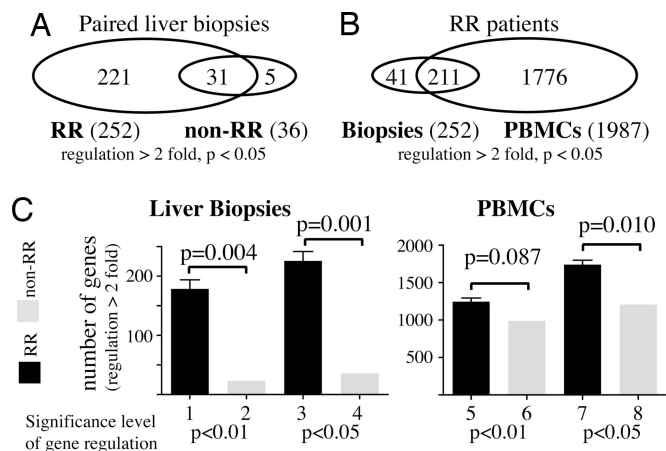


Fig. 1. PegIFN α 2b induced regulation of gene expression in liver and PBMCs. (A) Venn diagram of genes significantly (paired *t* test, $P < 0.05$) up- or down-regulated >2 -fold in response to pegIFN- α 2b in $>50\%$ of the 10 RR and 6 non-RR biopsy samples. (B) Venn diagram of genes significantly (paired *t* test, $P < 0.05$) up- or down-regulated >2 -fold in response to pegIFN- α 2b in biopsy and PBMC samples of $>50\%$ of RR patients. (C) RR up- or down-regulate significantly more genes in the liver in response to pegIFN- α 2b than non-RR patients. Shown are the mean (\pm SEM) number of genes changed >2 -fold at significance levels $P < 0.01$ (lanes 1, 2, 5, and 6) and $P < 0.05$ (lanes 3, 4, 7, and 8) in $>50\%$ of patients within each response group in liver biopsies and PBMCs.

differences between the RR and non-RR samples were statistically significant (Fig. 1C).

Not surprisingly, many of the regulated genes represent known ISGs. However, contrary to our expectations, expression levels of most of these ISGs were not higher in post-pegIFN α 2b treatment biopsies from RR patients compared with non-RRs. Only 7.5% of the 252 genes significantly regulated in $>50\%$ of 10 RR patients were higher in the B-2 samples of RRs (see Table S1). Rather, non-RR patient samples had a higher level of ISG expression already in B-1, and the fold change in the B-2 samples was therefore only minor. This is illustrated in Fig. 2A at the example of four ISGs. The genes show a very low expression in biopsies from individuals without hepatitis C (controls) and in B-1s of RR patients. The six non-RR patients had a high expression of these genes before treatment, and pegIFN α 2b administration did not increase or only minimally increased their expression. There were very few exceptions to this rule (an example is shown in Fig. 2B). These genes had low expression in the pretreatment biopsies, and pegIFN α 2b induced them in all patients. Nevertheless, the predominant pattern of gene expression resembled this shown in Fig. 2A. A complete list and a heat map of the expression of 252 genes significantly ($P < 0.05$) changed >2 -fold between B-1 and B-2 in the RR group are shown for all biopsy samples in Table S1 and Fig. S1.

There was a considerable overlap of pegIFN α 2b-regulated genes in liver and PBMCs (Fig. 1B). Interestingly, in all patients, pegIFN α 2b regulated more genes in PBMCs than in liver. However, the difference in the up-regulation of ISGs was more pronounced in biopsies compared with the PBMCs (Fig. 1C). In PBMCs, no preactivation of ISGs was found, and pegIFN α 2b treatment induced ISGs in both RR and non-RR patients (Fig. 1C and Fig. S2). This indicates that chronic HCV infection has strong local effects on the IFN system in liver but little effect in PBMCs.

A Subset of Genes That Predicts Response to Treatment. Supervised classifier analysis of array data allows the identification of a subset of genes that best predicts the outcome, in our case rapid response vs. nonresponse at week 4. All liver biopsy and PBMC

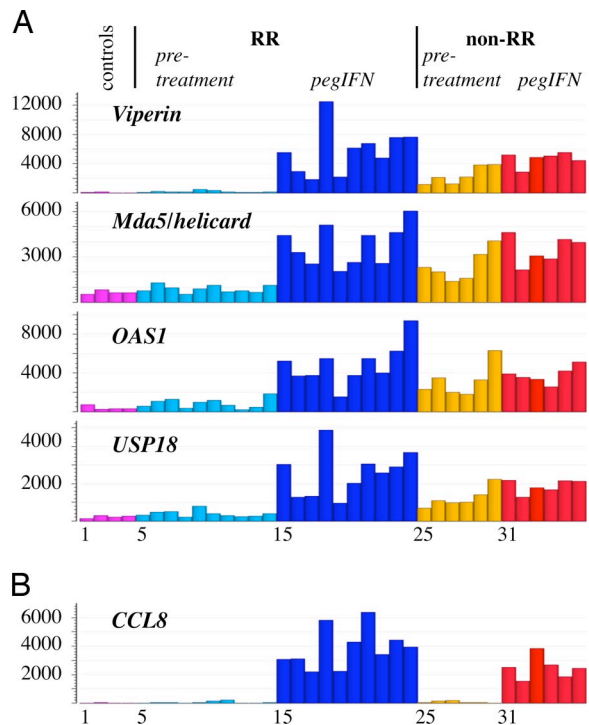


Fig. 2. PegIFN α 2b induced gene regulation in HCV-infected patients shows major differences between livers of RR and non-RR patients. (A) Four ISGs (Viperin, Mda5/helicard, OAS1, USP18) were chosen from the list of genes significantly regulated >2 -fold between B-1 and B-2 in RR patients. In the liver of non-RR patients, expression of these genes is already high before treatment (lanes 25–30) and does not further increase after pegIFN α (lanes 31–36). In RR patients, pretreatment expression (lanes 5–14) is similar to controls (lanes 1–4), and pegIFN α induces a strong up-regulation (lanes 15–24). The y axes display absolute expression values. (B) An example of a gene (CCL8) up-regulated in liver in response to pegIFN- α 2b in both RR and non-RR patients. The x axis represents individual biopsy samples. Lanes 5–14 (B-1) and 15–24 (B-2) correspond to RR patients number 1–10 in Table 1 (in the same order), and lanes 25–30 (B-1) and 31–36 (B-2) correspond to non-RR patients numbers 11–16.

datasets were subjected to supervised classifier prediction using the response at 4 weeks of treatment as grouping criteria. For PBMC samples, the analysis did not identify a subset of genes that could predict the treatment outcome (Fig. S3C and D). In contrast, a subset of 16 genes was identified in the liver B-2 samples that predicted response to treatment with an error rate of 16.1% using the K Nearest Neighbors test (Fig. S3B). An even better prediction was possible with a subset of 29 genes in the pretreatment biopsies B-1, where the error rate was 4.3% (Fig. S3A). In this set, there were 22 genes up-regulated by pegIFN α 2b (Table S2). Therefore, 76% best predictor genes represent ISGs.

Contrary to the predominance of ISGs in the best predictor set from pretreatment biopsies, only 3 (19%) of the 16 best predictor genes derived from an analysis of the B-2 biopsies were ISGs (Table S3). These results support the findings shown in Fig. 2 that expression levels of most ISGs in B-2 do not differ between RR and non-RR samples and therefore are not suited for the discrimination of responders from nonresponders. Among the non-ISGs present in the B-1 and B-2 liver biopsy lists discussed above are genes having functions in signal transduction, cell cycle regulation, apoptosis, and amino acid metabolism.

RT-qPCR Analysis of ISG Expression in Liver Biopsies. Array analysis of the paired liver biopsies emphasized the importance of ISG expression in B-1 biopsies for the outcome of therapy. To confirm these data, we measured by real-time quantitative PCR

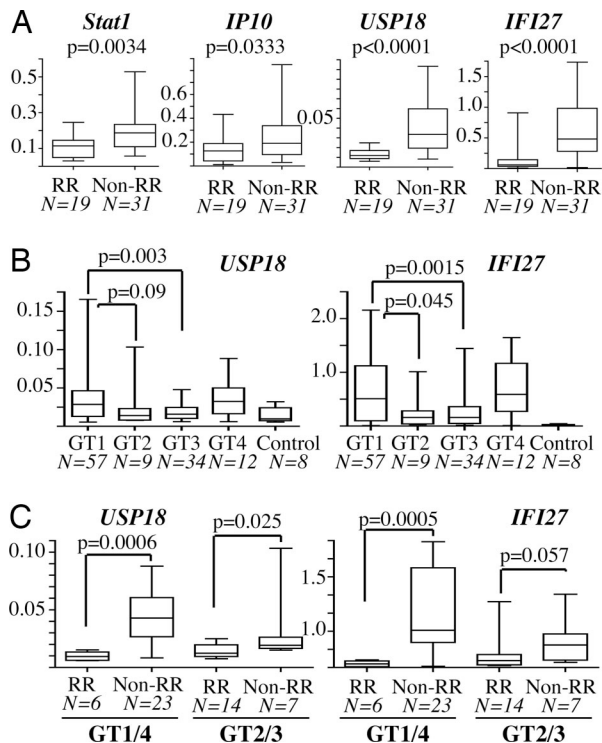


Fig. 3. RT-qPCR analysis of selected ISGs. (A) The expression level of selected ISGs in pretreatment biopsies is lower in RR than in non-RR patients. (B) Expression levels of USP18 and IFI27 in pretreatment biopsies are significantly higher in patients infected with genotype 1 (GT1) compared with GT 3. (C) Expression levels of USP18 and IFI27 are higher in non-RR patients also after stratification of the patients in a GT1/4 (“difficult-to-treat”) and a GT2/3 group. In A–C, the y axis shows expression relative to that of GAPDH. The *P* values were obtained with the Mann–Whitney test. *N* = number of patients in each group.

(RT-qPCR) the expression of selected ISGs in 16 patients with B-1 and B-2 biopsies and in pretreatment biopsies of 96 additional patients with CHC (Tables S4 and S5). In the 16 patients with paired biopsies, the RT-qPCR values matched well the array expression, validating the quality of the array data (Fig. S4A and data not shown). The expression of all four ISGs in pretherapy

biopsies was significantly different between the RR and non-RR groups (Fig. 3A), further supporting the conclusion that there is an inverse correlation between the pretreatment expression of ISGs in liver and the response to IFN α therapy. A significant up-regulation of ISGs correlated also with nonresponse at week 12 and with final treatment outcome (Fig. S4 B–D).

Pretreatment ISG Expression Levels Correlate with HCV Genotype. We also analyzed the expression of ISGs with regard to the HCV genotype (GT) (Fig. 3B). Interestingly, the investigated ISGs showed significantly higher expression in patients infected with the “difficult-to-treat” GTs 1 and 4 than with GTs 2 and 3, which can be successfully treated in >80% of patients. Importantly, the expression levels of ISGs were higher in non-RR than RR patients independently from the HCV GT (Fig. 3C). Therefore, the increased ISG expression level in non-RR patients (Fig. 3A) cannot simply be explained by the fact that GT 1 is overrepresented in the non-RR group. Rather, that patients with HCV GT 1 and 4 more frequently have an increased expression of ISGs in their liver provides a plausible explanation for the poor response of these patients to IFN therapy.

IFN-Induced Jak-STAT Signaling. The injected pegIFN α 2b binds to IFN receptors and activates the Jak-STAT pathway. A central event in this activation is the phosphorylation of STAT1 on tyrosine 701 (25). We analyzed extracts from all B-1 and B-2 biopsies by Western blot using a phospho-specific STAT1 antibody (Fig. 4A). A semiquantitative analysis of the phospho-STAT1 bands revealed a median induction of 3.6-fold in RR patients and 1.6-fold in non-RR patients (*P* = 0.03).

Phosphorylated STAT1 translocates into the nucleus and binds as a dimer to specific response elements of ISG promoters (25). Immunohistochemical analysis of phospho-STAT1 localization in paired biopsies of RR patients revealed a minimal nuclear staining in B-1 samples and a strong staining in most hepatocyte nuclei in B-2 samples (Fig. 4B and Fig. S5A). In contrast, all but one (number 11) non-RR patients showed a remarkably different staining pattern. In the pretreatment biopsies, a large proportion of hepatocytes already had an appreciable nuclear staining, which did not increase in B-2 samples. Interestingly, there was a visible increase of phospho-STAT1 staining in nuclei of Kupffer cells (liver macrophages) in B-2 samples of non-RR patients (Fig. 4B).

STAT1 DNA binding was assessed in extracts of B-1 and B-2

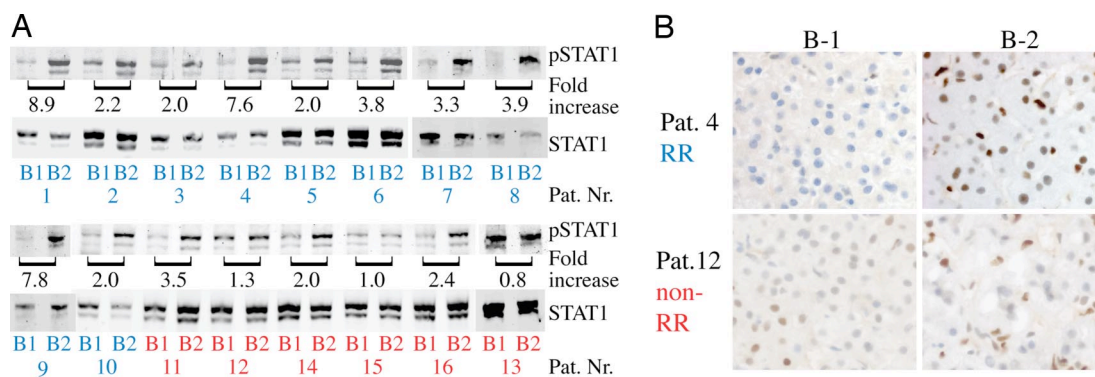


Fig. 4. Analysis of Jak-STAT signaling in liver biopsies. (A) STAT1 phosphorylation in extracts of liver biopsies collected before (B-1) and after (B-2) pegIFN- α 2b injection. Extracts were analyzed by Western blot analysis by using antibodies specific for PY (701)-STAT1. Signals were quantified by using Odyssey Imaging Software to calculate the integrated intensity (kilo counts \times mm²). The values represent the fold increase of phosphorylation in B-2 samples. RR patient numbers are shown in blue, non-RR patients in red. Blots were stripped and reprobed for total STAT1 used as a loading control for each pair of samples. (B) Representative examples of B-1 and B-2 of RR and non-RR patients. No nuclear staining is evident in pretreatment biopsies of RR patients (Pat. 4). The light-blue color of the nuclei originates from the counterstaining with hematoxylin. Four hours after pegIFN α , most hepatocytes show strong nuclear staining. In non-RR patients (Pat. 12), weak nuclear staining is already present in pretreatment biopsies, and pegIFN α induces little change in hepatocytes. The visible increased nuclear staining is confined to Kupffer cells.

biopsies by EMSAs. All RRs showed a marked increase in STAT1 DNA binding in the B-2 samples. In contrast, most non-RR patients showed a minimal or no increase of the gel-shift signal upon pegIFN α application (Fig. S5B). Taken together, the data demonstrate substantial differences in the IFN-induced Jak-STAT signaling between RR and non-RR patients.

Discussion

To learn more about possible mechanisms underlying differential response of HCV-infected patients to IFN therapy, we investigated the IFN-induced signaling and ISG induction in paired liver biopsies collected from patients with CHC before and during therapy with pegIFN α . Comparison of IFN signaling in two liver samples obtained from the same patient and comparison with the ISG induction in matching PBMC samples originating from the same patient allowed us to obtain unequivocal evidence that patients who respond poorly to therapy show preactivation of their IFN system, and that the preactivation is confined to the liver and is not evident in PBMCs. Importantly, in patients with low initial ISG expression, representing future responders to therapy, expression of ISGs in response to pegIFN α did not exceed that seen in nonresponders, either before or after therapy. This could suggest that patients with the initial preactivation of the IFN system, future nonresponders, have some defects at steps downstream of ISG expression, making them refractory to both endogenous IFN and IFN therapy. These findings in human patients are in accordance with observations in chimpanzees chronically infected with HCV (19). A human study reported a blunted response to IFN α in PBMCs of patients with a relative lack of viral response to treatment (26). In our group of 16 patients, we also detected a difference in the number of genes significantly changed at $P < 0.05$ in PBMCs between RR and non-RR patients (Fig. 1C), but this difference was less pronounced compared to the liver biopsies.

IFN α -induced STAT1 phosphorylation was stronger in RR than in non-RR patients, but there was still a clear activation of STAT1 in four of the six non-RR patients (Fig. 4A). The immunohistochemical analysis revealed a more pronounced difference. In non-RR samples, pegIFN α strongly induced nuclear STAT1 translocation in Kupffer cells, contrary to RR samples, where nuclear STAT1 accumulation was induced predominantly in hepatocytes. Interestingly, most non-RR patients had nuclear phospho-STAT1 already present in pretreatment biopsies. This is consistent with the observation that ISG transcripts are up-regulated in pretreatment biopsies of later nonresponders. How this preactivation of the Jak-STAT pathway is connected to the refractoriness of the IFN system in non-RR patients requires further investigation.

Over the last few years, important insights into the interference of HCV with the innate immune system revealed the ability of HCV to inhibit both TLR3-TRIF-IRF3 and the RIG-I/MDA5-Cardif signaling pathways of IFN β induction (27, 28). This capacity of HCV could help explain why the virus often establishes a chronic infection. However, our data and previously published results (20) demonstrate that the endogenous IFN system is constantly activated in many patients. Moreover, patients with a preactivated IFN system seem to respond poorly to IFN therapy. This finding is counterintuitive (one would expect that an active innate immune system would help eliminate the virus during IFN α therapy), but it is largely supported by other published data from chimpanzees and human patients (16, 17, 20). From the analyses of ISG expression in liver biopsies, it is apparent that in some patients, HCV induces (or at least does not block) the endogenous IFN system, whereas in others it successfully represses it, possibly by cleaving TRIF and/or Cardif. Paradoxically, this difference has no apparent impact on the ability of HCV to maintain a chronic infection.

In patients without a preactivated IFN system, pegIFN α 2b induced a robust up-regulation of many ISGs in the liver within 4 h. Similar high ISG expression was already present in the pretreatment biopsies of patients who later did not show a RR at week 4. It is somewhat perplexing why the latter patients do not resolve the chronic HCV infection spontaneously despite the strong activation of the IFN system. One possibility is that ISG proteins that are up-regulated in both cases possess different posttranscriptional modifications. In an alternative scenario, nonresponse to both endogenous and exogenous IFN α may be caused by the lack of induction of a few critical ISGs that are specifically required for the elimination of HCV. We cannot exclude this possibility, but an array analysis performed on paired liver samples did not reveal ISGs that were specifically up-regulated in RRs. Furthermore, this model cannot explain why preactivation of the endogenous IFN system is so closely linked to later nonresponse to treatment.

Alternatively, the kinetics of induction of the IFN response could be decisive. In patients without a preactivated IFN system, the injection of exogenous IFN α during treatment should induce an antiviral state very rapidly in most liver cells, and HCV would not have “enough” time to escape from the IFN-induced defense. However, the buildup of the antiviral state could be slow in the other group of patients, which would give HCV enough time to adapt to and evade the intracellular antiviral defense system, making it also resistant to the subsequent IFN therapy.

How could the induction of the endogenous IFN system compromise the success of IFN α therapy? Clearly, the activation of negative feedback loops that inhibit IFN signaling could play a role. Prominent candidates among the negative regulators are suppressors of cytokine signaling 1 (SOCS1) and SOCS3 (29), two IFN-induced proteins that bind to the IFN receptor and inhibit the activity of Jak1 and Tyk2, and the more recently described regulator Ubp43 (protein of the USP18 gene), an IFN-stimulated protein that binds to IFN α receptor 2 (IFNAR2) and blocks the access of Jak1 to it (30). However, we could not find a significant difference in the expression levels of these negative regulators in the pegIFN α 2b-stimulated liver biopsies of RR compared with non-RR patients (data not shown). Moreover, a general up-regulation of negative regulators such as SOCSs and Ubp43 is not compatible with the observed strong constitutive expression of a large number of ISGs in the subset of patients that poorly respond to IFN therapy. If IFN α signaling were indeed inhibited by the induction of SOCSs and Ubp43 in the majority of liver cells, then one should not observe such a pronounced preactivation of ISGs in pretreatment livers.

Notably, although the preactivation of tested ISGs occurred more frequently in liver biopsies of patients infected with HCV GT 1 and 4 than with GT 2 or 3, it did occur in both groups. Preactivation of ISGs was found in non-RR patients with GT 2/3, whereas RR patients with GT 1/4 had no induction in pretreatment biopsies (Fig. 3C). Therefore, preactivation of the endogenous IFN system is strongly linked to the later response to treatment independent of the HCV GT. Our finding that the frequency and degree of preactivation of the endogenous IFN system depend on the HCV GT could provide an explanation for the observation that GT 2 and 3 infections can be cured in >80% of patients, compared with <50% of infections with GT 1 (4). Perhaps HCV GTs 2 and 3 are more successful in preventing the activation of innate immunity in the liver. The success of the virus in preventing the induction of the endogenous IFN system would, however, come at the cost of being more susceptible to IFN α therapies. Of note, a single chimpanzee infected with GT 3 has been shown to have lower ISG expression levels than animals infected with GT 1 (17).

We have shown that HCV inhibits the IFN α -induced signaling via the Jak-STAT pathway by up-regulating a protein phosphatase PP2A (12, 14, 31, 32). Inhibition of IFN α signaling by HCV

by this or other mechanisms could explain why the strong preactivation of the endogenous IFN system does not lead to a spontaneous elimination of HCV. If one assumes that not all hepatocytes are infected by HCV, but rather a minority, then the induction of ISGs observed in pretreatment biopsies of non-RR patients could occur predominantly in noninfected hepatocytes. In infected cells, IFN would be ineffective because of the inhibition of the Jak-STAT signaling pathway. The IFN responsible for the preactivation of the system would be secreted by hepatocytes infected with a virus that is not successful in preventing IFN production. Because of the HCV-induced inhibition of the Jak-STAT pathway, the secreted IFN β would not induce an antiviral state in the infected hepatocytes but rather in noninfected neighbor cells. To gain further insights into the pathobiology of CHC, future studies should focus on analysis at the single-cell level. Unfortunately, the detection of HCV-infected hepatocytes in liver biopsies is still unsatisfactory, making such studies difficult.

Although the precise mechanism of the HCV escape from the immune defense system still remains to be elucidated, the impairment of hepatitis C therapy by preactivation of the endogenous IFN system is now well established. It would be interesting to investigate whether this preactivation is a reversible process. The injection of neutralizing anti-IFN α/β antibodies or other factors blocking the IFN response before treatment could return the endogenous IFN system to a “naive” state and potentially enhance the response to IFN α -based therapies.

Materials and Methods

Patient Samples and Treatment. From January 2006 to April 2007, patients with CHC referred to the outpatient liver clinic of University Hospital Basel were asked for permission to use part of their diagnostic liver biopsy (B-1) for

research purposes. Patients who then were treated with pegylated-IFN α 2b (PegIntron) and ribavirin (Rebetol, both from Essex Chemie) were asked to participate in this study. Sixteen patients agreed to undergo a second liver biopsy (B-2) 4 h after the first injection of 1.5 μ g/kg body weight pegIFN α 2b (PegIntron). All were Caucasians. The first dose of ribavirin was given after this second biopsy to avoid further confounding factors. The protocol was approved by the Ethics Committee of the University Hospital Basel. Written informed consent was obtained from all patients. Blood for PBMC isolation was collected before treatment and 4 h after the first pegIFN α 2b injection. Patients were treated with pegIFN α 2b (1.5 μ g/kg body weight) and ribavirin (weight-based dosing: <65 kg: 800 mg/d; 65–85 kg: 1 g/d; >85 kg: 1.2 g/d). HCV RNA was quantified before treatment initiation and at weeks 4 and 12 of the treatment (Table 1). Treatment duration was 24 weeks for patients with genotypes 2/3 and 48 weeks for genotypes 1/4. As non-CHC controls, four patients who underwent ultrasound-guided liver biopsies of focal lesions gave informed consent for a biopsy from normal liver tissue outside the focal lesion. Pretreatment liver biopsies from 96 additional patients (all but one were Caucasians) with CHC were used for RT-qPCR for selected ISGs (patient data shown in Table S4).

Measurement of IFN α in Serum. Pretreatment IFN α levels and the concentration of pegIFN α 2b 4 h after the first injection were measured in serum using the human IFN α ELISA kit from PBL Biomedical Laboratories according to the manufacturer’s instructions. This kit has been shown to recognize both unpegylated and pegylated human IFN α (22).

RNA Isolation, Western Blots, EMSA, Immunohistochemistry, and Microarray and RT-qPCR Analyses. The procedures are described in detail in *SI Materials and Methods*. All original array data are being deposited in the National Center for Biotechnology Information (NCBI) Gene Expression Omnibus (GEO) database.

ACKNOWLEDGMENTS. We thank the patients who participated in this study. This work was supported by Swiss National Science Foundation Grant 32-116106, Swiss Cancer League Grant KLS-01832-02-2006, Grant 8/05 from the Krebsliga Basel, and a grant from the Roche Research Foundation (to M.S.-F.). Friedrich Miescher Institute is supported by the Novartis Research Foundation.

- Meylan E, Tschopp J (2006) Toll-like receptors and RNA helicases: Two parallel ways to trigger antiviral responses. *Mol Cell* 22:561–569.
- Gale M, Jr, Foy EM (2005) Evasion of intracellular host defence by hepatitis C virus. *Nature* 436:939–945.
- Strader DB, Wright T, Thomas DL, Seeff LB (2004) Diagnosis, management, and treatment of hepatitis C. *Hepatology* 39:1147–1171.
- Hadziyannis SJ, et al. (2004) Peginterferon-alpha2a and ribavirin combination therapy in chronic hepatitis C: A randomized study of treatment duration and ribavirin dose. *Ann Intern Med* 140:346–355.
- Fried MW, et al. (2002) Peginterferon alfa-2a plus ribavirin for chronic hepatitis C virus infection. *N Engl J Med* 347:975–982.
- Ferenci P, et al. (2005) Predicting sustained virological responses in chronic hepatitis C patients treated with peginterferon alfa-2a (40 KD)/ribavirin. *J Hepatol* 43:425–433.
- Davis GL, et al. (2003) Early virologic response to treatment with peginterferon alfa-2b plus ribavirin in patients with chronic hepatitis C. *Hepatology* 38:645–652.
- Yu JW, Wang GQ, Sun LJ, Li XG, Li SC (2007) Predictive value of rapid virological response and early virological response on sustained virological response in HCV patients treated with pegylated interferon alpha-2a and ribavirin. *J Gastroenterol Hepatol* 22:832–836.
- Sen GC (2001) Viruses and interferons. *Annu Rev Microbiol* 55:255–281.
- Darnell JE, Jr, Kerr IM, Stark GR (1994) Jak-STAT pathways and transcriptional activation in response to IFNs and other extracellular signaling proteins. *Science* 264:1415–1421.
- de Veer MJ, et al. (2001) Functional classification of interferon-stimulated genes identified using microarrays. *J Leukocyte Biol* 69:912–920.
- Blindenbacher A, et al. (2003) Expression of hepatitis C virus proteins inhibits interferon alpha signaling in the liver of transgenic mice. *Gastroenterology* 124:1465–1475.
- Heim MH, Moradpour D, Blum HE (1999) Expression of hepatitis C virus proteins inhibits signal transduction through the Jak-STAT pathway. *J Virol* 73:8469–8475.
- Duong FH, Filipowicz M, Tripodi M, La Monica N, Heim MH (2004) Hepatitis C virus inhibits interferon signaling through up-regulation of protein phosphatase 2A. *Gastroenterology* 126:263–277.
- Gale M, Jr, et al. (1998) Control of PKR protein kinase by hepatitis C virus nonstructural 5A protein: Molecular mechanisms of kinase regulation. *Mol Cell Biol* 18:5208–5218.
- Bigger CB, Brasky KM, Lanford RE (2001) DNA microarray analysis of chimpanzee liver during acute resolving hepatitis C virus infection. *J Virol* 75:7059–7066.
- Bigger CB, et al. (2004) Intrahepatic gene expression during chronic hepatitis C virus infection in chimpanzee. *J Virol* 78:13779–13792.
- Thimme R, et al. (2002) Viral and immunological determinants of hepatitis C virus clearance, persistence, and disease. *Proc Natl Acad Sci USA* 99:15661–15668.
- Lanford RE, et al. (2007) Lack of response to exogenous interferon-alpha in the liver of chimpanzees chronically infected with hepatitis C virus. *Hepatology* 46:999–1008.
- Chen L, et al. (2005) Hepatic gene expression discriminates responders and nonresponders in treatment of chronic hepatitis C viral infection. *Gastroenterology* 128:1437–1444.
- Brodsky LI, et al. (2006) A novel unsupervised method to identify genes important in the anti-viral response: Application to interferon/ribavirin in hepatitis C patients. *PLoS ONE* 1:e584.
- Lanford RE, et al. (2006) Genomic response to interferon-alpha in chimpanzees: Implications of rapid downregulation for hepatitis C kinetics. *Hepatology* 43:961–972.
- Ji X, et al. (2003) Interferon alfa regulated gene expression in patients initiating interferon treatment for chronic hepatitis C. *Hepatology* 37:610–621.
- Silva M, et al. (2006) A randomised trial to compare the pharmacokinetic, pharmacodynamic, and antiviral effects of peginterferon alfa-2b and peginterferon alfa-2a in patients with chronic hepatitis C (COMPARE). *J Hepatol* 45:204–213.
- Darnell JE, Jr (1997) STATS and gene regulation. *Science* 277:1630–1635.
- Taylor MW, et al. (2007) Changes in gene expression during pegylated interferon and ribavirin therapy of chronic hepatitis C virus distinguish responders from nonresponders to antiviral therapy. *J Virol* 81:3391–3401.
- Li K, et al. (2005) Immune evasion by hepatitis C virus NS3/4A protease-mediated cleavage of the Toll-like receptor 3 adaptor protein TRIF. *Proc Natl Acad Sci USA* 102:2992–2997.
- Meylan E, et al. (2005) Cardif is an adaptor protein in the RIG-I antiviral pathway and is targeted by hepatitis C virus. *Nature* 437:1167–1172.
- Krebs DL, Hilton DJ (2001) SOCS proteins: Negative regulators of cytokine signaling. *Stem Cells* 19:378–387.
- Malakhova OA, et al. (2006) UBP43 is a novel regulator of interferon signaling independent of its ISG15 isopeptidase activity. *EMBO J* 25:2358–2367.
- Christen V, Treves S, Duong FH, Heim MH (2007) Activation of endoplasmic reticulum stress response by hepatitis viruses up-regulates protein phosphatase 2A. *Hepatology* 46:558–565.
- Duong FH, Christen V, Filipowicz M, Heim MH (2006) S-adenosylmethionine and betaine correct hepatitis C virus induced inhibition of interferon signaling *in vitro*. *Hepatology* 43:796–806.

Supporting Information

Sarasin-Filipowicz et al. 10.1073/pnas.0707882105

SI Materials and Methods

Western Blots and EMSA. Whole cell, cytoplasmic and nuclear extracts were prepared as described (1, 2). 10 μg of total protein from human liver lysates was loaded for SDS/PAGE and transferred onto a nitrocellulose membrane (Schleicher & Schuell, Switzerland). The membranes were blocked in 3% BSA/milk (1:1)-0.1% Triton X-100 for 1 h, washed with Tris-buffered saline Tween-20 (TBST), and incubated with the primary antibody overnight at 4°C.

Proteins were detected with primary antibodies specific to phosphorylated STAT1 (PY (701)-STAT1; #9171; Cell Signaling) and STAT1 (carboxy-terminus; Transduction Laboratories, BD Biosciences, PharMingen). After 3 washes with TBST, membranes were incubated with infrared fluorescent secondary goat anti-mouse (IRDye 680) or anti-rabbit (IRDye 800) antibodies (both from LI-COR Biosciences) for 1 h at room temperature. Blots were analyzed by Odyssey Infrared Imaging System from LI-COR. The infrared image was obtained in a single scan and the signal was quantified using the integrated intensity.

EMSAs were performed using 2 μg of nuclear extracts and ^{32}P -radiolabeled DNA-oligonucleotide duplex of the serum inducible element (SIE)-m67, corresponding to STAT response element sequences (3).

Immunohistochemistry. Standard indirect immunoperoxidase procedures were used for immunohistochemistry (ABC-Elite, Vectra Laboratories). 4-mm-thick sections were cut from paraffin blocks, rehydrated, pretreated (20' in ER2 solution) incubated with a monoclonal rabbit antibody against phospho-STAT1 (dilution 1:200, #9167 Cell Signaling) and counterstained with haematoxylin. The whole staining procedure (dehydration, pretreatment, incubation, counterstaining and mounting) was performed with an automated stainer (Bond, Vision BioSystems Europe, Newcastle-upon-Thyne, U.K.). For quantification of nuclear phospho-STAT1 staining, 5 times 200 hepatocytes were counted for each B-1 and B-2 sample of each patient. In [SI Fig. S5A](#), the mean values with the standard deviations are shown.

RNA Isolation and Microarray Analysis. Total RNA was extracted from liver and PBMC samples using the RNeasy Mini Kit (Qiagen) according to manufacturer's instructions. RNA was aliquoted and stored at -80°C. Gene expression was assessed in liver and PBMCs by microarray analysis using Affymetrix Human Genome U133 Plus 2.0 arrays representing over 56,000 transcripts and variants with 11 perfect-match/mis-match probe pairs per transcript. The microarray hybridizations were performed at the functional genomics facility of the Friedrich Miescher Institute for Biomedical Research in Basel. Total RNA (1–2 μg) from each sample was reverse transcribed and biotinylated using the Affymetrix 1-cycle amplification kit as per manufacturer's instructions. Biotinylated cRNA (20 μg) was fragmented by heating with magnesium (as per Affymetrix's instructions) and 15 μg of fragmented cRNA was hybridized to Human U133 Plus 2.0 GeneChips according to the manufacturer's instructions. Quality control and background normalization was performed using Refiner 4.1 from Genedata AG (Basel, Switzerland). Expression value estimates were obtained using the GC-RMA implementation in Refiner 4.1. Quantile-normalization and median scaling of the genes called present (detection P value <0.04) to a value of 500 was performed in

Genedata's Analyst 4.1 package. These data will subsequently be referred to as "absolute" expression values in the text.

Data analysis was performed using Expressionist Analyst 4.1 from Genedata AG.

Genes were required to pass a paired *t* test with a $P < 0.05$ or $P < 0.01$ and have a fold change of 2 or greater between the paired patient samples in >50% of patients within each group. More precisely, for each patient, genes up- or down-regulated >2-fold in posttreatment samples (compared with pretreatment) were identified and saved in gene lists. The gene lists of all RR patients and those of all non-RR patients were combined to generate two extended lists. The genes of these lists were analyzed with a paired *t* test using the B-1 and B-2 samples of the patients in each response group. Genes had to pass the paired *t* test with a significance level of $P < 0.05$ or $P < 0.01$. Finally, genes up- or down-regulated >2-fold with $P < 0.05$ or $P < 0.01$ in >50% of patients within each of the response groups were selected.

A fold change of 2 was selected to provide a list of genes that were changing greatly within the samples. The false discovery rate (FDR) of the *t* test was estimated by setting the universe size to the number of genes that were detected with an Affymetrix detection P value <0.04 (often called "present") in at least one of the conditions (≈ 32000 genes). The FDR analysis was made using a permutation based false discovery estimate (4). In addition we performed Storey-Tibshirani (5) FDR estimates, maximal FDR values for which were 0.25 for $P < 0.05$ and 0.12 for $P < 0.01$.

The probability for the intersections in the Venn diagrams in [Fig. 1 A](#) and [B](#) occurring by chance was calculated using the hypergeometric test and was very low for both cases (4.91^{-40} and 6.03^{-192}). Both hypergeometric probabilities were calculated using the *p* hyper function in the R statistical package and Bonferroni corrections were applied.

To compare the number of significantly regulated genes between RR and non-RR patients in groups with equal number of patients, 15 groups of 6 out of 10 patients were selected using computer-generated pseudorandom numbers. In each group, the genes changed >2-fold with a significance level of $P < 0.05$ or $P < 0.01$ (paired *t* test) in >50% of patients were identified and counted. We then calculated the probability of the Non-RR derived result (i.e., 36 genes for $P < 0.05$) being part of the expected Normal sampling distribution of the results obtained from the 15 random RR samples using the "pnormal" function from the statistical package R. This gave *p*-values of 0.004 and 0.001 for the biopsy samples when considering the data from the *t* test at either the <0.01 or <0.05 level respectively ([Fig. 1C](#)).

To compare the mean ISG expression levels in B-2 samples of RRs and non-RRs, a Welch *t* test was performed using the list of 252 genes significantly regulated >2-fold in >50% of RR patients. Only 19 genes (7.5%) passed the test ($P < 0.05$) with a minimum of a 2-fold difference between RR and non-RR.

The heat map in [Fig. S1](#) was generated by hierarchical clustering of the 252 genes significantly regulated >2-fold in >50% of RR patients.

For the supervised classifier prediction of liver biopsy samples and PBMCs using the response at week 4 as a grouping criterion, 4 supervised clustering algorithms were used (Support Vector Machine, Sparse Linear Discriminant Analysis, Fisher Linear Discriminant Analysis, K Nearest Neighbors). The misclassification rates could be determined for every algorithm used and K Nearest Neighbors (KNN) was selected to generate the list of

genes best predicting treatment response at week 4 in biopsy samples (B-1 and B-2). In the case of Fig. S3A, Support Vector Machine rendered an even lower misclassification rate of 1.9% if compared with the 4.3% from KNN, but the lists of best predictors in B-1 were identical for both tests.

RNA Isolation, Reverse Transcription, and SYBR-PCR. The array data were validated by quantitative real-time RT-PCR analysis of several IFN regulated genes including STAT1, IP10, USP18 and IFI27. Total RNA was extracted as described above. The RNA was reverse transcribed by Moloney murine leukemia virus reverse transcriptase (Promega Biosciences, Inc.) in the presence of random hexamers (Promega) and deoxynucleoside triphosphate. The reaction mixture was incubated for 5 min at 70°C and then for 1 h at 37°C. The reaction was stopped by heating at 95°C for 5 min. SYBR-PCR was performed based on SYBR green

fluorescence (SYBR green PCR master mix; Applied Biosystems, Foster City, CA). Primers for GAPDH (glyceraldehyde-3-phosphate dehydrogenase), STAT1, IP10, USP18 and IFI27 were designed across exon-intron junctions (Table S5). The difference in the cycle threshold (Δ CT) value was derived by subtracting the CT value for GAPDH, which served as an internal control, from the CT value for transcripts of interest. All reactions were run in duplicate by using an ABI 7000 sequence detection system (Applied Biosystems). mRNA expression levels of the transcripts were calculated relative to GAPDH from the Δ CT values using the formula $2^{-\Delta$ CT. The change of expression in paired liver biopsy samples was calculated as a fold change according to the formula $2^{(\Delta$ CT B-1- Δ CT B-2).

Box plot diagrams and Mann-Whitney tests were performed using GraphPad Prism version 4.00 for Macintosh, GraphPad Software, www.graphpad.com.

1. Blindenbacher A, et al. (2003) Expression of hepatitis C virus proteins inhibits interferon alpha signaling in the liver of transgenic mice. *Gastroenterology* 124:1465-1475.
2. Duong FH, Filipowicz M, Tripodi M, La Monica N, Heim MH (2004) Hepatitis C virus inhibits interferon signaling through up-regulation of protein phosphatase 2A. *Gastroenterology* 126:263-277.
3. Heim MH, Moradpour D, Blum HE (1999) Expression of hepatitis C virus proteins inhibits signal transduction through the Jak-STAT pathway. *J Virol* 73:8469-8475.
4. Dean N, Raftery AE (2005) Normal uniform mixture differential gene expression detection for cDNA microarrays. *BMC Bioinformatics* 6:173.
5. Storey JD, Tibshirani R (2003) Statistical significance for genomewide studies. *Proc Natl Acad Sci USA* 100:9440-9445.

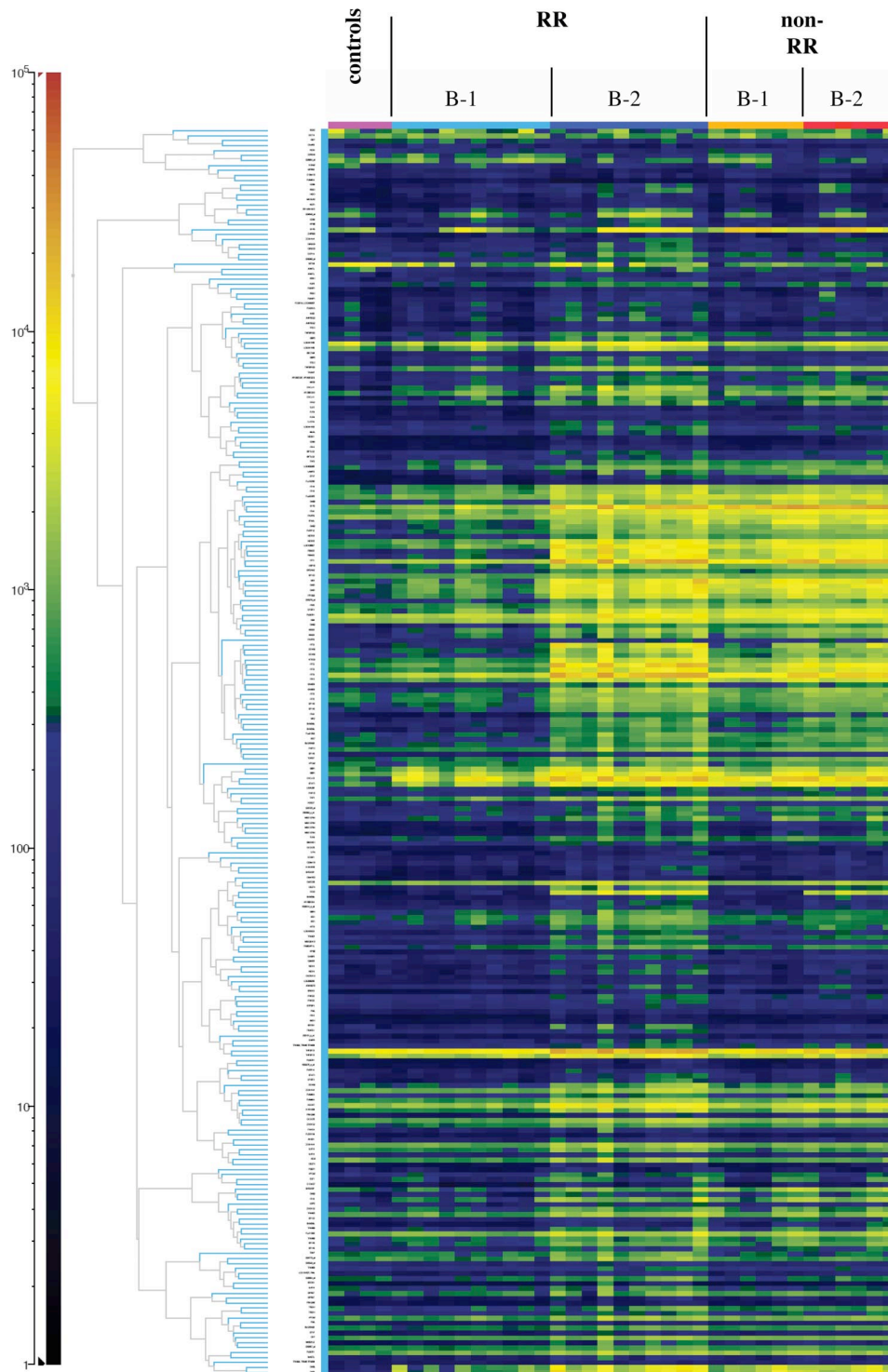
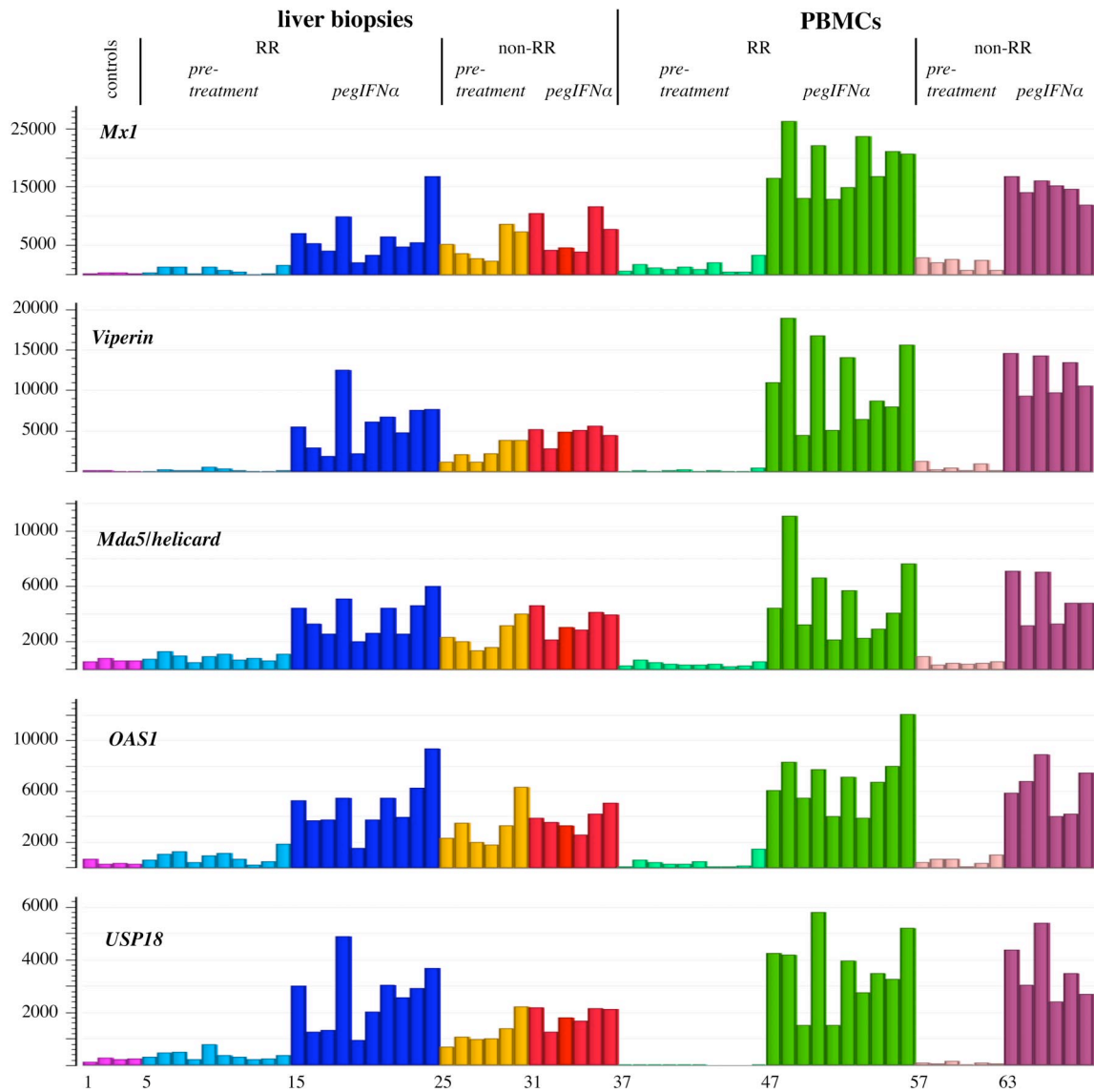


Fig. S1. The predominant pattern of gene expression in all patient biopsy samples is shown as a heat map. The map was generated with a hierarchical clustering analysis using a list of 252 genes that are altered >2 fold in $>50\%$ of all RRs with a p value of <0.05 . The color coding of the absolute expression values is shown on the left. Many genes have a low expression level in the control patients and the pretreatment biopsies of the RR patients (B-1). In RR patients, pegIFN α induces an up-regulation (B-2). In non-RR patients, many of the genes are already strongly induced in the pretreatment biopsy samples (B-1), and no further induction is then found after pegIFN α (B-2).

A



B

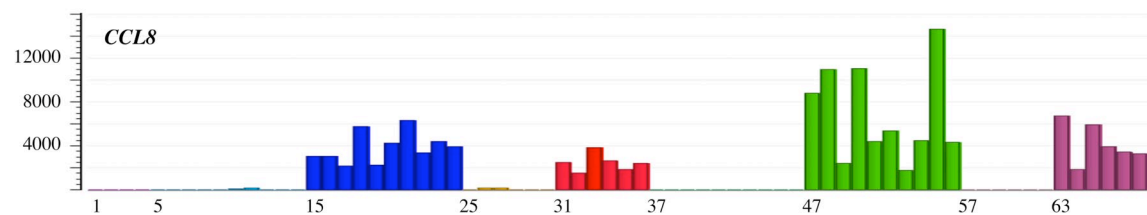


Fig. 52. PegIFN- α 2b induced gene regulation in HCV-infected patients shows major differences between RR and non-RR patients in the liver but not in PBMCs. (A) Five ISGs (*Mx1*, *viperin*, *Mda5/helicard*, *OAS1*, *USP18*) were chosen from the list of genes significantly ($P < 0.05$) regulated >2 -fold between B-1 and B-2 in RR patients. In the liver of non-RR patients, expression of these genes is already high before treatment (lanes 25–30), and does not further increase after pegIFN α (lanes 31–36). In RR patients, pretreatment expression (lanes 5–14) is similar to controls (lanes 1–4), and pegIFN α induces a strong up-regulation (lanes 15–24). No preactivation is found in PBMCs (lanes 37–46 and 57–62), and pegIFN α strongly induces these genes in both RR and non-RR patients (lanes 47–56 and 63–68). The y-axes display absolute expression values. (B) An example of a gene (*CCL8*) up-regulated in liver in response to pegIFN- α 2b in both RR and non-RR patients. The expression values in PBMCs are shown in lanes 37–68).

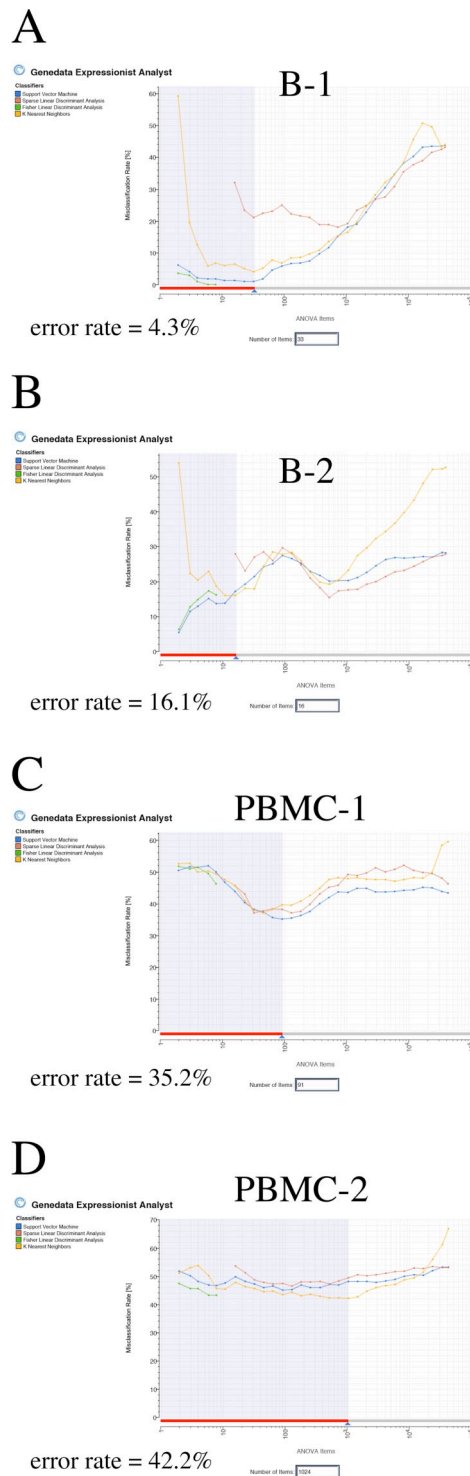


Fig. S3. Supervised classifier prediction in liver biopsy samples and PBMCs with response to treatment at week 4 as grouping criterion. (A) Supervised classifier prediction using the B-1 biopsies of the two response groups resulted in a list of 29 genes (33 transcripts) as best predictors of treatment outcome with a misclassification rate of 4.3% when using the K Nearest Neighbors test. (B) Supervised classifier prediction using the B-2 biopsies of the two response groups revealed a list of 16 genes (16 transcripts) as best predictors of treatment outcome with a misclassification rate of 16.1%. (C and D) Supervised classifier prediction of PBMC-1 and PBMC-2 samples did not generate a useful list of predictive genes with any of the 4 statistical tests used (Support Vector Machine, Sparse Linear Discriminant Analysis, Fisher Linear Discriminant Analysis, K Nearest Neighbors). The misclassification rates were 38.5% for PBMC-1 and 42.6% for PBMC-2.

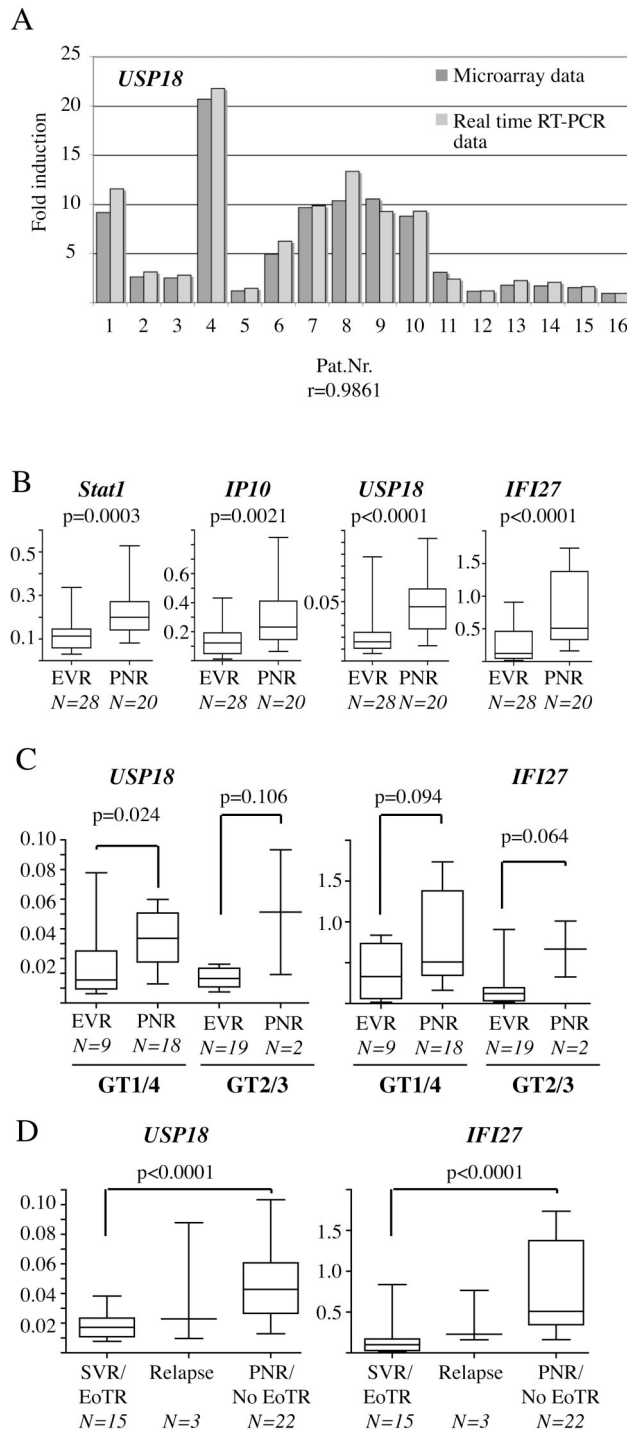


Fig. S4. RT-qPCR analysis of selected ISGs. (A) RT-qPCR analysis of the USP18 mRNA corroborates the array data. Depicted is the fold induction of USP18 mRNA between B-1 and B-2 in individual patients. The correlation coefficient between the RT-qPCR and microarray data is $r = 0.9861$. (B) The expression level of selected ISGs in pretreatment biopsies is lower in patients with early virological response (EVR = more than 2 log drop of viral load at week 12) than in patients with primary non-response (PNR = less than 2 log drop of viral load at week 12). (C) Both within the group of patients with genotype 1 and 4 ("difficult"-to-treat) and the group with genotype 2 and 3 ("easy"-to-treat) the PNR patients have higher pretreatment expression levels of USP18 and IFI27. In B and C, the y axis shows expression relative to that of GAPDH. Statistical significance was tested with the Mann-Whitney test. n = number of patients in each group. (D) Patients with sustained virological response (SVR = undetectable HCV RNA 6 months after end of treatment) or end-of-treatment response (EoTR) show significantly lower expression of USP18 and IFI27 than patients with PNR or no EoTR.

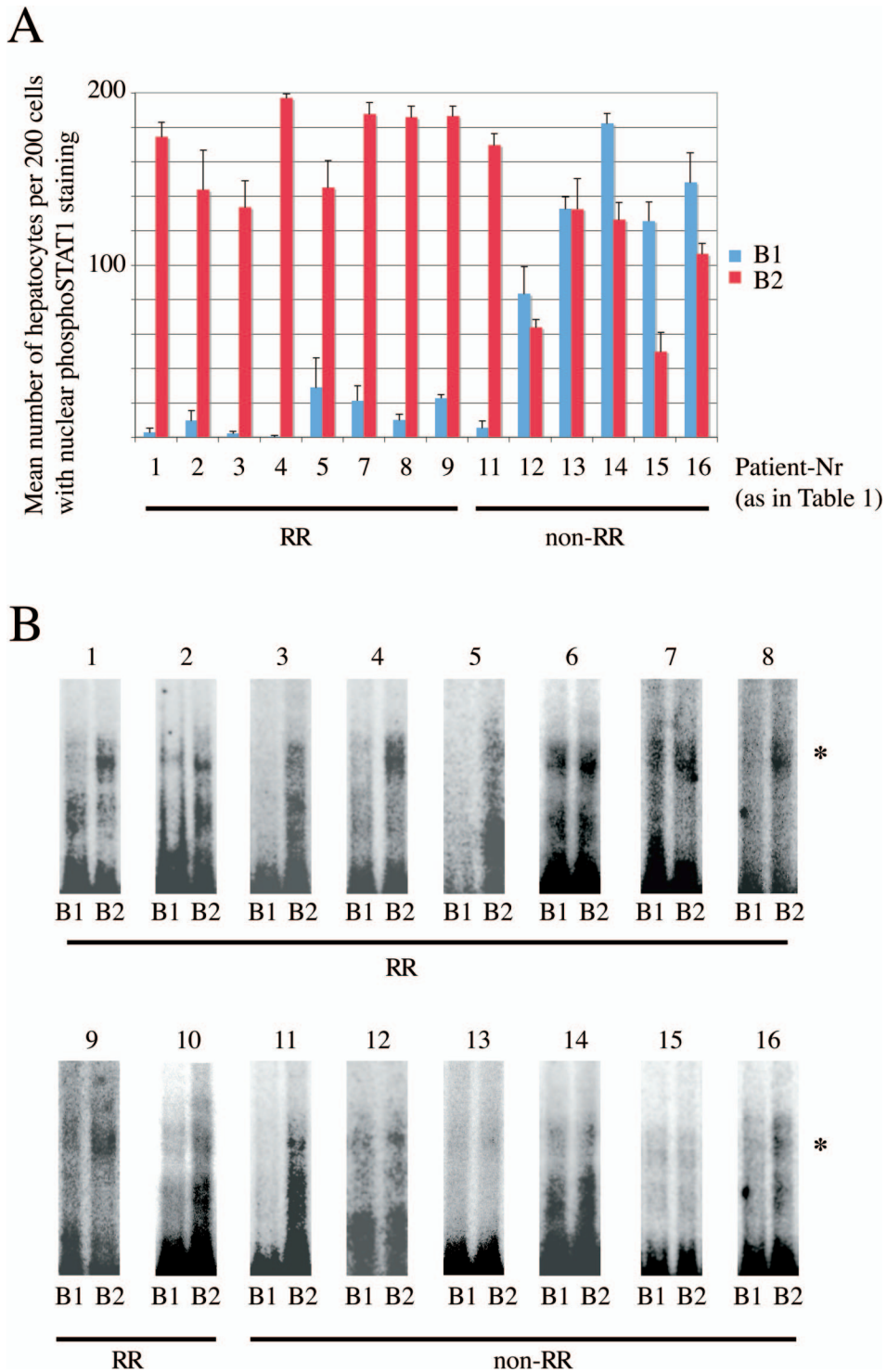


Fig. S5. (A) Semiquantitative assessment of immunohistochemical staining of phospho-STAT1 in liver biopsies. Nuclear staining of hepatocytes was quantified by repeated counting (5 times) in 200 hepatocytes in B-1 (blue) and B-2 (red) samples of the indicated patients (patient numbers correspond to the numbers in table 1). In five out of six non-RR patients, a considerable proportion of hepatocytes had a weak but clear nuclear staining already in the pretreatment biopsies. All of the RR patients had no phospho-STAT1 signals in the nuclei before treatment, but showed a strong induction after pegIFN α . (B) The induction of STAT-DNA binding in response to pegIFN α 2b is impaired in most of the non-RR patients. Nuclear extracts from B-1 and B-2 samples were analyzed with EMSAs using the radiolabeled SIE-m67 oligonucleotide probe. The asterisk (*) depicts the signal of the activated STAT1 dimers that have bound the oligonucleotide sequence. The numbers above the gel shift panels represent the patient numbers as already used in table 1. The upper panel shows the 10 patients with a rapid response at week 4 (numbers 1–10). The lower panel shows the 6 non-RR patients (numbers 11–16).

Table S1. List of 252 genes changed >2-fold from B-1 to B-2 in >50% of 10 RR patients with a significance of $P < 0.05$ (paired t test)

Name	Description	Gene Symbol	RR Mean B2/B1	non-RR Mean B2/B1
214038_at	chemokine (C-C motif) ligand 8	CCL8	55.42	29.45
217502_at	interferon-induced protein with tetratricopeptide repeats 2	IFIT2	31.50	2.75
213797_at	radical S-adenosyl methionine domain containing 2	RSAD2	28.47	1.93
214059_at	Interferon-induced protein 44	IFI44	14.02	2.84
227458_at	<i>CD274 antigen</i>	<i>CD274</i>	13.79	3.82
226757_at	interferon-induced protein with tetratricopeptide repeats 2	IFIT2	12.84	2.45
204994_at	myxovirus (influenza virus) resistance 2 (mouse)	MX2	12.06	3.16
210302_s.at	mab-21-like 2 (C. elegans)	MAB21L2	11.76	1.37
204747_at	interferon-induced protein with tetratricopeptide repeats 3	IFIT3	11.67	1.97
210001_s.at	<i>suppressor of cytokine signaling 1</i>	<i>SOCS1</i>	11.34	2.21
239979_at	Epithelial stromal interaction 1 (breast)	EPSTI1	9.60	2.69
230036_at	sterile alpha motif domain containing 9-like	SAMD9L	9.29	2.47
222793_at	DEAD (Asp-Glu-Ala-Asp) box polypeptide 58	DDX58	8.97	1.86
203153_at	interferon-induced protein with tetratricopeptide repeats 1, interferon-induced protein with tetratricopeptide repeats 1	IFIT1	8.51	1.63
202086_at	myxovirus (influenza virus) resistance 1, interferon-inducible protein p78 (mouse), myxovirus (influenza virus) resistance 1, interferon-inducible protein p78 (mouse)	MX1	8.33	1.44
209999_x.at	<i>suppressor of cytokine signaling 1</i>	<i>SOCS1</i>	8.28	1.37
218943_s.at	DEAD (Asp-Glu-Ala-Asp) box polypeptide 58	DDX58	8.03	1.86
226702_at	hypothetical protein LOC129607	LOC129607	7.98	1.42
219691_at	sterile alpha motif domain containing 9	SAMD9	7.96	1.87
1557078_at	likely ortholog of mouse schlafen 5	MGC19764	7.83	1.97
243271_at	Sterile alpha motif domain containing 9-like	SAMD9L	7.80	4.93
219352_at	hect domain and RLD 6	HERC6	7.75	1.42
204439_at	interferon-induced protein 44-like	IFI44L	7.12	1.31
223298_s.at	5'-nucleotidase, cytosolic III	NT5C3	7.05	1.76
230314_at	Similar to hypothetical protein 628	LOC440424	6.89	1.89
1553055_a.at	likely ortholog of mouse schlafen 5	MGC19764	6.83	1.76
1555464_at	interferon induced with helicase C domain 1	IFIH1	6.71	2.42
229450_at	Interferon-induced protein with tetratricopeptide repeats 3	IFIT3	6.56	1.59
228230_at	peroxisomal proliferator-activated receptor A interacting complex 285	PRIC285	6.49	1.64
219211_at	ubiquitin specific peptidase 18	USP18	6.46	1.51
210873_x.at	apolipoprotein B mRNA editing enzyme, catalytic polypeptide-like 3A	APOBEC3A	6.38	3.10
205483_s.at	interferon, alpha-inducible protein (clone IFI-15K)	G1P2	6.31	1.22
231956_at	KIAA1618	KIAA1618	6.13	1.72
228439_at	hypothetical protein BC012330	MGC20410	6.11	2.24
204972_at	2'-5'-oligoadenylate synthetase 2, 69/71kDa	OAS2	6.00	1.36
242234_at	XIAP associated factor-1	BIRC4BP	5.95	1.68
219684_at	28kD interferon responsive protein	IFRG28	5.78	1.39
242961_x.at	DEAD (Asp-Glu-Ala-Asp) box polypeptide 58	DDX58	5.77	1.75
243999_at	likely ortholog of mouse schlafen 5	MGC19764	5.72	1.74
1552309_a.at	nexilin (F actin binding protein)	NEXN	5.58	1.76
202869_at	2',5'-oligoadenylate synthetase 1, 40/46kDa	OAS1	5.48	1.18
219863_at	hect domain and RLD 5	HERC5	5.39	1.34
205569_at	lysosomal-associated membrane protein 3	LAMP3	5.31	1.59
218400_at	2'-5'-oligoadenylate synthetase 3, 100kDa	OAS3	5.27	1.38
210797_s.at	2'-5'-oligoadenylate synthetase-like	OASL	5.23	1.26
232375_at	Signal transducer and activator of transcription 1, 91kDa	STAT1	5.22	1.59
211122_s.at	<i>chemokine (C-X-C motif) ligand 11</i>	<i>CXCL11</i>	5.19	1.59
241916_at	Phospholipid scramblase 1	PLSCR1	5.16	2.30
205660_at	2'-5'-oligoadenylate synthetase-like	OASL	5.04	1.26
202672_s.at	activating transcription factor 3	ATF3	4.91	3.21
230000_at	chromosome 17 open reading frame 27	C17orf27	4.89	1.20

Table 1 (continued)

Name	Description	Gene Symbol	RR Mean B2/B1	non-RR Mean B2/B1
238439_at	<i>ankyrin repeat domain 22</i>	<i>ANKRD22</i>	4.84	3.23
204804_at	tripartite motif-containing 21	TRIM21	4.80	1.81
208392_x.at	SP110 nuclear body protein	SP110	4.79	1.52
225076_s.at	KIAA1404 protein	KIAA1404	4.76	1.68
223834_at	<i>CD274 antigen</i>	<i>CD274</i>	4.74	1.82
220059_at	BCR downstream signaling 1	BRDG1	4.72	2.19
223980_s.at	SP110 nuclear body protein	SP110	4.45	1.51
211267_at	homeo box (expressed in ES cells) 1	HESX1	4.43	3.10
228468_at	<i>microtubule associated serine/threonine kinase-like</i>	<i>MASTL</i>	4.43	1.51
33304_at	interferon stimulated exonuclease gene 20kDa	ISG20	4.39	1.62
202988_s.at	regulator of G-protein signalling 1	RGS1	4.37	4.66
235276_at	gb:AA781795/DB XREF = gi:2841126/DB XREF = ai51d05.s1/CLONE = 1360521/FEA = EST /CNT = 14/TID = Hs.122587.0/TIER = ConsEnd /STK = 1/UG = Hs.122587/UG TITLE = ESTs		4.27	1.43
219209_at	interferon induced with helicase C domain 1	IFIH1	4.24	1.44
209762_x.at	SP110 nuclear body protein	SP110	4.24	1.77
236156_at	lipase A, lysosomal acid, cholesterol esterase (Wolman disease)	LIPA	4.19	2.42
226103_at	nexilin (F actin binding protein)	NEXN	4.16	1.64
203805_s.at	Fanconi anemia, complementation group A, Fanconi anemia, complementation group A	FANCA	4.15	1.17
227609_at	epithelial stromal interaction 1 (breast)	EPST11	4.14	1.22
208436_s.at	interferon regulatory factor 7	IRF7	4.11	1.37
239196_at	ankyrin repeat domain 22	ANKRD22	4.06	2.08
1556314_a.at	CDNA FLJ33375 fis, clone BRACE2006137		3.99	2.34
228152_s.at	hypothetical protein FLJ31033	FLJ31033	3.94	1.42
225557_at	AXIN1 up-regulated 1	AXUD1	3.93	1.72
211012_s.at	promyelocytic leukemia, hypothetical protein LOC161527	LOC161527, PML	3.93	1.79
210163_at	chemokine (C-X-C motif) ligand 11	CXCL11	3.88	1.69
226725_at	Transcribed locus		3.83	1.52
222881_at	heparanase	HPSE	3.71	1.95
235157_at	Poly (ADP-ribose) polymerase family, member 14	PARP14	3.69	1.44
221680_s.at	ets variant gene 7 (TEL2 oncogene)	ETV7	3.62	1.27
1554519_at	CD80 antigen (CD28 antigen ligand 1, B7-1 antigen)	CD80	3.61	2.23
206715_at	transcription factor EC	TFEC	3.60	2.38
206513_at	absent in melanoma 2	AIM2	3.56	1.96
218543_s.at	poly (ADP-ribose) polymerase family, member 12	PARP12	3.55	1.34
204187_at	guanosine monophosphate reductase, guanosine monophosphate reductase	GMPR	3.55	1.42
216020_at	Interferon induced with helicase C domain 1	IFIH1	3.54	1.50
209824_s.at	aryl hydrocarbon receptor nuclear translocator-like	ARNTL	3.54	1.42
209457_at	dual specificity phosphatase 5	DUSP5	3.45	2.46
213038_at	<i>IBR domain containing 3</i>	<i>IBRDC3</i>	3.44	1.38
224225_s.at	ets variant gene 7 (TEL2 oncogene)	ETV7	3.44	1.36
229625_at	<i>Guanylate binding protein 5</i>	<i>GBP5</i>	3.42	2.02
203595_s.at	interferon-induced protein with tetratricopeptide repeats 5	IFIT5	3.39	1.39
225344_at	nuclear receptor coactivator 7	NCOA7	3.38	1.57
213361_at	tudor domain containing 7	TDRD7	3.36	1.37
220104_at	zinc finger CCCH-type, antiviral 1	ZC3HAV1	3.33	1.79
208965_s.at	interferon, gamma-inducible protein 16	IFI16	3.33	1.66
238025_at	mixed lineage kinase domain-like	MLKL	3.31	1.51
205875_s.at	three prime repair exonuclease 1	TREX1	3.30	1.36
225291_at	polyribonucleotide nucleotidyltransferase 1	PNPT1	3.25	1.49
210029_at	<i>indoleamine-pyrrole 2,3 dioxygenase</i>	<i>INDO</i>	3.20	1.00
206553_at	2'-5'-oligoadenylate synthetase 2, 69/71kDa	OAS2	3.18	1.37
228362_s.at	Hypothetical protein LOC441168	RP1-93H18.5	3.17	1.70
204286_s.at	phorbol-12-myristate-13-acetate-induced protein 1	PMAIP1	3.15	3.03

Table S1. (continued)

Name	Description	Gene Symbol	RR Mean B2/B1	non-RR Mean B2/B1
214586.at	G protein-coupled receptor 37 (endothelin receptor type B-like)	GPR37	3.14	0.85
238581.at	<i>Guanylate binding protein 5</i>	GBP5	3.13	1.74
228304.at	Transcribed locus		3.11	1.63
238743.at	Coiled-coil domain containing 75	CCDC75	3.10	1.42
209795.at	CD69 antigen (p60, early T-cell activation antigen)	CD69	3.10	3.82
209892.at	fucosyltransferase 4 (alpha (1,3) fucosyltransferase, myeloid-specific)	FUT4	3.09	2.22
235175.at	guanylate binding protein 4	GBP4	3.08	1.61
206332.s.at	interferon, gamma-inducible protein 16	IFI16	3.08	1.52
36564.at	IBR domain containing 3	IBRDC3	3.06	1.53
216834.at	regulator of G-protein signalling 1	RGS1	3.06	2.51
221766.s.at	family with sequence similarity 46, member A	FAM46A	3.04	1.48
212657.s.at	interleukin 1 receptor antagonist	IL1RN	3.03	1.49
1559051.s.at	chromosome 6 open reading frame 150	C6orf150	3.03	3.24
208966.x.at	interferon, gamma-inducible protein 16	IFI16	3.01	1.57
203610.s.at	tripartite motif-containing 38	TRIM38	3.01	1.32
218625.at	<i>neurtin 1</i>	NRN1	3.01	1.67
202912.at	adrenomedullin	ADM	2.97	1.32
216243.s.at	<i>interleukin 1 receptor antagonist</i>	IL1RN	2.95	1.31
238725.at	<i>Interferon regulatory factor 1</i>	IRF1	2.94	1.19
203596.s.at	interferon-induced protein with tetratricopeptide repeats 5	IFIT5	2.94	1.46
224973.at	Family with sequence similarity 46, member A	FAM46A	2.94	1.40
219011.at	pleckstrin homology domain containing, family A (phosphoinositide binding specific) member 4	PLEKHA4	2.92	1.32
219885.at	likely ortholog of mouse schlafen 3	FLJ10260	2.92	1.58
204285.s.at	phorbol-12-myristate-13-acetate-induced protein 1	PMAIP1	2.91	3.12
211013.x.at	promyelocytic leukemia	PML	2.87	1.26
223501.at	tumor necrosis factor (ligand) superfamily, member 13b	TNFSF13B	2.87	2.00
35254.at	TRAF-type zinc finger domain containing 1	TRAFD1	2.86	1.61
1563075.s.at	Clone IMAGE:110987 mRNA sequence		2.81	1.68
213294.at	Coiled-coil domain containing 75	CCDC75	2.80	1.28
232517.s.at	peroxisomal proliferator-activated receptor A interacting complex 285	PRIC285	2.79	1.53
214933.at	calcium channel, voltage-dependent, P/Q type, alpha 1A subunit	CACNA1A	2.79	1.89
238430.x.at	likely ortholog of mouse schlafen 5	MGC19764	2.79	1.36
209417.s.at	interferon-induced protein 35	IFI35	2.79	1.24
238039.at	CDNA FLJ26339 fis, clone HRT02975		2.77	1.23
219403.s.at	heparanase	HPSE	2.77	1.28
230383.x.at	Transcribed locus, moderately similar to NP_060190.1 signal-transducing adaptor protein-2; brk kinase substrate [Homo sapiens]		2.76	1.45
207375.s.at	interleukin 15 receptor, alpha	IL15RA	2.75	1.27
225443.at	DCP1 decapping enzyme homolog A (<i>S. cerevisiae</i>)	DCP1A	2.71	1.16
205739.x.at	zinc finger protein 588	ZNF588	2.70	1.66
223502.s.at	tumor necrosis factor (ligand) superfamily, member 13b	TNFSF13B	2.70	1.99
214995.s.at	apolipoprotein B mRNA editing enzyme, catalytic polypeptide-like 3G, apolipoprotein B mRNA editing enzyme, catalytic polypeptide-like 3F	APOBEC3F, APOBEC3G	2.68	1.61
218501.at	Rho guanine nucleotide exchange factor (GEF) 3	ARHGEF3	2.67	1.87
222816.s.at	zinc finger, CCHC domain containing 2	ZCCHC2	2.66	1.17
243296.at	Pre-B-cell colony enhancing factor 1	PBEF1	2.66	1.05
230405.at	hypothetical gene supported by AL713721	LOC441109	2.65	1.40
210218.s.at	nuclear antigen Sp100	SP100	2.64	1.10
204533.at	chemokine (C-X-C motif) ligand 10	CXCL10/IP-10	2.63	1.42
34689.at	three prime repair exonuclease 1	TREX1	2.63	1.29
202446.s.at	phospholipid scramblase 1	PLSCR1	2.62	1.37

Table S1. (continued)

Name	Description	Gene Symbol	RR Mean B2/B1	non-RR Mean B2/B1
209969_s.at	signal transducer and activator of transcription 1, 91kDa	STAT1	2.60	1.14
203567_s.at	tripartite motif-containing 38	TRIM38	2.58	1.32
202307_s.at	transporter 1, ATP-binding cassette, sub-family B (MDR/TAP)	TAP1	2.57	1.43
209631_s.at	G protein-coupled receptor 37 (endothelin receptor type B-like)	GPR37	2.57	0.94
213982_s.at	RAB GTPase activating protein 1-like	RABGAP1L	2.56	1.46
202269_x.at	guanylate binding protein 1, interferon-inducible, 67kDa, guanylate binding protein 1, interferon-inducible, 67kDa	GBP1	2.56	1.44
202531_at	<i>interferon regulatory factor 1</i>	<i>IRF1</i>	2.56	1.26
226773_at	MRNA (clone ICRFp50711077)		2.56	1.37
229391_s.at	hypothetical protein LOC441168	LOC441168	2.55	2.15
216202_s.at	serine palmitoyltransferase, long chain base subunit 2	SPTLC2	2.55	1.64
204211_x.at	eukaryotic translation initiation factor 2-alpha kinase 2	EIF2AK2	2.54	1.28
212659_s.at	interleukin 1 receptor antagonist	IL1RN	2.54	1.34
221432_s.at	solute carrier family 25, member 28, solute carrier family 25, member 28	SLC25A28	2.53	1.39
219062_s.at	zinc finger, CCHC domain containing 2	ZCCHC2	2.53	1.29
229543_at	gb:AV734646 /DB XREF = gi:10852191 /DB XREF = AV734646 /CLONE = cdAAGE02 /FEA = EST /CNT = 18 /TID = Hs.54277.2 /TIER = ConsEnd /STK = 0 /UG = Hs.54277 /LL = 9130 /UG GENE = DXS9928E /UG TITLE = DNA segment on chromosome . . .		2.52	1.73
1557236_at	Apolipoprotein L, 6	APOL6	2.52	1.09
216598_s.at	chemokine (C-C motif) ligand 2	CCL2	2.51	2.52
223192_at	solute carrier family 25, member 28	SLC25A28	2.50	1.41
235543_at	gb:A1928184 /DB XREF = gi:5664148 /DB XREF = wo95b05.x1 /CLONE = IMAGE:2463057 /FEA = EST /CNT = 12 /TID = Hs.122011.0 /TIER = ConsEnd /STK = 2 /UG = Hs.122011 /UG TITLE = ESTs		2.48	1.23
206133_at	XIAP associated factor-1	BIRC4BP	2.46	1.13
219364_at	likely ortholog of mouse D11lgp2	LGP2	2.45	1.32
224806_at	tripartite motif-containing 25	TRIM25	2.45	1.23
202688_at	tumor necrosis factor (ligand) superfamily, member 10, tumor necrosis factor (ligand) superfamily, member 10	TNFSF10	2.44	1.44
204415_at	interferon, alpha-inducible protein (clone IFI-6-16)	G1P3	2.44	1.08
227807_at	poly (ADP-ribose) polymerase family, member 9	PARP9	2.43	1.55
212420_at	E74-like factor 1 (ets domain transcription factor)	ELF1	2.42	1.28
221865_at	chromosome 9 open reading frame 91	C9orf91	2.39	2.07
214329_x.at	tumor necrosis factor (ligand) superfamily, member 10, tumor necrosis factor (ligand) superfamily, member 10	TNFSF10	2.39	1.38
210971_s.at	aryl hydrocarbon receptor nuclear translocator-like	ARNTL	2.39	1.21
213051_at	zinc finger CCCH-type, antiviral 1	ZC3HAV1	2.37	1.31
219716_at	apolipoprotein L, 6	APOL6	2.37	1.29
220146_at	toll-like receptor 7	TLR7	2.35	2.24
218986_s.at	hypothetical protein FLJ20035	FLJ20035	2.35	1.14
209893_s.at	fucosyltransferase 4 (alpha (1,3) fucosyltransferase, myeloid-specific)	FUT4	2.34	1.77
225634_at	zinc finger CCCH-type, antiviral 1	ZC3HAV1	2.33	1.20
219357_at	GTP binding protein 1	GTPBP1	2.32	1.34
205932_s.at	msh homeo box homolog 1 (Drosophila)	MSX1	2.32	1.42
206247_at	MHC class I polypeptide-related sequence B	MICB	2.31	1.59
38269_at	protein kinase D2	PRKD2	2.30	1.40
235737_at	<i>thymic stromal lymphopoietin</i>	<i>TSLP</i>	2.30	1.09
208912_s.at	2',3'-cyclic nucleotide 3' phosphodiesterase	CNP	2.29	1.17

Table S1. (continued)

Name	Description	Gene Symbol	RR Mean B2/B1	non-RR Mean B2/B1
232383.at	transcription factor EC	TFEC	2.29	1.60
226474.at	nucleotide-binding oligomerization domains 27	NOD27	2.27	1.45
232150.at	Chromosome 20 open reading frame 18	C20orf18	2.25	1.53
203127.s.at	serine palmitoyltransferase, long chain base subunit 2	SPTLC2	2.24	1.76
231577.s.at	guanylate binding protein 1, interferon-inducible, 67kDa	GBP1	2.24	1.38
217497.at	endothelial cell growth factor 1 (platelet-derived)	ECGF1	2.24	1.54
209282.at	protein kinase D2	PRKD2	2.23	1.42
205151.s.at	gb:NM 014817.1 /DB XREF = gi:7662219 /GEN = KIAA0644 /FEA = FLmRNA /CNT = 48 /TID = Hs.21572.0 /TIER = FL + Stack /STK = 11 /UG = Hs.21572 /LL = 9865 /DEF = Homo sapiens KIAA0644 gene product (KIAA0644), mRNA. /PROD = KI . . .		2.22	1.43
230110.at	mucolipin 2	MCOLN2	2.22	1.27
204961.s.at	neutrophil cytosolic factor 1 (47kDa, chronic granulomatous disease, autosomal 1)	NCF1	2.21	1.35
214511.x.at	Fc fragment of IgG, high affinity Ia, receptor (CD64), Fc-gamma receptor I B2	FCGR1A, LOC440607	2.19	1.82
206503.x.at	promyelocytic leukemia	PML	2.19	1.40
204205.at	apolipoprotein B mRNA editing enzyme, catalytic polypeptide-like 3G	APOBEC3G	2.19	1.46
216950.s.at	Fc fragment of IgG, high affinity Ia, receptor (CD64)	FCGR1A	2.17	1.82
212660.at	PHD finger protein 15	PHF15	2.17	1.64
227877.at	similar to annexin II receptor	LOC389289	2.17	1.42
213716.s.at	secreted and transmembrane 1	SECTM1	2.16	1.27
221044.s.at	tripartite motif-containing 34, tripartite motif-containing 6 and tripartite motif-containing 34	TRIM34, TRIM6-TRIM34	2.16	1.40
203236.s.at	lectin, galactoside-binding, soluble, 9 (galectin 9)	LGALS9	2.16	1.57
231876.at	tripartite motif-containing 56	TRIM56	2.15	1.15
1568592.at	hypothetical gene supported by BC031266	LOC400368	2.15	1.27
229390.at	hypothetical protein LOC441168	LOC441168	2.15	1.78
203964.at	N-myc (and STAT) interactor	NMI	2.15	1.32
212577.at	structural maintenance of chromosomes flexible hinge domain containing 1	SMCHD1	2.11	1.37
209732.at	C-type lectin domain family 2, member B	CLEC2B	2.10	1.59
224175.s.at	tripartite motif-containing 34, tripartite motif-containing 6 and tripartite motif-containing 34	TRIM34, TRIM6-TRIM34	2.10	1.37
202864.s.at	nuclear antigen Sp100	SP100	2.09	1.11
241869.at	apolipoprotein L, 6	APOL6	2.08	1.47
229723.at	T-cell activation GTPase activating protein	TAGAP	2.08	1.70
206271.at	toll-like receptor 3	TLR3	2.08	1.15
218999.at	hypothetical protein FLJ11000	FLJ11000	2.07	1.20
205692.s.at	<i>CD38 antigen (p45)</i>	<i>CD38</i>	2.05	1.12
217546.at	<i>metallothionein 1M</i>	<i>MT1M</i>	2.03	1.01
202430.s.at	phospholipid scramblase 1	PLSCR1	1.97	1.11
239587.at	Transcribed locus		1.94	1.13
223220.s.at	poly (ADP-ribose) polymerase family, member 9	PARP9	1.90	1.18
208960.s.at	Kruppel-like factor 6	KLF6	1.87	1.66
225973.at	transporter 2, ATP-binding cassette, sub-family B (MDR/TAP)	TAP2	1.72	1.21
230252.at	G protein-coupled receptor 92	GPR92	0.57	0.51
44790.s.at	chromosome 13 open reading frame 18	C13orf18	0.56	0.67
227410.at	family with sequence similarity 43, member A	FAM43A	0.56	0.64
206765.at	potassium inwardly-rectifying channel, subfamily J, member 2	KCNJ2	0.53	0.51
209218.at	squalene epoxidase	SQLE	0.53	1.42
202887.s.at	DNA-damage-inducible transcript 4	DDIT4	0.52	0.89

Table S1. (continued)

Name	Description	Gene Symbol	RR Mean B2/B1	non-RR Mean B2/B1
209782_s.at	D site of albumin promoter (albumin D-box) binding protein	DBP	0.47	0.61
227285_at	chromosome 1 open reading frame 51	C1orf51	0.46	0.61
202861_at	period homolog 1 (Drosophila)	PER1	0.46	0.56
228854_at	Transcribed locus		0.42	0.33
205883_at	zinc finger and BTB domain containing 16	ZBTB16	0.33	0.38

Shown are the average fold changes from B-1 to B-2 in RR and non-RR patients. Nineteen genes (shown in *italics*) had significantly ($P < 0.05$, Welch t test) higher mean expression values in B-2 samples from RR vs. non-RR patients.

Table S2a. Analysis of gene expression in pretreatment biopsies (B-1)

Gene symbol	Description	Affy-ID	Mean (SEM) expression in 10 RRs	Mean (SEM) expression in 6 non-RRs	Non-RR/RR	Function
IFI44L	interferon-induced protein 44-like	204439_at	306 (50)	3392 (903)	11.10	cell cycle
RSAD2	radical S-adenosyl methionine domain containing 2	242625_at	272 (41)	2405 (425)	8.83	innate immune response
G1P2	interferon, alpha-inducible protein (clone IFI-15K)	205483_s_at	2238 (397)	17375 (2762)	7.76	innate immune response
IFI27	interferon, alpha-inducible protein 27	202411_at	3320 (714)	24927 (2441)	7.51	innate immune response
LAMP3	lysosomal-associated membrane protein 3	205569_at	96 (22)	665 (108)	6.97	cell proliferation
OAS3	2'-5'-oligoadenylate synthetase 3, 100kDa	218400_at	319 (46)	1842 (296)	5.77	innate immune response
HERC6	hect domain and RLD 6	219352_at	144 (32)	795 (93)	5.53	immune response
HIST1H2BD	Histone 1, H2bd	235456_at	40 (4)	202 (33)	5.02	DNA packaging
IFIT1	interferon-induced protein with tetratricopeptide repeats 1	203153_at	2209 (165)	9995 (1706)	4.53	innate immune response
LOC129607	hypothetical protein LOC129607	226702_at	970 (143)	4135 (520)	4.26	amino acid metabolism
IFI44	interferon-induced protein 44	214453_s_at	1101 (153)	4183 (405)	3.80	innate immune response
HERC5	hect domain and RLD 5	219863_at	963 (93)	3144 (552)	3.26	protein ubiquitination
LGALS3BP	lectin, galactoside-binding, soluble, 3 binding protein	200923_at	1537 (238)	4960 (475)	3.23	response to stress
SAMD9	sterile alpha motif domain containing 9	228531_at	323 (32)	997 (166)	3.08	unknown

Table S2b. Analysis of gene expression in pretreatment biopsies (B-1)

IFIT2	interferon-induced protein with tetratricopeptide repeats 2	226757_at	951 (63)	2744 (510)	2.89	innate immune response
LOC286208	hypothetical protein LOC286208	1560089_at	39 (3)	110 (18)	2.86	-
IRF7	interferon regulatory factor 7	208436_s_at	240 (16)	679 (107)	2.82	innate immune response
FLJ20035	hypothetical protein FLJ20035	218986_s_at	1191 (84)	3341 (378)	2.80	Helicase
IFIT3	Interferon-induced protein with tetratricopeptide repeats 3	229450_at	2760 (213)	7703 (1327)	2.79	innate immune response
RALGPS1	Ral GEF with PH domain and SH3 binding motif 1	204199_at	22 (2)	61 (8)	2.70	signal transduction
PARP12	poly (ADP-ribose) polymerase family, member 12	218543_s_at	437 (36)	1158 (60)	2.65	poly (ADP-ribose) polymerase family
HIST1H2BG	histone 1, H2bg	210387_at	13 (1)	29 (3)	2.13	DNA packaging
PARP9	poly (ADP-ribose) polymerase family, member 9	223220_s_at	1386 (111)	2868 (263)	2.07	poly (ADP-ribose) polymerase family
PNPT1	polyribonucleotide nucleotidyltransferase 1	225291_at	518 (23)	971 (105)	1.88	RNA catabolism
CCDC75	Coiled-coil domain containing 75	213294_at	776 (40)	1382 (105)	1.78	-
CNP	2',3'-cyclic nucleotide 3' phosphodiesterase	208912_s_at	682 (24)	1054 (70)	1.55	nucleotide metabolism
HTATIP2	HIV-1 Tat interactive protein 2, 30kDa	209448_at	3317 (130)	4451 (74)	1.34	Apoptosis
RPLP0	ribosomal protein, large, P0, ribosomal protein, large, P0	211720_x_at	16980 (404)	13294 (439)	0.78	protein biosynthesis
LOC402560	Hypothetical LOC401384	227554_at	562 (95)	90 (20)	0.16	-

List of 29 genes best predicting treatment outcome at week 4 (IFN stimulated genes shaded in grey; genes that differ between RR and non-RR but are not regulated by IFN are not shaded).

Table S3. Analysis of gene expression in biopsies obtained 4 h after pegIFN α (B-2)

Gene symbol	Description	Affy-ID	Mean (SEM) expression in 10 RRs	Mean (SEM) expression in 6 non-RRs	Non-RR /RR	Function
IFI27	interferon, alpha-inducible protein 27	202411_at	4540 (735)	25501 (2372)	5.62	innate immune response
LGALS3BP	lectin, galactoside-binding, soluble, 3 binding protein	200923_at	1728 (282)	5223 (386)	3.02	response to stress
ZFP3	zinc finger protein 3 homolog (mouse)	235728_at	33 (4)	75 (7)	2.28	ion binding
MYH14	myosin, heavy polypeptide 14	234290_x_at	33 (2)	64 (5)	1.98	cell morphogenesis
PARP6	poly (ADP-ribose) polymerase family, member 6	219639_x_at	149 (8)	285 (23)	1.92	poly (ADP-ribose) polymerase family
GPR143	G protein-coupled receptor 143	206696_at	18 (1)	28 (2)	1.54	signal transduction
BRUNOL5	bruno-like 5, RNA binding protein (Drosophila)	232416_at	13 (0.3)	19 (1)	1.43	RNA binding
ATP5A1	ATP synthase, H ⁺ transporting, mitochondrial F1 complex, alpha subunit, isoform 1, cardiac muscle	213738_s_at	14472 (290)	17712 (487)	1.22	cellular metabolism
CHMP4A	chromatin modifying protein 4A	228764_s_at	348 (11)	234 (6)	0.67	protein localization
IDS	iduronate 2-sulfatase (Hunter syndrome)	206342_x_at	185 (7)	122 (5)	0.66	carbohydrate metabolism
	gb:AI341383 /DB_XREF=gi:4078310 /DB_XREF=qx91a06.x1 /CLONE=IMAGE:2009842 /FEA=EST /CNT=52 /TID=Hs.112751.2 /TIER=Stack /STK=42 /UG=Hs.112751 /LL=23383 /UG_GENE=KIAA0892 /UG_TITLE=KIAA0892 protein	227092_at	475 (24)	254 (17)	0.54	
VISA	Virus-induced signaling adapter	229741_at	167 (7)	77 (4)	0.46	innate immune response

Table S3b. Analysis of gene expression in biopsies obtained 4 h after pegIFN α (B-2)

PCOLCE	procollagen C-endopeptidase enhancer	202465_at	1297 (135)	539 (56)	0.42	development
IRF1	Interferon regulatory factor 1	238725_at	1106 (109)	449 (30)	0.41	innate immune response
PSMAL	prostate-specific membrane antigen-like	211303_x_at	793 (76)	278 (68)	0.35	Unknown
LOC402560	Hypothetical LOC401384	227554_at	578 (85)	83 (17)	0.14	-

List of 16 genes best predicting treatment outcome at week 4 (IFN stimulated genes shaded in grey; genes that differ between RR and non-RR but are not regulated by IFN are not shaded).

Table S4a. Study patients' characteristics

Biopsy number	Sex	Age	HCV genotype	Baseline VL IU/ml	Metavir	4 week response	12 week response	Follow-up
A 810	m	53	3	6112502	A3/F4	-	-	EoTR, Relapse
A 643	f	52	2a/c	72157	A2/F4	-	-	EoTR, Relapse
A 441	m	45	1b	2910319	A1/F4	Non-RVR	EVR	EoTR, Relapse
A 502.b	m	67	1b	2137002	A1/F2	Non-RVR	EVR	No EoTR
A 626	m	63	1	1752158	A3/F4	Non-RVR	EVR	No EoTR
A 517	f	53	3a	204455	A2/F4	Non-RVR	EVR	No EoTR
A 454	m	45	1	684000	A1/F4	Non-RVR	PNR	PNR
A 478	m	45	1	5632925	A2/F3	Non-RVR	PNR	PNR
A 606	m	41	1	12328724	A2/F3	Non-RVR	PNR	PNR
A 795	m	54	1	222053	A3/F4	Non-RVR	PNR	PNR
A 603	f	38	2	5780000	A2/F3	Non-RVR	PNR	PNR
A 733	f	58	2	5262008	A2/F4	Non-RVR	PNR	PNR
A 770	m	49	4	8048807	A3/F4	Non-RVR	PNR	PNR
A 535	f	49	1a	>700'000	A1/F2	Non-RVR	PNR	PNR
A 558.c	f	47	1a	1444062	A2/F2	Non-RVR	PNR	PNR
A 578	f	43	1a	1300504	A1/F2	Non-RVR	PNR	PNR
A 595	f	52	1a	4458717	A2/F2	Non-RVR	PNR	PNR
A 745	f	37	1a	953556	A3/F3	Non-RVR	PNR	PNR

Table S4b. Study patients' characteristics

A 756	m	61	1a	5545733	A2/F4	Non-RVR	PNR	PNR
A 759	m	62	1a	5624281	A3/F4	Non-RVR	PNR	PNR
A 521.b	f	44	1b	248000	A2/F2	Non-RVR	PNR	PNR
A 555.b	m	60	1b	7636130	A2/F3	Non-RVR	PNR	PNR
A 563	m	48	1b	713046	A3/F4	Non-RVR	PNR	PNR
A 615	m	59	1b	191299	A3/F3	Non-RVR	PNR	PNR
A 664	m	56	1b	7790643	A2/F3	Non-RVR	PNR	PNR
A 709	m	48	1b	2949376	A2/F4	Non-RVR	PNR	PNR
A 518	m	48	4	45523	A1/F4	Non-RVR	EVR	treatment interrupted
A 685	m	40	3a	2531993	A3/F3	Non-RVR	EVR	ongoing
A 673	f	38	1b	8002763	A2/F3	Non-RVR	EVR	ongoing
A 570.b	f	54	3	6655260	A1/F2	Non-RVR	EVR	EoTR
A 704	m	41	3a	15538256	A1/F1	Non-RVR	EVR	EoTR
A 536	m	49	3a	2283557	A1/F2	Non-RVR	EVR	SVR
A 376	m	42	3a	352000	A1/F1	-	EVR	SVR
A 502.c	m	37	3a	247290	A2/F2	-	EVR	SVR
A 558.b	f	45	3a	6409813	A1/F2	-	EVR	EoTR
A 475	f	45	4c/d	1718991	A3/F3	-	EVR	SVR
A 764	m	38	4	12000	A2/F2	RR		ongoing
A 590	f	48	1a	3107291	A3/F4	RR		ongoing
A 720	f	50	1b	16639113	A1/F2	RR		ongoing
A 706	m	56	3	178919	A3/F4	RR		ongoing
A 542	f	28	3	423000	A2/F1	RVR	EVR	SVR
A 601	f	63	2a/c	3306636	A2/F3	RVR	EVR	SVR
A 609	f	53	2a/c	1196303	A3/F3	RVR	EVR	EoTR
A 614	m	33	2b	1867778	A1/F2	RVR	EVR	EoTR
A 623	m	47	2b	4663883	A3/F4	RVR	EVR	EoTR
A 426	m	26	3a	87458	A1/F1	RVR	EVR	EoTR
A 534	m	52	3a	13773866	A2/F2	RVR	EVR	SVR

Table S4c. Study patients' characteristics

A 584	m	37	3a	78684	A1/F2	RVR	EVR	EoTR
A 594	m	38	1a	9638894	A2/F1	RVR	EVR	ongoing
A 792	f	16	1a	3378	A3/F1	RVR	EVR	ongoing
A 662	m	49	3a	12381160	A2/F2	RVR	EVR	ongoing
A 688	f	48	3a	13538256	A2/F3	RVR	EVR	ongoing
A 748	m	29	3a	11879263	A2/F2	RVR	EVR	ongoing
A 707	f	24	1b	440	A2/F2	RVR		ongoing
A 740	f	24	3a	805551	A2/F3	RVR		ongoing
A 767	m	31	3a	282100	A3/F3	RVR		ongoing
A 789	m	34	4	173000	A2/F2			ongoing
A 809	f	41	1a	4652760	A2/F1			ongoing
A 515	f	54	3a	75644	A2/F4			ongoing
A 642	m	33	3a	1683442	A2/F1			ongoing
A 774	m	43	3a	51326	A3/F4			ongoing
A 658	m	57	1	10327448	A1/F1	-	-	No treatment
A 675	f	53	1	-	A3/F4	-	-	No treatment
A 701	m	27	1	13157175	A2/F2	-	-	No treatment
A 726	f	28	1	340000	A2/F2	-	-	No treatment
A 727	f	56	1	895473	A2/F2	-	-	No treatment
A 514	f	32	1a	460169	A2/F2	-	-	No treatment
A 531	m	39	1a	3427262	A1/F2	-	-	No treatment
A 532	m	55	1a	788024	A1/F1	-	-	No treatment
A 544.b	m	46	1a	1218968	A1/F1	-	-	No treatment
A 566	m	42	1a	3556921	A1/F1	-	-	No treatment
A 574	m	43	1a	792776	A1/F1	-	-	No treatment
A 586	m	46	1a	761368	A2/F2	-	-	No treatment
A 619	f	41	1a	4519497	A2/F1	-	-	No treatment
A 667	f	32	1a	259633	A1/F1	-	-	No treatment
A 698	m	35	1a	3378710	A1/F1	-	-	No treatment

Table S4d. Study patients' characteristics

A 725	m	48	1a	36108528	A1/F2	-	-	No treatment
A 735	m	35	1a	222771	A1/F1	-	-	No treatment
A 753	m	49	1a	-	A3/F4	-	-	No treatment
A 765	f	37	1a	2351514	A1/F1	-	-	No treatment
A 799	f	41	1a	14028196	A2/F2	-	-	No treatment
A 525	m	63	1b	117458	A1/F1	-	-	No treatment
A 549	m	69	1b	1810000	A2/F2	-	-	No treatment
A 551	m	46	1b	69000000	A1/F2	-	-	No treatment
A 559.b	f	39	1b	1350000000	A1/F1	-	-	No treatment
A 567	m	29	1b	384525	A2/F2	-	-	No treatment
A 577	f	40	1b	300359	A1/F1	-	-	No treatment
A 582	m	35	1b	17594	A1/F2	-	-	No treatment
A 687	f	69	1b	1686605	A1/F2	-	-	No treatment
A 694	m	68	1b	5652771	A3/F4	-	-	No treatment
A 705	m	44	1b	67587	A2/F4	-	-	No treatment
A 641	m	58	2b	4853209	A2/F3	-	-	No treatment
A 732	m	32	2	1144075	A2/F2	-	-	No treatment
A 564	m	31	3	759000	A2/F2	-	-	No treatment
A 469	m	26	3a	24626114	A1/F0	-	-	No treatment
A 500	m	36	3a	1480000	A1/F1	-	-	No treatment
A 524	m	47	3a	337115	A2/F4	-	-	No treatment
A 539	m	35	3a	1152145	A2/F2	-	-	No treatment
A 541	f	31	3a	961000	A1/F1	-	-	No treatment
A 548	m	60	3a	951896	A3/F4	-	-	No treatment
A 621	m	45	3a	134785	A2/F1	-	-	No treatment
A 638	m	50	3a	1274215	A1/F2	-	-	No treatment
A 650	f	44	3a	319000	A2/F2	-	-	No treatment
A 689	f	67	3a	265382	A3/F4	-	-	No treatment
A 768	m	36	3a	1140000	A3/F3	-	-	No treatment

Table S4e. Study patients' characteristics

A 485.b	m	42	4	191686	A1/F2	-	-	No treatment
A 622	f	48	4	88216	A1/F1	-	-	No treatment
A 734	m	34	4	521210	A2/F2	-	-	No treatment
A 744	m	52	4	585000	A3/F4	-	-	No treatment
A 757	m	39	4	104945	A1/F2	-	-	No treatment
A 804	m	45	4	321000	A2/F2	-	-	No treatment
A 656	m	51	4e	864372	A3/F4	-	-	No treatment

Table S5. Primer sequences used for real-time RT-PCR analysis

Gene	Primer 1 sequence	Primer 2 sequence
GAPDH	5' GTCCTCCTGTTGACAGTCA 3'	5' ACCTTCCCATGGTG TCTGA 3'
STAT1	5' TCCCA GGCCCTTGTTG 3'	5' CAAGCTGCTGAAGTTGGTACCA 3'
IP10	5' CGATTCTGATTTGCTGCCTTAT 3'	5' GCAGGTACAGCGTACGGTTCT 3'
USP18	5' CTC AGTCCCGACGTGGA 3'	5' ATCTCTCAAGCGCCATGCA 3'
IFI27	5' CCTCGGGCAGCCTTGTG 3'	5' AATCCGGAGATCCAGTTGCT 3'

4.2 Cardif cleavage in CHC and correlation with ISG induction

4.2.1 Cardif is cleaved in human HCV infected liver and cleavage occurs more often in patients infected with genotypes 2 and 3

The NS3-4A protease has been reported to target and inactivate Cardif *in vitro* (154). We assessed whether Cardif cleavage can be detected in the livers of patients infected with HCV. Liver whole cell extracts from 40 chronically infected HCV patients, 10 HBV patients and two controls (healthy liver tissue) were subjected to Western blot analysis. Representative examples for detection of full-length (FL) and cleaved Cardif are shown in *Figure 4.2.A*. The two bands correspond to Cardif FL (aa 1-540) and Cardif in the cleaved form (aa 1-508). As a control for Cardif FL, lysates from Huh7.5 cells that only contain uncleaved Cardif, and as a control for cleaved Cardif, lysates from the replicon cell line HCVrepBB7 (B-7; ref.(177)) were loaded on each gel. The 40 HCV samples showed a variable degree of Cardif cleavage: some samples had only FL, some samples only cleaved Cardif, and most samples had partial cleavage of Cardif. None of the 10 HBV patients and 2 controls showed Cardif cleavage (*Figure 4.2.A* and data not shown).

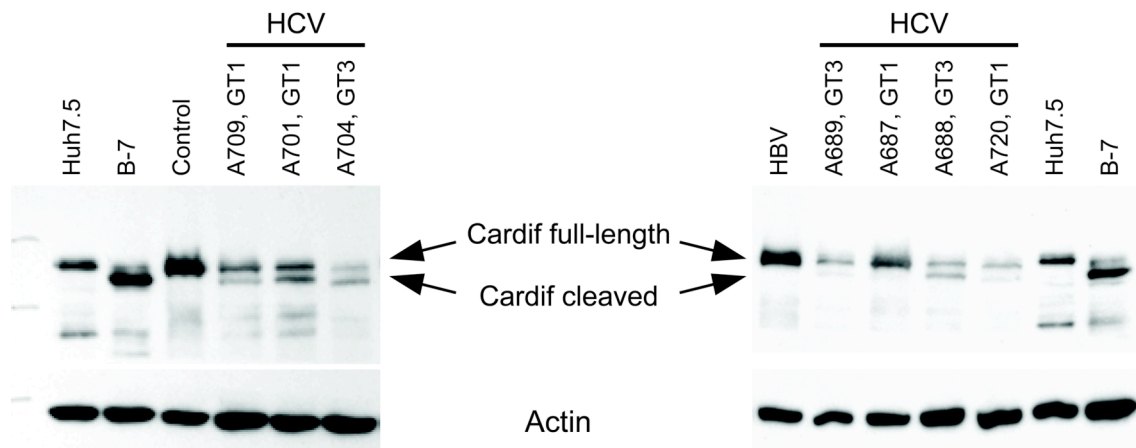


Figure 4.2.A. Levels of Cardif full-length and cleaved Cardif in human liver biopsies

Proteins from cells and liver biopsies were extracted using RIPA buffer (50mM Tris pH 8.0, 150mM NaCl, 1% NP40, 0.5 % DOC, 0.1% SDS, 1 mM sodium orthovanadate, 10 mM NaF and a cocktail of protease inhibitors). Cardif protein was assessed by Western blot. For Cardif detection, monoclonal antibody Adri-1 or polyclonal antibody AT107 (both gifts from Olivier Donzé, Apotech Corporation, Lausanne) were used at a 1:2500 dilution. As control, actin was detected using a monoclonal antibody AC15 from Sigma. Detection of the proteins was revealed by chemiluminescence using the ECL Advance Western Blotting Detection kit (Amersham Biosciences).

We then analyzed whether the different HCV genotypes have different abilities to cleave Cardif. As the cleaved form of Cardif often seems to be degraded and quantification of the cleaved form therefore is difficult, we assessed the amount of Cardif FL in the 40 HCV biopsy lysates and stratified the results into the “difficult-to-treat” GTs 1 and 4 versus the more treatment susceptible GTs 2 and 3. Interestingly, the amount of Cardif FL is higher in biopsies from patients with GTs 1 and 4 than GTs 2 and 3 (*Figure 4.2.B, left panel*). It is therefore very likely, that HCV GTs 2 and 3 are more successful in cleaving Cardif. As expected, there was also a statistically significant difference in the protein amount of Cardif FL between HCV and HBV samples. Importantly, Cardif mRNA amounts are not different between HCV GTs 1/4 and 2/3 (*Figure 4.2.B, right panel*). Moreover, healthy control samples had similar amounts of Cardif mRNA in the liver as HCV samples.

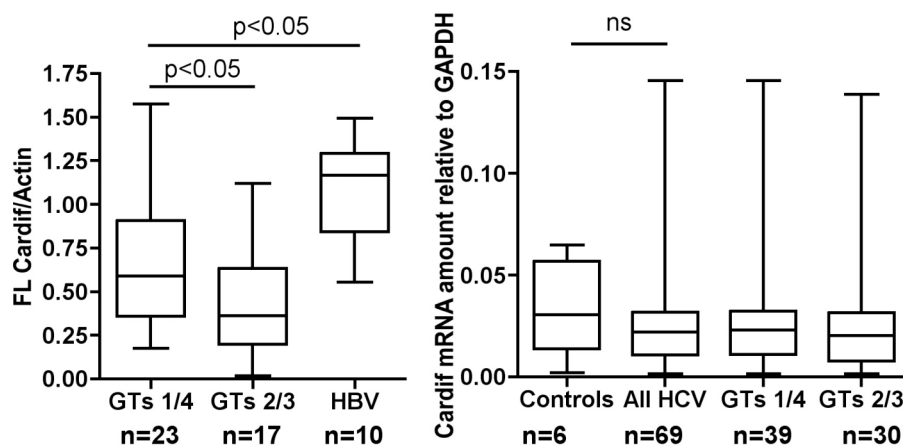


Figure 4.2.B. Quantification of Cardif full-length (FL) and Cardif mRNA according to HCV genotype

Left panel: Cardif FL protein was assessed by Western blot. Densitometric scanning was performed using an ImageScanner (Amersham Pharmacia Biotech). The bands corresponding to Cardif FL and actin were quantified with the ImageMaster TotalLab software (Amersham Pharmacia Biotech). Data expressed as Cardif FL correspond to densitometric value of the Cardif FL band divided by the densitometric value of actin. Depicted is the amount of FL Cardif in HCV (stratified into genotypes 1/4 versus 2/3) and HBV patients. Statistical analysis was performed using Mann-Whitney t-tests. The horizontal line in the box plot represents the median of the sample values. The lower and upper quartile is shown within the box below and above the line that represents the median. The lower whisker depicts the smallest observation, the upper whisker ends at the largest observation.

Right panel: Cardif mRNA expression in the liver was assessed in 69 HCV and 6 healthy control samples by RT-qPCR using the primers C212fd ACTTCATTGCGGCACTGAGG and C522rev TCTGGATTCCTTGGGATGGC. Statistical analysis was performed using Mann-Whitney t-test and revealed no significance (ns) between controls and HCV samples.

4.2.2 Expression of full-length Cardif correlates with ISG pre-activation in the liver

It is unknown whether the ISG activation status of chronic HCV patients (with future non-responders to treatment showing a pre-activated endogenous IFN system in the liver) is dependent on the viral sensory pathways and therefore also on Cardif function. We aimed to investigate whether there is a correlation between protein expression of Cardif FL in the HCV infected liver and the mRNA levels of known ISGs. Indeed, we observed that high protein levels of Cardif FL are often associated with high expression of ISG transcripts. An example of an ISG (IFI27) is shown in *Figure 4.2.C*. Some patients with high Cardif FL protein expression showed, however, no pre-activation of the endogenous IFN system, arguing that in these patients viral sensory pathways are affected at other levels, either upstream or downstream of Cardif.

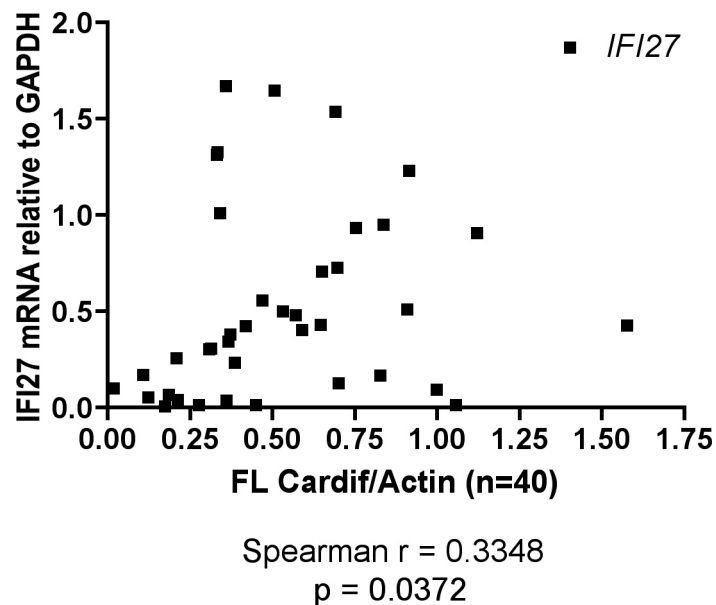


Figure 4.2.C. Correlation of Cardif FL protein with IFI27 mRNA expression in the liver

Cardif FL protein in 40 HCV liver biopsies was assessed by Western blot. Densitometric scanning was performed using an ImageScanner (Amersham Pharmacia Biotech). The bands corresponding to Cardif FL and actin were quantified with the ImageMaster TotalLab software (Amersham Pharmacia Biotech). IFI27 mRNA expression in the liver was assessed in the same 40 HCV liver biopsies by RT-qPCR. Nonparametric correlation analysis was performed and the Spearman correlation coefficient is $r=0.3348$.

4.2.3 Activation of STAT1 in hepatocytes correlates with levels of ISG mRNAs in the liver of patients with CHC

To elucidate whether the increase in ISG transcripts observed in HCV infected livers results from an activated Jak-STAT signaling pathway in hepatocytes, we assessed the levels of phosphorylated STAT1 (p-STAT1) by immunohistochemistry in a cohort of 80 HCV patients and 8 controls (healthy liver tissue). Nuclear p-STAT1 signal was quantified in hepatocytes and each biopsy sample was assigned to one of four categories (-, +, ++, +++; see *Figure 4.2.D* for details). There was a correlation of nuclear p-STAT1 staining in hepatocytes with the expression of ISGs in the liver (*Figure 4.2.D*).

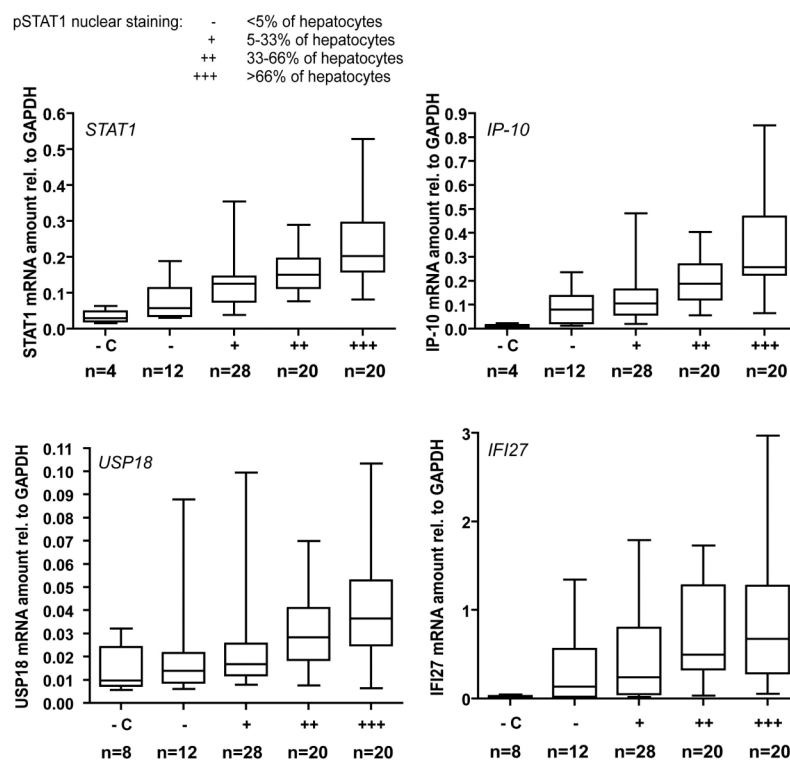


Figure 4.2.D. Quantification of p-STAT1 nuclear staining in hepatocytes of HCV patients and correlation to mRNA levels of four different ISGs (STAT1, IP-10/CXCL10, USP18, IFI27)

Standard indirect immunoperoxidase procedures were used for immunohistochemistry (ABC-Elite, Vectra Laboratories). 4-mm-thick sections were cut from paraffin blocks, rehydrated, pretreated (20' in ER2 solution) incubated with a monoclonal rabbit antibody against phospho-STAT1 (dilution 1:200, #9167 Cell Signaling) and counterstained with haematoxylin. The whole staining procedure (dehydration, pre-treatment, incubation, counterstaining and mounting) was performed with an automated stainer (Bond®, Vision BioSystems Europe, Newcastle-upon-Thyne, UK). The p-STAT1 signal

ISG mRNA expression in the liver was assessed in 80 HCV liver biopsies by RT-qPCR. The ISG expression levels were calculated relative to the expression of GAPDH as internal control.

4.3. Interferon alpha induces long-lasting refractoriness of Jak-STAT signaling in the mouse liver through induction of USP18/UBP43

Sarasin-Filipowicz M. et al.

Manuscript in preparation, 2008

	Page
- Abstract	74
- Introduction	75
- Materials and methods	78
- Results	82
- Discussion	87
- References	90
- Figures	93

Interferon alpha induces long-lasting refractoriness of Jak-STAT signaling in the mouse liver through induction of USP18/UBP43

Magdalena Sarasin-Filipowicz^{1,2}, Xueya Wang¹, Ming Yan³, Francois H.T. Duong¹, Valeria Poli⁴, Douglas J. Hilton⁵, Dong-Er Zhang³, Markus H. Heim^{1,2*}

¹Department of Biomedicine, University Basel, CH-4031 Basel, Switzerland, ²Division of Gastroenterology and Hepatology, University Hospital Basel, CH-4031 Basel, Switzerland, ³Moores UCSD Cancer Center, University of California San Diego, La Jolla, CA 92093, USA, ⁴Department of Genetics, Biology and Biochemistry, University of Turin, 10126 Turin, Italy, ⁵Division of Molecular Medicine, The Walter and Eliza Hall Institute of Medical Research, 1G Royal Parade, Parkville, Victoria 3050, Australia

Character Count: 29739 (without spaces)

Keywords: Interferon alpha, phosphorylated STAT1, refractoriness, UB43

Abbreviations: SOCS, suppressor of cytokine signaling; CHC, chronic hepatitis C; SVR, sustained virological response; pegIFN, pegylated interferon; ISG, interferon stimulated gene; IFNAR, interferon alpha receptor; IRGs, interferon regulated genes; ISRE, interferon stimulated response element; GAS, gamma-activated sequence; PIAS, protein inhibitor of activated STAT; USP18, ubiquitin specific peptidase 18; HCV, hepatitis C virus; EMSA, electrophoretic mobility shift assay.

M. Sarasin-Filipowicz and X.Wang contributed equally to this work.

Acknowledgements

The work was supported by Swiss National Science foundation grant 320000-116106 and Swiss Cancer League grant KLS-01832-02-2006, grant 8/05 from the Krebsliga Basel, and a grant from the Roche Research Foundation to M.S-F.

Abstract.

Recombinant interferon- α (IFN α) is used for the treatment of chronic viral hepatitis and some forms of cancer. During these therapies recombinant IFN α is injected once daily or every second day for several months. Recently, a long-acting form of IFN α , pegylated IFN α (pegIFN α) has replaced the standard IFN α in therapies of chronic hepatitis C because it is more effective, supposedly due to inducing a long-lasting activation of IFN signaling pathways. IFN signaling in cultured cells, however, becomes refractory within hours, and little is known about the pharmacodynamic effects of continuously high IFN α serum concentrations. To investigate the behaviour of the IFN system *in vivo*, we repeatedly injected mice with IFN α and analyzed its effects in the liver. Within hours after the first injection, IFN signaling became refractory to further stimulation for up to two days. An analysis of the negative regulators of IFN α signaling revealed that suppressor of cytokine signaling 1 (SOCS1) is rapidly upregulated after IFN α administration and is likely responsible for the early termination of IFN α signaling. For the longlasting refractoriness, neither SOCS1 nor SOCS3 appear to be instrumental. Rather, USP18/UBP43, an inhibitor of Jak1 that was recently found to be involved in the control of hepatitis C virus (HCV) and the responsiveness to pegIFN α treatment is the key mediator. Our results indicate that the current therapeutic practice using the long-lasting pegIFN α is not well adapted to the intrinsic properties of the IFN system and is not exploiting the full therapeutic potential of recombinant IFN α .

Introduction

Since their discovery in 1957, type I interferons (IFNs) have become valuable and widely used clinical drugs [1, 2]. IFN α is used in the treatment of chronic hepatitis B and hepatitis C and of some forms of cancer, whereas IFN β is effective for treating multiple sclerosis. With an estimated 3% of the global population affected, chronic hepatitis C (CHC) represents a major health concern since it can lead to liver cirrhosis and hepatocellular carcinoma [3]. Treatment of CHC with recombinant IFN α 2 injected 3 times a week achieved sustained virological responses (SVR) in 15-20% of patients. A major improvement of the SVR to 35-40% was observed by the addition of the broad-spectrum antiviral agent ribavirin [4]. The introduction of a pegylated, long-acting form of IFN α 2 (pegIFN α 2) further increased the SVR to 50-55% of patients [5, 6]. The reasons for the improved efficacy of pegIFN α are not known, but it is assumed that the constant high serum concentrations achieved with pegIFN α provide for un-interrupted anti-viral activity through a permanent stimulation of the IFN signaling pathways, whereas the serum concentrations of standard IFN α (with a elimination half-life of 4 to 10 h) decline below pharmacologically active levels in the second half of each 48 hour dosing interval [7, 8]. There is, however, no experimental evidence for the hypothesis that continuously high IFN α concentrations achieve a better activation of the IFN α induced antiviral effector systems. In fact, there is evidence against this hypothesis provided by cell culture experiments.

It has been known for many years that cultured cells become refractory to IFN within hours and remain unresponsive for up to 3 days [9]. Maximal activation of the IFN signaling pathways is observed within the first two hours of IFN treatment. Continuous exposure to IFN results in a “desensitization” characterized by a return to pretreatment levels of interferon stimulated gene (ISG) transcription. Moreover, during the 48 to 72 h following the initial IFN α stimulation of the cells, any further IFN treatment fails to reinduce the transcription of ISGs. Currently it is not known, whether refractoriness also occurs during IFN therapies in patients. Such knowledge would be important for a rational design of IFN therapies. Dosing intervals shorter than the period of refractoriness would strongly reduce the efficacy of the injected IFN. Likewise, use of modified IFN α with a prolonged serum half-life such as pegIFN α with the aim to achieve constant (peg)IFN α serum concentrations would not increase efficacy either, if the target cells remain unresponsive during most of the

dosing interval. Admittedly, the clinical experience showing an improved therapeutic response rate with pegIFN α argues against the occurrence of desensitization in patients. To investigate if the liver becomes refractory to IFN α *in vivo*, we investigated IFN α signaling in mice injected repeatedly with IFN α .

Type I IFNs (IFN α s and IFN β) exert their effects through the Jak-STAT signaling pathway [10]. Upon binding of IFN α to its cell surface receptor (IFNAR), the receptor-associated tyrosine kinases Jak1 and Tyk2 become activated and phosphorylate tyrosines on the cytoplasmic tails of IFNAR chains 1 and 2. The phosphorylated receptors provide specific docking sites for signal transducers and activators of transcription (STAT) 1, 2 and 3. STATs are activated at the receptor-kinase complex by tyrosine phosphorylation [11, 12]. Activated STATs dissociate from the receptor and translocate to the nucleus where they act as transcription factors binding to specific regions in the promoters of IFN regulated genes (IRGs) [13]. In response to IFN α , STAT1-STAT2 heterodimers combine with IRF9 to form the transcription complex ISGF3, which binds to IFN stimulated response elements (ISREs) within the promoters of IRGs [14]. IFN α also activates homo- and heterodimers of STAT1 and STAT3, which bind to gamma-activated sequence (GAS) response elements [15].

The activation of the Jak-STAT pathway is tightly controlled by several negative regulatory mechanisms. Suppressors of Cytokine Signaling (SOCS) 1 and 3 prevent STAT activation by inhibiting Jaks [16]. Further downstream, the protein inhibitor of activated STAT (PIAS) 1 binds to hypomethylated STAT dimers and inhibits STAT-DNA interaction [17-19]. STATs are deactivated by the nuclear phosphatase TC-PTP, followed by nuclear export [20]. Recently, ubiquitin specific peptidase 18 (USP18/UBP43) has been described as a negative regulator in type I IFN signaling. USP18/UBP43 was originally identified as a protease cleaving ubiquitin-like modifier ISG15 from target proteins, but recently found to play a negative regulatory role independently of its ISG-deconjugating ability [21, 22]. UBP43 was reported to inhibit the activation of Jak1 by interfering with its interaction with IFNAR2 [23]. UBP43 deficient mice show a severe phenotype characterized by brain cell injury, poly-I:C hypersensitivity, and premature death [24, 25]. Interestingly, they are resistant to otherwise fatal cerebral infections with lymphocytic choriomeningitis virus and vesicular stomatitis virus [26]. USP18/UBP43 is elevated in livers of future non-responders to pegIFN α therapy [27]. Moreover, USP18/UBP43 silencing in cells with a replicating

chimeric HCV genome results in deregulation of STAT1 signaling and potentiation of IFNs ability to inhibit HCV-RNA replication [28].

To investigate the sensitivity of the liver during prolonged exposure to therapeutic concentrations of IFN α , we treated mice repeatedly with subcutaneous injections of IFN α and prepared extracts from their livers at various time points. IFN α signaling was investigated by phospho-STAT Western blots, gel shifts and quantification of IFN α target gene induction. In this manuscript we report that liver cells *in vivo* become refractory within hours after the first injection of IFN α and remain so for at least 2 days. A systematic analysis of the negative regulators of IFN α signaling surprisingly revealed that SOCS are responsible for the early inhibition of STAT phosphorylation within the first 2-4 h, but not for the observed long-term refractoriness. Rather, a long lasting upregulation of USP18/UBP43 was found to be responsible for the observed unresponsiveness of liver cells to prolonged IFN α exposure. Strikingly, in the absence of USP18/UBP43, even a strong upregulation of SOCS1 did not prevent activation of STAT1 and STAT2, suggesting that SOCS1 inhibitory effects on IFN α signaling depend on USP18/UBP43.

Taken together, our results demonstrate a refractoriness of IFN α signaling *in vivo*, and indicate that USP18/UBP43 plays a crucial role in the observed long-term desensitization of this signal transduction pathway in the mouse liver. Our findings have implications for the treatment of patients with chronic hepatitis C. Strategies aimed at restoring sensitivity to IFN α , for example targeting the upregulation of USP18/UBP43 in liver cells, could increase the efficacy of IFN α therapies.

Materials and Methods

Animals.

C57/BL6 mice were obtained from BRL (Biological Research Laboratories, Füllinsdorf, Switzerland), IL-10 deficient mice and Alb-Cre (strain name: B6.Cg-Tg(Alb-cre)21Mgn/J) transgenic mice were obtained from Jackson Laboratory, Bar Harbor, Maine 04609 USA. STAT3^{lox/lox} mice and SOCS3^{lox/lox} mice were described previously [29, 30]. STAT3^{lox/lox} and SOCS3^{lox/lox} mice were crossed to Alb-Cre transgenic mice to generate AlbCre⁺STAT3^{lox/lox} and AlbCre⁺SOCS3^{lox/lox} conditional knockout mice, respectively. All transgenic mice were viable and fertile. AlbCre⁻STAT3^{lox/lox} and AlbCre⁻SOCS3^{lox/lox} littermates were used as negative controls in the experiments. The generation of UBP43^{-/-} mice on a FVB background was described previously [24, 31]. Genotyping for the Cre transgene was performed by PCR using the following nucleotides: Cre-1, 5'-CACCATTGCCCTGTTTCACTATC-3'; Cre-2, 5'-GCCAGGCGTTTTCTGAGCATAC-3'. Genotyping for the IL-10 deficient mice: IL10-1, 5'GCCTTCAGTATAAAAGGGGGA CC-3'; IL10-2, 5'-GTGGGTGCAGTTATTGTCTTC CCG-3'; IL10-Neo, 5'-AATCCA TCTTGTTCAATGGCCGATC-3'. STAT3^{lox/lox} genotyping was performed using the following primers: APRF 11 Up, 5'-CACCAACACATGCTA TTTGTAGG-3'; APRF 11 Down, 5'-CCTGTCTCTGACAGGCCATC-3'; APRF14 Down, 5'-GCAGCAGAATACTCTACA GCTC-3'. SOCS3^{lox/lox} genotyping was performed with: SR221, 5'-GAGTTTTCTCTGGGCGTCCTCCTAG-3' and SR222, 5'-TGGTACTCGCTT TTGGAGCTGAA-3'. The animals were maintained on a 12 h day and 12 h night schedule with *ad libitum* access to food and drinking water. Mice were bred in a specific pathogen-free environment. Procedures with the animals were conducted with the approval of the animal care committee of the Kanton Basel, Switzerland. All UBP43^{-/-} animals used in the studies were handled in accordance with guidelines of The Scripps Research Institute and procedures were approved by the Institutional Animal Care and Use Committee of the institute.

6 to 8 weeks old male animals were used for all experiments.

Animals were anaesthetized with isofluorane before blood drawing from tail vessels. The animals were euthanized by CO-narcosis. The resected liver lobes were immediately frozen in liquid nitrogen and kept at -70°C until further processing; one lobe of liver was frozen in Trizol for RNA isolation. The subcutaneous injections with PBS or mouse Interferon-alpha (mIFN α) were performed between 8.00 am and 5.00 pm. Recombinant mIFN α was purchased from CalBiochem (Juro Supply GmbH, Switzerland). PBS was from the

University Hospital Basel. Mouse IL-10 MAb was from Pierce (Perbio Science Switzerland SA, Lausanne) and was injected intraperitoneally at a dose of 100 μ g 30 min prior to mIFN α injections.

ELISA.

To isolate serum from mIFN α or PBS injected C57/BL6 mice, 20 to 30 μ l of blood from mouse tail was collected at different timepoints, kept 10 min at RT, 30 min at 4°C, then centrifuged at 2500 g for 20 min at 4°C. The supernatant was again spun at 1500 g for 10 minutes at 4°C. For measurement of mIFN α , the serum was diluted 1:100 in dilution buffer and ELISA was performed using Mouse Interferon ELISA Kit (PIERCE, Perbio Science Switzerland SA, Lausanne) according to manufacturer's instructions.

For Measurement of mIL-10, the serum was diluted 1:4 in dilution buffer and ELISA was performed using the Quantakine Mouse IL-10 Immunoassay from R&D Systems Inc., 14 McKinley Place NE, Minneapolis, MN 55413 according to manufacturer's instructions.

Protein preparation and Western Blot Analysis.

30 to 50 mg of liver tissue were homogenized in a buffer containing 100 mM NaCl, 50 mM Tris pH 7.5, 1 mM EDTA, 0.1 % TX-100, 10 mM NaF, 1 mM PMSF, 1 mM Vanadate and 1x Protease inhibitor cocktail tablets (Roche Diagnostics GmbH, Mannheim, Germany). Samples were kept at 4°C for 30 and centrifuged for 5 min at 15000 rpm at 4°C. Protein concentration was determined using Lowry (BioRad Protein Assay, Bio-Rad Laboratories AG, Reinach, Switzerland).

10-20 μ g of total protein from mouse liver lysates was loaded for SDS-PAGE and transferred onto a nitrocellulose membrane (Schleicher & Schuell, Switzerland). The membranes were blocked in 3% BSA/milk-0.1% Triton X-100 for 1 h, washed with Tris-buffered saline Tween-20 (TBST), and incubated with the primary antibody overnight at 4°C.

Proteins were detected with primary antibodies specific to phospho-Stat1 (Tyr 701) (#9171), phospho-Stat3 (Tyr 705) (#9131, Cell Signalling, Bioconcept, Allschwil, Switzerland) and phospho-Stat2 (Tyr 689) (#07-224, Upstate, Lake Placid, NY). Stat1 p84/p91 (sc-346), Stat2 (sc-950) and Stat3 (sc-482) were purchased from Santa Cruz (LabForce AG, Nunningen, Switzerland). Mouse monoclonal STAT1-ab (carboxy-terminus; #610186) was from Transduction Laboratories, BD Biosciences, Pharmingen. Anti-SOCS-1 (ab3691) was purchased from Abcam, Cambridge, UK. Anti- β -Actin was from Sigma, Sigma-Aldrich

Chemie GmbH, Steinheim, Germany. Blot-FastStain was obtained from Geno Technology, Inc. (Cell Concepts GmbH, Umkirch, Germany).

After 3 washes with TBST, membranes were incubated with Anti-rabbit antibody-HRP and anti-mouse antibody-HRP obtained from Cell Signaling (Bioconcept, Allschwil, Switzerland) and signals were detected with SuperSignal West Pico Chemiluminescent Substrate (PIERCE, Perbio Science Switzerland SA, Lausanne, Switzerland). Alternatively, signals were detected using the Odyssey Infrared Imaging System from LI-COR after incubation with infrared fluorescent secondary goat anti-mouse (IRDye 680) or anti-rabbit (IRDye 800) antibodies (both from LI-COR Biosciences) for 1 h at room temperature. The infrared image was obtained in a single scan and the signal was quantified using the integrated intensity.

EMSA.

Nuclear extracts from 150 - 200 mg liver tissue were prepared as previously described [32]. 2 μ l of nuclear extract (= 5 to 10 ng protein sample) aliquots were incubated with a ³²P-radiolabeled mutated serum-inducible element oligonucleotide designated m67-hSIE with the sequence 5'-CATTTCCTCCGTAATCAT-3' for STAT1 and STAT3 or the interferon stimulated response element (ISRE) probe derived from the interferon stimulated gene 15 promoter (ISRE-015) with the sequence 5'- GAAAGGGAAACCGAACTGAAGC-3' [33]. For supershift experiments, 1 μ l of antibody specific for STAT1, STAT2 or STAT3 was added to the gel shift incubation reactions.

The samples were loaded on a 5% non-denaturing polyacrylamide gel and electrophoresis was performed for 4 h at 400 V at 4°C. The gel was dried and visualized by autoradiography.

RNA Isolation and Northern Blot Analysis.

RNA was purified using Trizol (Tri Reagent) provided by Molecular Research Center, Inc, (Lucerna Chem AG, Lucerne, Switzerland). RNA was aliquoted and stored at -75°C. The denatured RNA was separated on a 1.2% Agarose Formaldehyde MOPS gel and transferred to a Hybond-N+ Nylon membrane (Amersham Pharmacia Biotech Europe GmbH, Dübendorf, Switzerland) by capillary diffusion using 20x SSC buffer. The membranes were hybridized to ³²P labeled SOCS1 and SOCS3 probes at 65°C for overnight in the Quickhyb oven (Stratagene Europe, Switzerland) and washed twice with 2x SSC, 0.2% SDS at 42°C for 15 min, then twice with 0.2x SSC, 0.1% SDS at 42°C for 10 min. Results were visualized by autoradiography.

Real-time RT-qPCR.

RNA was purified from frozen liver tissue (< 20 mg) with Nucleo Spin RNA II kit (Macherey-Nagel, Düren, Germany) according to manufacturer's instructions. RNA was stored at -75°C. RNA was reverse transcribed by Moloney murine leukemia virus reverse transcriptase (Promega Biosciences, Inc., Wallisellen, Switzerland) in the presence of random hexamers (Promega) and deoxynucleoside triphosphate. The reaction mixture was incubated for 5 min at 70°C and then for 1 h at 37°C. The reaction was stopped by heating at 95°C. SYBR-PCR was performed based on SYBR green fluorescence (SYBR green PCR master mix; Applied Biosystems, Foster City, CA). The Δ CT value was derived by subtracting the threshold cycle (CT) value for mouse ribosomal protein L19 (mRPL19), which served as internal control, from the CT values for SOCS1, SOCS3, and USP18. Primers were designed across exon-intron junctions to prevent influence from genomic DNA amplification. Primers for mRPL19 were ATCCGCAAGCCT GTGACTGT and TCGGGCCAGGGTGTTTTT, for mSOCS1 GTGGTTGTGGAGGGTGAG ATG and GGGATGAGGTCTCCAGCCA, for mSOCS3 were CCTTTCTTATCCGCGACAGC and CGCTCAACGTGAAGAAGTGG, for USP18 were CGTGCTTGAGAGGGTCATTTG and GGTCCGGAGTCCACAACCTTC. All reactions were run in duplicate using the ABI 7000 Sequence Detection System (Applied Biosystems). mRNA expression level between T0 and Tn was expressed as a fold increase according to the formula $2^{\Delta\text{CT}(T0)-\Delta\text{CT}(Tn)}$. mRNA expression levels of transcripts were calculated relative to GAPDH from the Δ CT values using the formula $2^{-\Delta\text{CT}}$.

Results.

Pharmacokinetics of mouse IFN α

We first studied the pharmacokinetics of subcutaneously administered mIFN α by measuring the serum concentration in mice at different time points after injection. A single dose of 1000 IU/g body weight resulted in a fast increase to 10000 to 12000 pg/ml in 60 min followed by a decline to pretreatment levels 8 h after the injection (Figure 1A). The serum concentration half-life was 4-5 h. To achieve constantly elevated serum concentrations as obtained by pegylated human IFN α , we then used a priming dose of 1000 IU/g body weight mIFN α followed by repeated injections of 300 IU/g body weight to obtain IFN α serum concentrations between 6000 and 10000 pg/ml for up to 16 h (Figure 1B).

IFN α signaling in the mouse liver

To study the IFN α induced activation of the Jak-STAT pathway and its termination by negative regulators we sacrificed mice at different time points after mIFN α injections and analyzed the activation of pathway components in liver extracts. To simulate the clinical setting of treatment of patients with chronic hepatitis C with standard IFN α , where IFN α serum concentrations decline below pharmacologically active levels in the second half of each 48 h dosing interval [7, 8], mice were given a second injection of mIFN α 8 h after the first injection, when serum concentrations were again at baseline levels (Figure 2A). After the first injection, a strong phosphorylation of STAT1 was observed within 30 minutes. STAT1 activation reached its maximum after 1 to 2 h, and then declined within 4 h after the initial injection (Figure 3A). Surprisingly, the second injection at time point 8 h induced very little STAT1 phosphorylation, although the amount of STAT1 in the liver was strongly induced by the first IFN α injection (Figure 3A). Moreover, in a long-term experiment with 7 injections given every 8 h, we did not observe restoration of IFN α sensitivity for up to 48 h (data not shown). To control for circadian variations and stress, a number of mice were injected at the same time points with PBS (left panel of Figure 3A). Indeed, there was a variation of STAT1 expression during the 16 h of the experiment, but mIFN α induced much higher expression levels. As expected, no STAT1 phosphorylation was induced by PBS.

Treatment with mIFN α also resulted in STAT3 phosphorylation in liver cells. The maximal activation occurred at 2 h and, contrary to STAT1, the activation pattern was similar after the second injection. There was no upregulation of STAT3 expression after mIFN α

treatment (Fig 3A).

These results were confirmed by electrophoretic mobility shift assay (EMSA). Phosphorylated STATs form dimers that can translocate into the nucleus and bind specific response elements such as the GAS element. The first injection of mIFN α induced a strong STAT1 homodimer gel shift using the m67-SIE oligonucleotide (a GAS element), whereas the second injection had little effect (Figure 3B). On the other hand, STAT3 homodimers were strongly induced after both the first and the second injection. IFN α also induces ISGF3, a heterotrimeric transcription factor composed of activated STAT1 and STAT2, and IRF9. ISGF3 activity was also induced only after the first, but not after the second injection of mIFN α (Figure 3C).

Taken together, these data indicate that IFN α induced Jak-STAT signaling in the mouse liver is transient and furthermore refractory to a second IFN α dose applied 8 h later, at a time point when serum concentrations of IFN α have returned to pretreatment levels.

We hypothesized that this surprisingly long-lasting refractoriness of the signal transduction pathway could be a reason why anti-HCV therapies with standard IFN α had limited success, because the IFN α injected 48 h after the previous dose could encounter a still refractory signal transduction system. Since pegylated IFN α s with their long half-life are more potent, we next analyzed if the continuous presence of high serum concentrations of IFN α could prevent the induction of refractoriness.

Since pegylated mouse IFN α is not available, mice were injected with 1000 IU/g of mIFN α as a priming dose, followed by four injections of 300 IU/g of mIFN α as maintenance doses. With this regimen, steady concentrations of 6000-10000 pg/ml were maintained for up to 16 h mimicking the pharmacokinetics of pegIFN α in patients (Figure 1B). Again, mice were sacrificed at different time points (Figure 2B) and IFN α signaling was analyzed with Western blots and EMSAs. There was strong but transient phosphorylation of STAT1 and STAT2 in the first 2 h after initial injection of mIFN α , but subsequent injections failed to induce further STAT1 phosphorylation, although STAT1 expression was highly upregulated (Figure 4A). Accordingly, the ISGF3 gel shift signal was only detectable at time point 1 hour after the initial injection (Figure 4B). Contrary to STAT1 and STAT2, activation of STAT3 was prolonged in continuous presence of mIFN α (Figure 4A).

In conclusion, IFN α treatment of mice induces a strong initial activation of signaling in the liver followed by a rapid inhibition of STAT1 and STAT2 activation and a persistent refractoriness even in the continuous presence of IFN α .

Negative regulation of IFN α signaling by SOCS1 and SOCS3 in the mouse liver

Within hours, IFN α induces the transcriptional upregulation of SOCS1 and SOCS3, two negative regulators of the Jak-STAT pathway that are instrumental for the termination of STAT phosphorylation at the receptor-kinase complex [16]. We therefore tested if the long-term refractoriness of the IFN signal transduction system in mouse liver would be due to a continuous high-level expression of SOCS proteins. SOCS1 mRNA was detectable after 1 h until 3 h, but not during the later time points despite the continuously high serum concentrations of mIFN α (Figure 4C). SOCS1 protein was upregulated after 3 h, but was barely detectable at later time points (Figure 4D). Induction of SOCS3 showed a different pattern. In continuous presence of high mIFN α levels, SOCS3 mRNA expression was induced after 1 hour and remained high during the entire 16 h (Figure 4C). The observed SOCS3 upregulation could be caused by the prolonged STAT3 activation, because STAT3 is a transcriptional inducer of the SOCS3 gene [34]. And since SOCS3 is known to inhibit IFN α induced STAT1 phosphorylation [35], the prolonged *in vivo* refractoriness of the IFN system could indeed be due to the observed SOCS3 induction.

The role of IL-10, STAT3 and SOCS3 in long-term refractoriness of IFN α signal transduction

Because the IFN α receptor-kinase complex is inhibited by SOCS3, the signals that maintain high SOCS3 expression cannot be transmitted through the IFN receptor, but have to be derived from a cytokine receptor that is not inhibited by SOCS3. IL-10 was an attractive candidate, because it is a strong activator of STAT3 and inducer of SOCS3, and, importantly, the IL-10 receptor is not inhibited by SOCS3 [36]. We therefore measured mIL-10 serum levels upon a single injection of mIFN α (Figure 5A, upper panel) or in response to multiple injections of mIFN α (Figure 5A, lower panel) and indeed found strong induction of IL-10. After a single mIFN α injection, the IL-10 serum concentrations were transiently elevated, but in the setting of multiple injections with the resulting constantly elevated serum IFN α concentration, IL-10 levels remained high. Apparently, the IFN α induced pathways that stimulate IL-10 expression do not become refractory.

To clarify the role of IL-10 in the observed refractoriness of IFN α signaling, we used IL-10 deficient mice and injected them with two doses of mIFN α given 8 h apart. STAT1 activation in these mice was assessed one hour after the first (time 1h) and one hour after the

second injection (time 9h) (Figure 5B). Contrary to our expectations, the IFN α signal transduction became refractory in the IL-10 deficient mice as well. While the first mIFN α injection induced a strong phospho-STAT1 signal after one hour, the second injection 8 h later had little effect on STAT1 phosphorylation (time point 9h) both in the wildtype and the IL-10 deficient mice (Figure 5B). The same results were observed when wildtype mice were injected with neutralizing IL-10 antibodies 30 minutes before the mIFN α injections (data not shown). Of note, there was no decrease of STAT3 phosphorylation in the IL-10 deficient mice. We conclude that the elevated serum IL-10 concentrations induced by mIFN α injections are not necessary for the prolonged activation of STAT3 and the induction of a refractory state.

We then used hepatocyte specific STAT3 and SOCS3 deficient mice to test if the activation of STAT3 or the upregulation of SOCS3 is required for the induction of the refractory state. To that aim, we crossed STAT3^{lox/lox} mice [29] and SOCS3^{lox/lox} mice [30] with albumin-Cre transgenic mice [37]. The refractoriness of the IFN α signal transduction pathway was then assessed in these mice during repeated mIFN α injections. Neither the deletion of STAT3 nor SOCS3 could restore responsiveness to the second injection of mIFN α (Figure 5C), disproving the hypothesis that STAT3 and SOCS3 are mediators of IFN α refractoriness.

Prolonged upregulation of USP18/UBP43 is responsible for IFN α refractoriness

Recently USP18/UBP43 emerged as an important negative regulator in type I IFN signaling [21-23, 28]. We therefore measured USP18 mRNA levels in the liver of wildtype, IL-10 deficient, and hepatocyte specific STAT3 and SOCS3 deficient mice after injections of mIFN α . In all these mice, USP18 mRNA was strongly induced one hour after the first injection, and also 1 hour after the second injection (time point 9h) (Figure 6A). In the setting of repeated injections (Figure 2B) with constantly elevated serum IFN α concentrations, USP18 mRNA was upregulated one hour after the first injection, and then stayed more than 5 fold induced at all later time points for up to 16 h (data not shown). This expression profile would be consistent with an important role of USP18/UBP43 for the induction and maintenance of a refractory state of the IFN α signaling pathway in the liver.

We therefore assessed IFN α signaling in UBP43 deficient mice [24, 25]. After the first injection of mIFN α , UBP43^{-/-} mice showed an even stronger STAT1 phosphorylation in

the liver than the wildtype controls (Figure 6B and 6C). More importantly, UBP43^{-/-} mice were responsive to the second injection of mIFN α . At time point 9h, one hour after the second injection, the phospho-STAT1 and phospho-STAT2 signals were as strong as those found in wildtype mice one hour after the first injection (Figure 6B and 6C). Moreover, the phospho-STAT1 signals at 9h were stronger than those found at time points 4h and 8h after the first injection, demonstrating a stimulatory effect of the second mIFN α dose. We conclude that USP18/UBP43 is required for the induction of IFN α refractoriness in the liver of mice.

Finally, we assessed SOCS1 expression in wildtype and UBP43 deficient mice. Compared to wildtype mice, SOCS1 mRNA was hyper-induced in UBP43^{-/-} mice one hour after the first mIFN α injection, and at time point 9h, when SOCS1 mRNA was no longer induced in wildtype mice, it was even further induced in UBP43^{-/-} mice (Figure 6D). This finding is important, because at time point 9h all IFN α stimulated STATs showed a strong phosphorylation (Figure 6B). We therefore conclude that in the absence of USP18/UBP43, SOCS1 cannot inhibit IFN α induced phosphorylation and activation of STAT1, STAT2 and STAT3.

Discussion

Desensitization of the IFN signal transduction pathways during prolonged exposure of cultured cells to IFN α has been described more than 20 years ago [9], but very little was known if and to what extent IFN refractoriness occurs in animals and humans. Infections that activate the endogenous type I IFN system usually last for several days and weeks, and even years, as for example chronic viral hepatitis. Intuitively, one would assume that the IFN system remains sensitive and effective in at least all those situations where the infection is finally cleared. In the present work, however, we present strong evidence that the IFN α signaling pathways in mouse liver become unresponsive within hours after the first application of mIFN α and remain so for at least two days. Refractoriness was observed in mice that received multiple injections and had sustained IFN α serum concentrations between 6000 and 10000 pg/ml, i.e. concentrations that induce a strong STAT1 activation before the initiation of the refractory state (see 30 minutes time points in Figures 1A and 3A). Refractoriness was also observed in mice that received a second injection after 8 h, thus at a time when IFN α serum concentrations were again at pretreatment levels. The refractory state was characterized by an almost complete inhibition of tyrosine phosphorylation of STAT1 and STAT2. The residual STAT1 and STAT2 activation documented by the faint phospho-STAT1 and -STAT2 signals detected in Western blots did not induce target genes such as SOCS1, possibly also because the IFN α induced increase of total STAT1 and, to a lesser extent, also STAT2 protein amount further reduced the ratio of phosphorylated to unphosphorylated STATs. The induction pattern of SOCS1 is consistent with its well-known role in the early negative feedback regulation of IFN α signaling. Since SOCS1 is not expressed to any detectable degree at later timepoints (Figure 4C and 4D), SOCS1 clearly can not be responsible for the long-lasting inhibition of STAT1 and STAT2 phosphorylation.

STAT3 can be activated by IFN α to form transcriptionally active homodimers or STAT1-STAT3 heterodimers [38]. Interestingly, STAT3 showed an activation pattern that differed from STAT1 and STAT2. STAT3 was maximally phosphorylated after 1 hour, and remained activated during the entire time course of the multiple injection experiment (Figure 4A). Accordingly, SOCS3, a known target gene of STAT3, was also upregulated during the entire experiment (Figure 4C). However, if we assume that SOCS3 inhibits IFN α signaling in the mouse liver in the same way as has been reported in cells [35], then the continuous activation of STAT3 could not be due to IFN α signals. Instead, additional cytokine signals

would have to stimulate STAT3 activation. Interleukin-10 was an attractive candidate, because it is a strong activator of STAT3 but its receptor-kinase complex is not inhibited by SOCS3 [36]. Furthermore, IL-10 inhibits expression of IFN α induced genes in monocytes by suppressing STAT1 phosphorylation [39] and attenuates IFN α induced STAT1 phosphorylation in the mouse liver [40]. However, the induction of a refractory state in IL-10 deficient mice proves that IL-10 is not necessary for IFN α refractoriness (Figure 5B). Likewise, liver specific STAT3 and SOCS3 deficient mice were still refractory to prolonged IFN α stimulation (Figure 5C), a finding that further disproves an important role of the STAT3-SOCS3 axis for the induction of IFN α refractoriness.

USP18/UBP43 blocks Jak1 phosphorylation through a specific interaction with the IFNAR2 subunit of the receptor and thereby attenuates IFN signaling [23]. USP18/UBP43 is induced by IFN α [41, 42] and provides a negative feedback loop that restricts IFN α signals. In the liver, USP18/UBP43 shows a low constitutive expression [21], but we found a strong upregulation after treating mice with subcutaneous injections of mIFN α (Figure 6A). Contrary to SOCS1 with its transient upregulation after the first injection of mIFN α (Figure 4C), USP18/UBP43 was still highly induced 1 hour after a second injection of mIFN α (Figure 6A). Since the apparent half-life of USP18 mRNA is 3-4 h [43], this prolonged upregulation of USP18 was probably caused by the weak STAT1 activity observed after the second injection of mIFN α . Whatever the mechanism that maintains its prolonged upregulation, USP18/UBP43 is clearly important for the induction of IFN refractoriness, because no such desensitization to mIFN α was observed in USP18/UBP43 deficient mice (Figure 6B).

USP18/UBP43 restricts the IFN β induced upregulation of more than 700 genes, amongst them SOCS1 [44]. Indeed, SOCS1 was highly expressed in the liver of UB43^{-/-} mice injected with mIFN α (Figure 6D). Interestingly, in UB43^{-/-} mice SOCS1 expression was further increased after the second injection of mIFN α . Despite the very high expression of SOCS1 at the time point 9 h, the second injection of mIFN α induced a strong phosphorylation of STAT1 in UB43^{-/-} mice. This surprising result provides strong genetic evidence that the inhibitory activity of SOCS1 requires the presence of USP18/UBP43.

Our results have potentially important consequences for the treatment of patients with chronic viral hepatitis with recombinant IFN α . If we assume that the human liver also becomes refractory to IFN α within hours after the first injection of recombinant IFN α and that the liver cells remain unresponsive to further IFN α stimulation, then the current practice

of injecting pegylated IFN α (pegIFN α) with its very long half-life would lack a pharmacodynamic rationale, because during most of the dosing interval pegIFN α would not have any effect on its prime target cells, the HCV infected hepatocytes, but could still have unwanted secondary effects in other organ systems such as the central nervous system, the skin, the muscles and the joints. Clearly, the mechanisms underlying the increased efficacy of pegIFN α compared to standard IFN α remain unsolved. The results presented here should therefore motivate an in-depth analysis of the pharmacodynamic effects of the current pegIFN α treatments in the livers of patients with chronic hepatitis C.

References

1. Isaacs A, Lindenmann J. Virus interference. I. The interferon. *Proc R Soc Lond B Biol Sci* 1957;147:258-267.
2. Friedman RM. Clinical uses of interferons. *Br J Clin Pharmacol* 2008;65:158-162.
3. Lauer GM, Walker BD. Hepatitis C virus infection. *N Engl J Med* 2001;345:41-52.
4. McHutchison JG, Gordon SC, Schiff ER, Shiffman ML, Lee WM, Rustgi VK, Goodman ZD, et al. Interferon alfa-2b alone or in combination with ribavirin as initial treatment for chronic hepatitis C. Hepatitis Interventional Therapy Group. *N Engl J Med* 1998;339:1485-1492.
5. Fried MW, Shiffman ML, Reddy KR, Smith C, Marinos G, Goncales FL, Jr., Haussinger D, et al. Peginterferon alfa-2a plus ribavirin for chronic hepatitis C virus infection. *N Engl J Med* 2002;347:975-982.
6. Manns MP, McHutchison JG, Gordon SC, Rustgi VK, Shiffman M, Reindollar R, Goodman ZD, et al. Peginterferon alfa-2b plus ribavirin compared with interferon alfa-2b plus ribavirin for initial treatment of chronic hepatitis C: a randomised trial. *Lancet* 2001;358:958-965.
7. Barouki FM, Witter FR, Griffin DE, Nadler PI, Woods A, Wood DL, Lietman PS. Time course of interferon levels, antiviral state, 2',5'-oligoadenylate synthetase and side effects in healthy men. *J Interferon Res* 1987;7:29-39.
8. Wills RJ. Clinical pharmacokinetics of interferons. *Clin Pharmacokinet* 1990;19:390-399.
9. Larner AC, Chaudhuri A, Darnell JE, Jr. Transcriptional induction by interferon. New protein(s) determine the extent and length of the induction. *J Biol Chem* 1986;261:453-459.
10. Darnell JE, Jr., Kerr IM, Stark GR. Jak-STAT pathways and transcriptional activation in response to IFNs and other extracellular signaling proteins. *Science* 1994;264:1415-1421.
11. Shuai K, Stark GR, Kerr IM, Darnell JE, Jr. A single phosphotyrosine residue of Stat91 required for gene activation by interferon-gamma. *Science* 1993;261:1744-1746.
12. Heim MH, Kerr IM, Stark GR, Darnell JE, Jr. Contribution of STAT SH2 groups to specific interferon signaling by the Jak-STAT pathway. *Science* 1995;267:1347-1349.
13. Horvath CM. STAT proteins and transcriptional responses to extracellular signals. *Trends Biochem Sci* 2000;25:496-502.
14. Heim MH. The Jak-STAT pathway: cytokine signalling from the receptor to the nucleus. *J Recept Signal Transduct Res* 1999;19:75-120.
15. Darnell JE, Jr. STATs and gene regulation. *Science* 1997;277:1630-1635.
16. Krebs DL, Hilton DJ. SOCS proteins: negative regulators of cytokine signaling. *Stem Cells* 2001;19:378-387.
17. Liu B, Liao J, Rao X, Kushner SA, Chung CD, Chang DD, Shuai K. Inhibition of Stat1-mediated gene activation by PIAS1. *Proc Natl Acad Sci U S A* 1998;95:10626-10631.
18. Shuai K. Modulation of STAT signaling by STAT-interacting proteins. *Oncogene* 2000;19:2638-2644.
19. Mowen KA, Tang J, Zhu W, Schurter BT, Shuai K, Herschman HR, David M. Arginine methylation of STAT1 modulates IFN α /beta-induced transcription. *Cell* 2001;104:731-741.

20. *ten Hoeve J, de Jesus Ibarra-Sanchez M, Fu Y, Zhu W, Tremblay M, David M, Shuai K. Identification of a nuclear Stat1 protein tyrosine phosphatase. Mol Cell Biol 2002;22:5662-5668.*
21. *Liu LQ, Ilaria R, Jr., Kingsley PD, Iwama A, van Etten RA, Palis J, Zhang DE. A novel ubiquitin-specific protease, UBP43, cloned from leukemia fusion protein AML1-ETO-expressing mice, functions in hematopoietic cell differentiation. Mol Cell Biol 1999;19:3029-3038.*
22. *Malakhov MP, Malakhova OA, Kim KI, Ritchie KJ, Zhang DE. UBP43 (USP18) specifically removes ISG15 from conjugated proteins. J Biol Chem 2002;277:9976-9981.*
23. *Malakhova OA, Kim KI, Luo JK, Zou W, Kumar KG, Fuchs SY, Shuai K, et al. UBP43 is a novel regulator of interferon signaling independent of its ISG15 isopeptidase activity. Embo J 2006;25:2358-2367.*
24. *Ritchie KJ, Malakhov MP, Hetherington CJ, Zhou L, Little MT, Malakhova OA, Sipe JC, et al. Dysregulation of protein modification by ISG15 results in brain cell injury. Genes Dev 2002;16:2207-2212.*
25. *Malakhova OA, Yan M, Malakhov MP, Yuan Y, Ritchie KJ, Kim KI, Peterson LF, et al. Protein ISGylation modulates the JAK-STAT signaling pathway. Genes Dev 2003;17:455-460.*
26. *Ritchie KJ, Hahn CS, Kim KI, Yan M, Rosario D, Li L, de la Torre JC, et al. Role of ISG15 protease UBP43 (USP18) in innate immunity to viral infection. Nat Med 2004;10:1374-1378.*
27. *Chen L, Borozan I, Feld J, Sun J, Tannis LL, Coltescu C, Heathcote J, et al. Hepatic gene expression discriminates responders and nonresponders in treatment of chronic hepatitis C viral infection. Gastroenterology 2005;128:1437-1444.*
28. *Randall G, Chen L, Panis M, Fischer AK, Lindenbach BD, Sun J, Heathcote J, et al. Silencing of USP18 potentiates the antiviral activity of interferon against hepatitis C virus infection. Gastroenterology 2006;131:1584-1591.*
29. *Alonzi T, Maritano D, Gorgoni B, Rizzuto G, Libert C, Poli V. Essential role of STAT3 in the control of the acute-phase response as revealed by inducible gene inactivation [correction of activation] in the liver. Mol Cell Biol 2001;21:1621-1632.*
30. *Crocker BA, Krebs DL, Zhang JG, Wormald S, Willson TA, Stanley EG, Robb L, et al. SOCS3 negatively regulates IL-6 signaling in vivo. Nat Immunol 2003;4:540-545.*
31. *Kim KI, Yan M, Malakhova O, Luo JK, Shen MF, Zou W, de la Torre JC, et al. Ube1L and protein ISGylation are not essential for alpha/beta interferon signaling. Mol Cell Biol 2006;26:472-479.*
32. *Heim MH, Gamboni G, Beglinger C, Gyr K. Specific activation of AP-1 but not Stat3 in regenerating liver in mice. Eur J Clin Invest 1997;27:948-955.*
33. *Heim MH, Moradpour D, Blum HE. Expression of hepatitis C virus proteins inhibits signal transduction through the Jak-STAT pathway. J Virol 1999;73:8469-8475.*
34. *Auernhammer CJ, Bousquet C, Melmed S. Autoregulation of pituitary corticotroph SOCS-3 expression: characterization of the murine SOCS-3 promoter. Proc Natl Acad Sci U S A 1999;96:6964-6969.*
35. *Song MM, Shuai K. The suppressor of cytokine signaling (SOCS) 1 and SOCS3 but not SOCS2 proteins inhibit interferon-mediated antiviral and antiproliferative activities. J Biol Chem 1998;273:35056-35062.*
36. *Yasukawa H, Ohishi M, Mori H, Murakami M, Chinen T, Aki D, Hanada T, et al. IL-6 induces an anti-inflammatory response in the absence of SOCS3 in macrophages. Nat Immunol 2003;4:551-556.*

37. Postic C, Shiota M, Niswender KD, Jetton TL, Chen Y, Moates JM, Shelton KD, et al. Dual roles for glucokinase in glucose homeostasis as determined by liver and pancreatic beta cell-specific gene knock-outs using Cre recombinase. *J Biol Chem* 1999;274:305-315.
38. Heim MH. Intracellular signalling and antiviral effects of interferons. *Dig Liver Dis* 2000;32:257-263.
39. Ito S, Ansari P, Sakatsume M, Dickensheets H, Vazquez N, Donnelly RP, Larner AC, et al. Interleukin-10 inhibits expression of both interferon alpha- and interferon gamma- induced genes by suppressing tyrosine phosphorylation of STAT1. *Blood* 1999;93:1456-1463.
40. Shen X, Hong F, Nguyen VA, Gao B. IL-10 attenuates IFN-alpha-activated STAT1 in the liver: involvement of SOCS2 and SOCS3. *FEBS Lett* 2000;480:132-136.
41. Der SD, Zhou A, Williams BR, Silverman RH. Identification of genes differentially regulated by interferon alpha, beta, or gamma using oligonucleotide arrays. *Proc Natl Acad Sci U S A* 1998;95:15623-15628.
42. Malakhova O, Malakhov M, Hetherington C, Zhang DE. Lipopolysaccharide activates the expression of ISG15-specific protease UBP43 via interferon regulatory factor 3. *J Biol Chem* 2002;277:14703-14711.
43. Li XL, Blackford JA, Judge CS, Liu M, Xiao W, Kalvakolanu DV, Hassel BA. RNase-L-dependent destabilization of interferon-induced mRNAs. A role for the 2-5A system in attenuation of the interferon response. *J Biol Chem* 2000;275:8880-8888.
44. Zou W, Kim JH, Handidu A, Li X, Kim KI, Yan M, Li J, et al. Microarray analysis reveals that Type I interferon strongly increases the expression of immune-response related genes in Ubp43 (Usp18) deficient macrophages. *Biochem Biophys Res Commun* 2007;356:193-199.

Figures

Figure 1

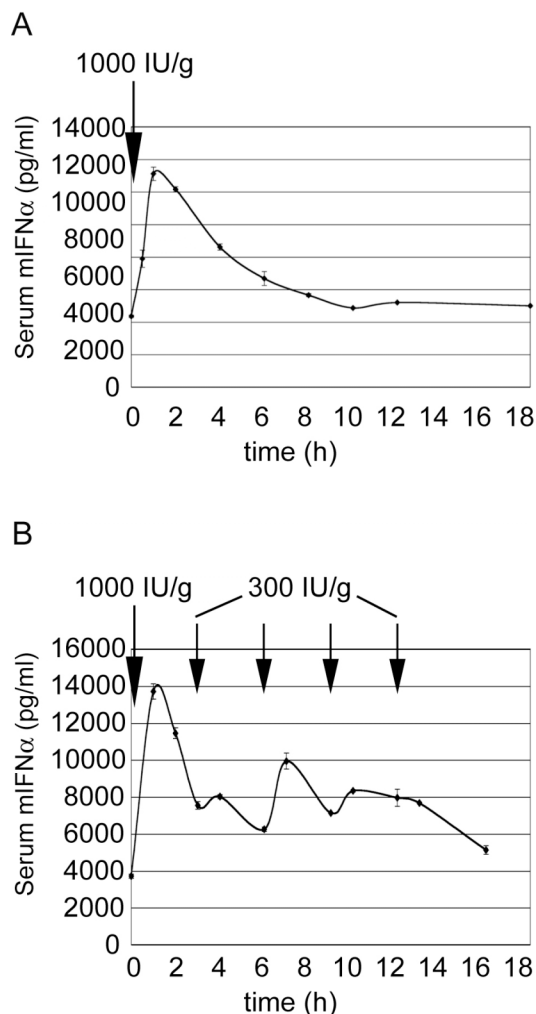


Figure 1. Pharmacokinetics of subcutaneous mIFN α injection into mice.

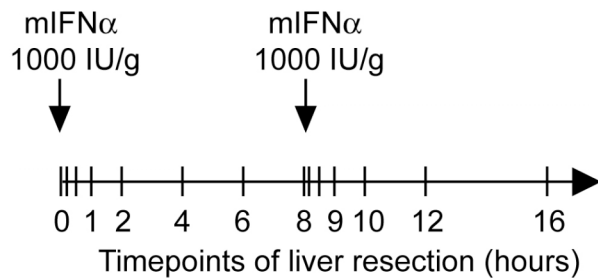
(A) Serum concentrations of mIFN α after subcutaneous injection of a single dose of 1000 IU/g.

The profile was obtained from two C57BL6 mice receiving mIFN α by subcutaneous (s.c.) injection. The peak of serum concentration was reached one hour after the injection. After 8 h, the concentration of mIFN α was back to pretreatment levels. The error bars represent the standard error of the mean.

(B) mIFN α serum concentration after multiple mIFN α injections. Two C57BL6 mice were injected s.c. with 1000 IU/g body weight of mIFN α as a priming dose, and four times with 300 IU/g body weight as maintenance doses every three hours. Sera were collected immediately before each injection and one hour after each injection. The black arrows indicate time points of mIFN α injections.

Figure 2

A



B

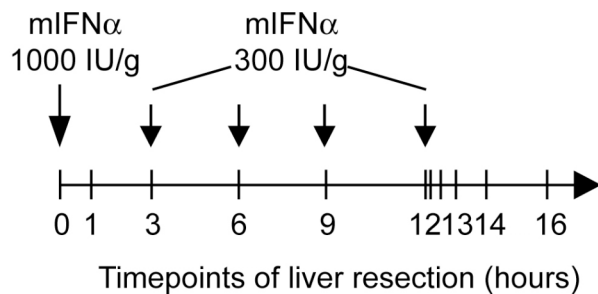


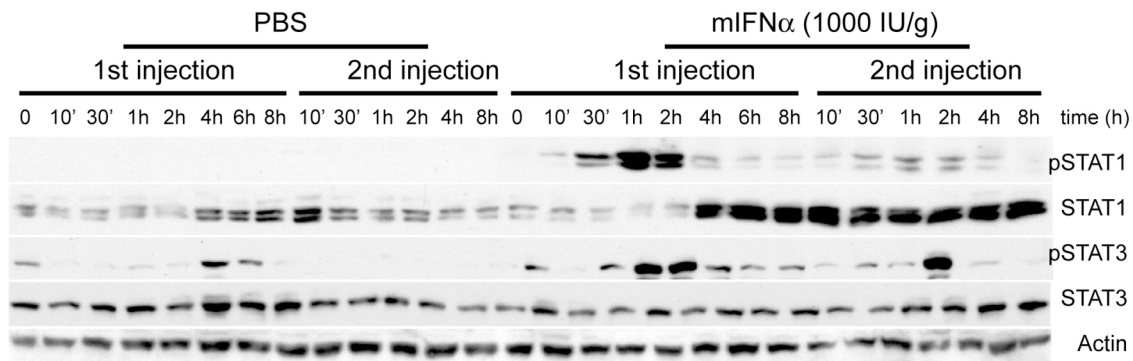
Figure 2. Schematic representation of the experimental outline for the analysis of IFN α signaling in mouse liver.

(A) Schematic diagram showing the time course of the experiment with two injections of mIFN α . The interval between the injections is 8 h and the vertical bars in the diagram indicate the time points of animal sacrifice and liver resection.

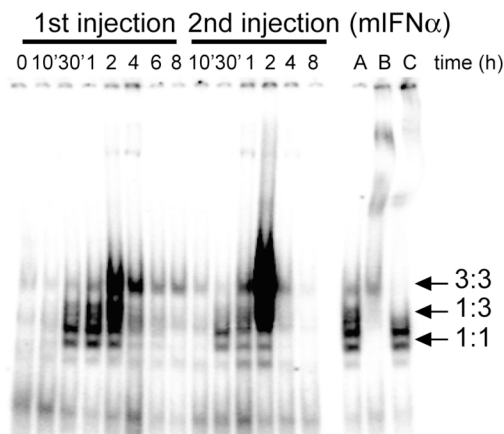
(B) Schematic diagram showing the time course of the multiple injection experiment. Mice were injected with 1000 IU/g of mIFN α as a priming dose, followed by four injections of 300 IU/g of mIFN α as maintenance doses. The vertical bars in the diagram indicate the time points of animal sacrifice and liver resection.

Figure 3

A



B



C

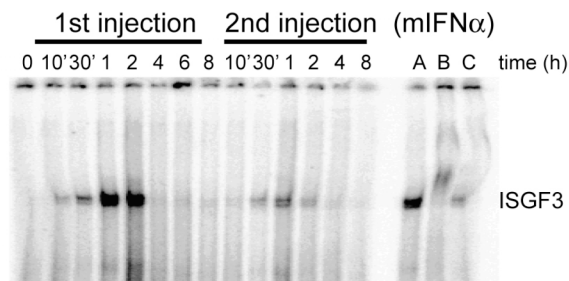


Figure 3. Activation of Jak/STAT signaling in response to two injections of mIFN α .

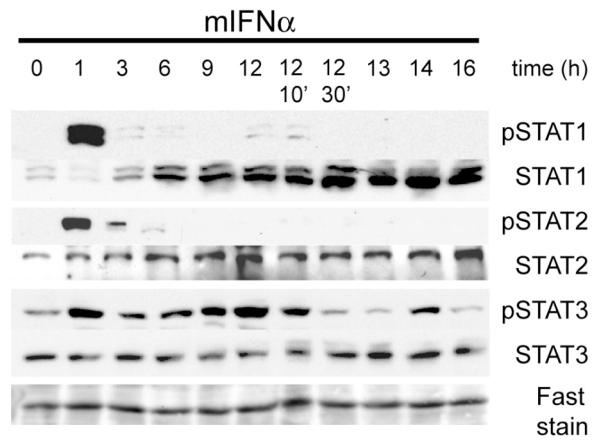
(A) C57BL/6 mice were treated with two injections of mIFN α (1000 IU/ml, right panel) or PBS (left panel) as indicated in the time course in Figure 2A. IFN- α -induced tyrosine phosphorylation of STAT1 and STAT3 was assessed by immunoblotting of liver whole cell extracts. Blots were stripped and reprobed for total STAT1 and STAT3 and for actin as a loading control.

(B) DNA binding of STAT1 and STAT3 homo- and heterodimers upon stimulation with mIFN α . Nuclear extracts of liver cells obtained at different time points from two times mIFN α injected mice were analyzed in electrophoretic mobility shift assays with the SIE-m67 oligonucleotide probe. Extract from mouse liver 1 hour after mIFN α stimulation was used as positive control (lane A). Antisera specific to STAT1 (lane B) and STAT3 (lane C) were used to shift STAT1 homodimers, STAT3 homodimers and STAT1:STAT3 heterodimers (marked with arrows).

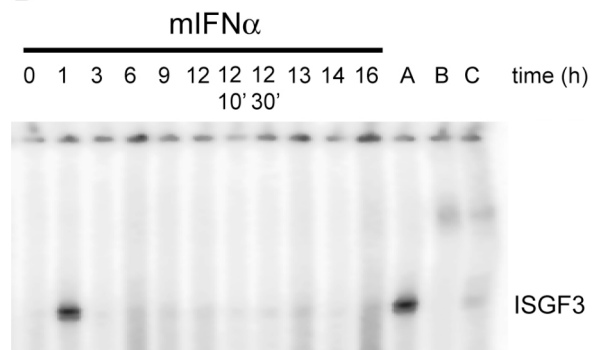
(C) DNA binding of ISGF3 in liver cells after two times mIFN α treatment. Liver Nuclear extracts of C57/BL6 mice were analyzed in EMSAs using ISRE oligonucleotide probes. Extract from mouse liver 1 hour after mIFN α stimulation was used as a positive control (lane A) and the ISGF3 band was shifted using antiserum specific for STAT1 (lane B) and STAT2 (lane C).

Figure 4

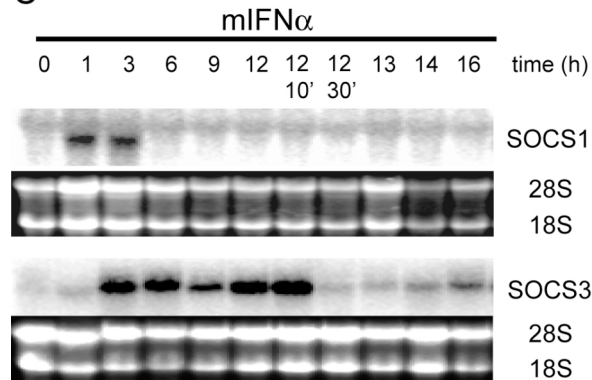
A



B



C



D

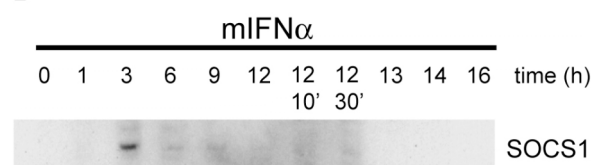


Figure 4. Activation of Jak/STAT signaling in response to continuous mIFN α treatment.

(A) Phosphorylation of STAT1, STAT2 and STAT3 was assessed by Western Blot using whole cell extracts of mouse liver after mIFN α treatment. Blots were stripped and reblotted for total STAT1/STAT2/STAT3 and stained with Blot-FastStain as loading control.

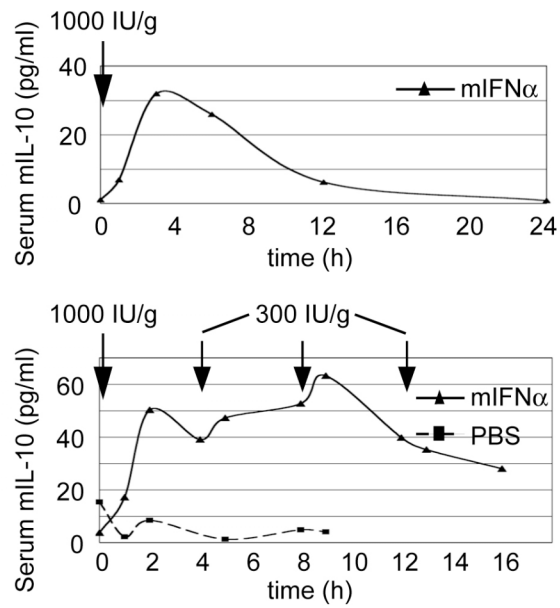
(B) DNA binding of ISGF3 in liver cells after continuous mIFN α treatment. Liver Nuclear extracts of C57/BL6 mice were analyzed in EMSAs using ISRE oligonucleotide probes. Nuclear extract from mouse liver 1 hour after mIFN α stimulation was used as a positive control (lane A) and shifts of the ISGF3 band were performed by using antiserum specific for STAT1 (lane B) and STAT2 (lane C).

(C) SOCS1 and SOCS3 mRNA expression level in the continuous presence of mIFN α . Total RNA from mIFN α injected mice was prepared and subjected to Northern Blot analysis for SOCS1 and SOCS3 mRNA expression. Equal loading of the gel was verified by ethidium bromide staining and comparing the intensities of the 28S rRNA and 18S rRNA bands.

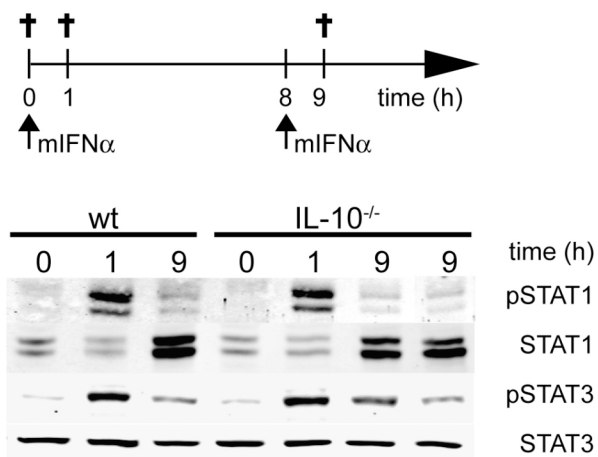
(D) SOCS1 protein expression was determined by Western blot using whole cell extracts of mouse liver after mIFN α treatment.

Figure 5

A



B



C

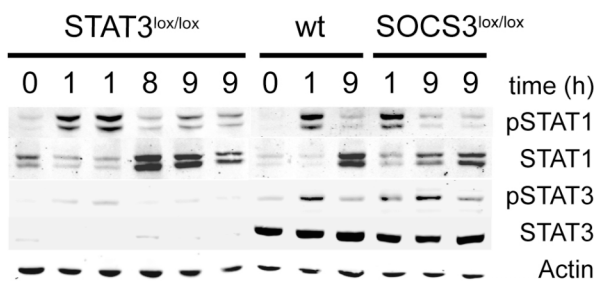


Figure 5. IL-10 serum concentrations and Jak-STAT signaling in mice deficient of IL-10, STAT3 or SOCS3.

(A) Upper panel: Injection of a single subcutaneous dose of mIFN α (1000 IU/g body weight) induces a transient increase in IL-10 serum concentrations. The level of mIL-10 as determined by ELISA is shown in the graph.

Lower panel: Repeated injections of 300 IU/g body weight of mIFN α every 4 h after an initial priming dose of 1000 IU/g body weight induces constantly high mIL-10 serum concentrations. During mIFN α maintenance doses, the concentration of mIL-10 stays at levels around 40 pg/ml (see graph with black triangles). As negative control, the level of serum mIL-10 was determined in a mouse multiply injected with PBS (see graph with black squares).

(B) Two times mIFN α injection experiment in IL-10 deficient mice.

Upper panel: Schematic representation of the experimental design with two mIFN α injections performed 8 h apart. Animals were sacrificed at time point 0 h (control), 1 hour and 9 hour (1 hour after the second injection). Immunoblotting for pSTAT1/STAT1 and pSTAT3/STAT3 is shown for C57/BL6 wild-type (wt) mice and for IL-10^{-/-} animals.

(C) Two times mIFN α injection experiment in mice with liver specific knockout of STAT3 and SOCS3. Immunoblotting for pSTAT1/STAT1, pSTAT3/STAT3 and actin is shown for wt C57/BL6 mice and for SOCS3^{lox/lox}Cre⁺ and STAT3^{lox/lox}Cre⁺ animals.

Figure 6

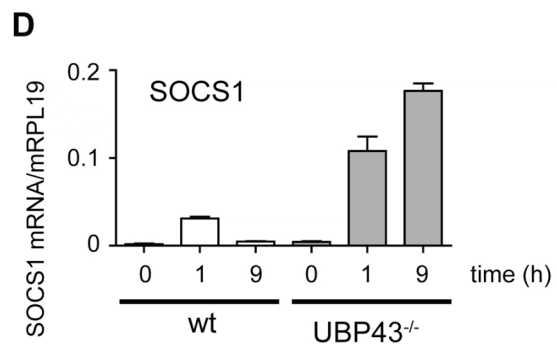
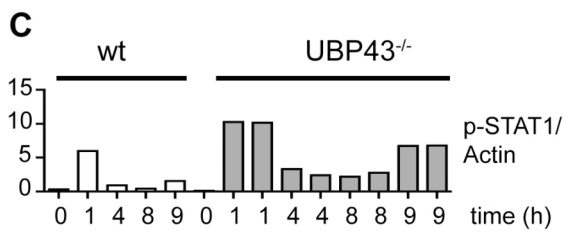
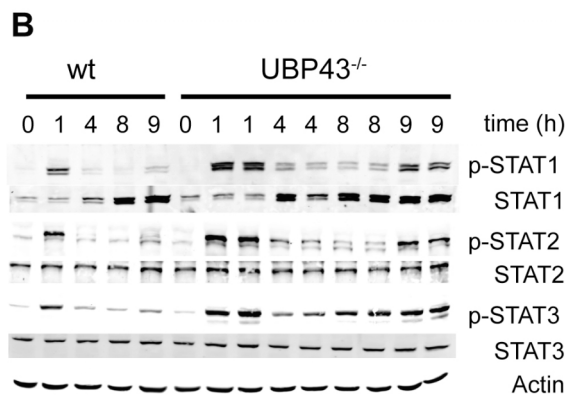
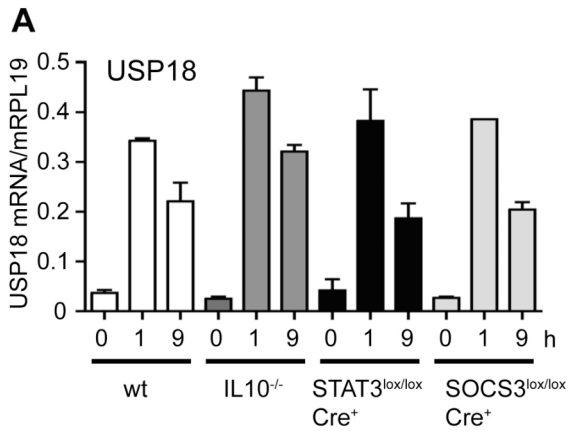


Figure 6. Role of USP18/UBP43 in IFN α refractoriness.

(A) Real time rt-qPCR analysis of USP18 mRNA expression in response to the first and the second injection of mIFN α . Total RNA was isolated from the livers of wt, IL10^{-/-}, SOCS3^{lox/lox}Cre⁺ and STAT3^{lox/lox}Cre⁺ animals at the timepoints 0, 1h, 9h (1h after the second injection). Data are plotted as the amount of USP18 mRNA relative to mRPL19 and are the means (+/- SEM) of two animals per timepoint for the knockout mice and 4 animals per timepoint for the wt mice.

(B) Activation of the Jak/STAT signaling pathway in response to the first and the second injection of mIFN α in wildtype and USP18/UBP43 deficient mice. Phosphorylation of STAT1, STAT2 and STAT3 was assessed by Western Blot using whole cell extracts of mouse liver from wt and USP18/UBP43^{-/-} mice. Blots were stripped and reblotted for total STAT1/STAT2/STAT3 and for actin as loading control.

(C) Bar diagram of phospho-STAT1 signals in wild-type and USP18/UBP43 deficient mice. Phospho-STAT1 and actin signals from figure 6B were quantified using the Odyssey Infrared Imaging System. The integrated intensities of phospho-STAT1 signals were divided by the actin values. The y-axis displays arbitrary units.

(D) Real time rt-qPCR analysis of SOCS1 mRNA expression in response to the first and the second injection of mIFN α in 2 wildtype and in 2 USP18/UBP43 deficient mice. Shown are mean values (with SEM) of the ratio of SOCS1 mRNA over mRPL19.

5. Discussion

5.1. Interferon regulated gene expression in the liver determines response to treatment in chronic hepatitis C

Response patterns to pegIFN α /ribavirin treatment in patients with CHC range from a complete non-response to a very rapid virological response (RVR) with undetectable HCV-RNA in the serum as soon as 4 weeks after treatment initiation. It is well known that 50-60% of patients infected with HCV genotype (GT) 1 and 20% of GT 2/3 patients are not cured by current standard treatment. To learn more about possible mechanisms underlying differential response of HCV infected patients to IFN therapy, we investigated IFN-induced signaling and ISG induction in paired liver biopsies collected from patients with CHC before (B-1) and during (B-2) therapy with pegIFN α . In addition to the liver samples, blood for PBMC isolation was collected before (PBMC-1) treatment and 4 hours after (PBMC-2) the first pegIFN α injection. Virological response early in the course of treatment is an excellent predictor of later sustained virological response (SVR), with the RVR being followed by an SVR in 85% of cases. Therefore, we divided the 16 patients from which paired liver biopsy samples were obtained into rapid responders (RRs) and non-RRs according to their response at week 4 of treatment.

Besides infecting human patients, HCV can also infect chimpanzees making them the only available animal model for *in vivo* studies. It is known that chimpanzees chronically infected with HCV have hundreds of ISGs induced in the liver (143). Interestingly however, all chimpanzees are non-responders to IFN based treatment (145) and therefore not suitable for studying the molecular basis underlying the treatment failure. Injection of pegIFN α into HCV infected chimpanzees does not result in an increase of ISG expression in liver, unlike in PBMCs, which respond to IFN normally. This finding and the fact that IFN responsive genes in PBMCs are known to differ from ISGs in liver tissue (146) underline the importance of tissue-specific differences when studying HCV infection in humans. Data obtained from human HCV patients demonstrated that future non-responders present with pre-

activation of the endogenous IFN system in the liver (131). In contrast to the observation that PBMCs in chimpanzees normally respond to IFN, a human study reported a blunted response to IFN α in PBMCs of patients with a relative absence of viral response to treatment (178).

In our analysis of the 16 paired liver biopsy samples, collected before and 4 hours after the first pegIFN α injection, pegIFN α induced STAT1 phosphorylation was stronger in RR than in non-RR patients when analyzed by Western blot. There was a considerable overlap between the two response groups, possibly due to heterogeneity of cells in the liver protein extract. Three out of six non-RR patients showed a 2-fold increase in the p-STAT1 signal in the B-2 sample if compared to B-1 (Figure 4A, see PNAS manuscript). A more prominent difference between the two response groups was evident from the immunohistochemical analysis of liver tissue (Figure 4B, see PNAS manuscript). In RR patients, there was no initial staining for phosphorylated STAT1 in hepatocyte nuclei, whereas administration of pegIFN α induced STAT1 nuclear translocation. In non-RR samples, pegIFN α strongly induced nuclear STAT1 translocation in Kupffer cells, whereas no increase in hepatocytes could be observed. Interestingly, most non-RR patients had nuclear phospho-STAT1 already present in pre-treatment B-1 biopsies. This is consistent with the observation that ISG transcripts are upregulated in pre-treatment biopsies of later non-responders (131). The analysis of IFN-regulated gene expression using Affymetrix U133 2.0 Plus microarrays revealed a pronounced difference in the number of genes regulated in the two response groups. 252 transcripts were significantly up- or down-regulated by >2-fold in the livers of RRs, whereas only a very low number of transcripts were induced in response to pegIFN α in the liver of non-RR patients in response to pegIFN α (Figure 1A, see PNAS manuscript). In contrast, many more genes were regulated in PBMCs in both patient groups and the difference between the two response groups was far less pronounced than in the liver, arguing for strong local defects of IFN α signaling in the liver (Figure 1C, see PNAS manuscript). To allow the identification of a subset of genes that best predicts the outcome, which we defined as rapid response versus non-response at week 4, we performed a supervised classifier analysis of the array data. For PBMC samples the analysis did not identify a subset of genes that could predict the treatment outcome, further corroborating that PBMCs are

not a good surrogate marker for the differences between RRs and non-RRs taking place in the liver (Figure S3, see PNAS manuscript). In contrast, a subset of 16 genes was identified in the liver B-2 samples that predicted response to treatment and an even better prediction was possible in the pre-treatment biopsies B-1. Remarkably, 22 of the 29 genes were ISGs. Taken together, clinical response to pegIFN α /ribavirin therapy was found exclusively in patients who have no pre-activation of the endogenous IFN system in the B-1 sample. The findings in non-responders support the interesting concept that activation of the endogenous IFN system in CHC not only is ineffective in spontaneously clearing the infection, but may also impede the response to therapy, most likely by inducing a refractory state of the IFN signaling pathway. Evidently, measures aiming at preventing or reversing pre-activation of ISGs in the HCV infected liver, if applied before IFN treatment initiation, could restore IFN responsiveness and effectiveness in all HCV infected patients.

5.2. Correlation of HCV genotype with ISG pre-activation in the liver and involvement of viral sensory pathways in inducing type I IFNs

Signaling through the Jak-STAT pathway is crucial for most of the known effects of IFNs, therefore inhibition of this pathway might well be a central effect target of HCV. Indeed, our laboratory has previously reported an inhibition of IFN induced binding of activated STATs to their cognate response elements by HCV proteins in cell lines and transgenic mice. Interestingly, this inhibition was not associated with induction of well-known Jak-STAT signaling inhibitors, but with an HCV induced upregulation of the catalytic subunit of PP2A finally resulting in STAT1 hypomethylation (118). HCV has a striking capability to establish a chronic infection, and attenuation of IFN signaling might be an important advantage of the virus early in the course of infection. Epidemiological studies suggest that 20-30% of patients resolve acute HCV infection without treatment suggesting that innate and/or adaptive immune responses are indeed capable of controlling the outcome of the infection. Evidently, HCV cannot block IFN signaling completely as demonstrated by the success of therapies based on the application of pharmacological doses of recombinant IFN α in some but not all patients with CHC. It is not well understood,

which host factors determine the response to IFN therapy. Likewise, the mechanisms leading to pre-activation of the Jak-STAT pathway in later non-responders and how the observed pre-activation is connected to the refractoriness of the IFN system requires further investigations. Why does the high level of ISG induction in the non-RR patient group not result in a spontaneous clearance of the virus? Is it because of defective IFN signaling or IFN effector systems in virus infected cells? Furthermore, it remains to be elucidated why therapeutic IFN is ineffective in patients with a pre-activation of the endogenous IFN system. Is their IFN system already maximally induced (all receptors saturated) and effector mechanisms are inhibited by the virus or does perhaps the upregulation of negative regulators of IFN signaling (SOCS, USP18/UBP43 etc.) prevent any further stimulation of the Jak-STAT signaling pathway? The negative effect of a pre-activation of the IFN system could be the result of a relative desensitization and refractoriness of the IFN α signal transduction pathways.

Interestingly, patients infected with HCV GT2 and GT3 very often show a favorable response to IFN-based treatment. Our finding that patients infected with HCV GT1/4 more often have an induced endogenous IFN system might therefore provide a plausible reason for the worse treatment prognosis of this patient group. Of note, a single chimpanzee infected with the GT3 has been shown to have lower ISG expression levels than animals infected with GT1 (143). Why the endogenous IFN system is activated in a (large) group of patients, but not in all of them, could be due to differences between viruses (genotypes, quasispecies) in their capacity to prevent IFN induction and/or to genetically determined variation in virus sensory pathways (involving RIG-I, Cardif, IRF3 and other molecules). We have analyzed the possibility that different HCV genotypes are differentially affecting the induction of type I IFN through the RIG-I/Cardif pathways. As the HCV NS3-4A protease has been described to cleave the adaptor protein Cardif *in vitro* (154), we assessed Cardif mRNA and protein expression and the presence of Cardif cleavage products in pre-treatment liver biopsies of HCV patients. Cardif cleavage was more often seen in livers of GT 2/3 patients. Moreover the expression of full-length Cardif correlated well with STAT1 hepatocyte nuclear staining in immunohistochemistry and the expression of ISGs in the liver of the same patient. This makes an intact RIG-

mediated signaling pathway a good candidate for inducing type I IFNs, STAT1 nuclear translocation and transcriptional induction of ISGs. Further studies will be needed to corroborate our findings. Especially, it would be of great interest to assess IRF-3 phosphorylation in liver biopsies and to find a correlation of IRF3 and STAT1 activation. Our finding that the frequency and degree of pre-activation of the endogenous IFN system depends on the HCV GT and that HCV GTs 2 and 3 show more frequent Cardif cleavage indicate that GT 2/3 are more successful in preventing the activation of innate immunity in the liver. The success of the virus in preventing the induction of the endogenous IFN system would however come at the cost of being more susceptible to IFN α -based therapies.

5.3 Refractoriness of IFN α signaling in the mouse liver

The clinical efficacy of pegIFN α is being attributed to the constantly high serum concentrations achieved with pegIFN α (unlike with unmodified IFN α), which may provide for un-interrupted antiviral activity through a permanent stimulation of the IFN signaling pathways. *In vitro* kinetics, however, showed a very rapid refractoriness of IFN signaling after an initial strong activation. Cultured cells became refractory to IFN within hours and remained unresponsive for up to 3 days (179). Continuous exposure to IFN resulted in a “desensitization” characterized by a return to pretreatment levels of ISG transcription. Moreover, during the 48 to 72 hours following the initial IFN α stimulation, any further IFN treatment failed to re-induce the transcription of ISGs in cell culture (179). The kinetic of *in vivo* IFN signaling has not been extensively studied. It is currently not known, whether refractoriness also occurs during IFN therapies in patients. Since the clinical experience shows improved therapeutic response rate with pegIFN α if compared to unmodified IFN α , and thus argues against the occurrence of desensitization in patients, we investigated whether the liver becomes refractory to IFN α *in vivo* by applying a mouse model. Due to inavailability of pegylated mouse IFN α , mice were repeatedly injected with unmodified mouse IFN α simulating the stable serum concentrations obtained in HCV patients.

Transient STAT activity in type I IFN-treated cells is mainly regulated by tyrosine phosphorylation (tyr-701 of STAT1, tyr-689 of STAT2, tyr-705 of STAT3) and dephosphorylation by active shut-off mechanisms. Tyrosine phosphorylation is essential for STAT dimer formation, nuclear translocation and DNA-binding. In our mouse model, we observed refractoriness in the activation of STAT1 and STAT2, but not STAT3. We hypothesized that prolonged STAT3 activation could be due to the presence of increased IL-10 levels that we found in the sera of the repeatedly injected mice. However, IFN signaling remained refractory to further doses in mice deficient in IL-10. We then investigated the possible involvement of known negative regulators of IFN α -induced Jak-STAT signaling, including SOCS and UBP43. The induction pattern of SOCS1 was consistent with its well-known role in the early negative feedback regulation of IFN α signaling. Since SOCS1 was not expressed to any detectable degree at late time-points (Figures 4C and 4D, see “refractoriness of Jak-STAT signaling” manuscript), it is highly unlikely that SOCS1 is responsible for the long-lasting inhibition of STAT1 and STAT2 phosphorylation. In contrast, the expression levels of SOCS3 were elevated for a prolonged time period (in accordance to the observed STAT3 phosphorylation), arguing for a possible role of SOCS3 in the long-term inhibition of STAT1 and STAT2 activation. However, a persisting refractoriness was also observed in mice deficient in SOCS3. The recently described specific type I IFN signaling inhibitor USP18/UBP43 blocks Jak1 phosphorylation through a specific interaction with the IFNAR2 subunit of the receptor and thereby attenuates IFN signaling (125). We found a strong upregulation of USP18/UBP43 after treating mice with subcutaneous injections of mIFN α (Figure 6A, see “refractoriness of Jak-STAT signaling” manuscript). Contrary to SOCS1 with its transient upregulation, USP18/UBP43 was still highly induced in late time-points of the kinetic. Remarkably, refractoriness of STAT1/2 phosphorylation could be overcome in USP18/UBP43 knockout mice. These data strongly indicate that UBP43 is the decisive factor in inducing a long-lasting refractory state in the IFN α signaling pathway *in vivo*. Moreover, the second injection of mIFN α induced a strong phosphorylation of STAT1 in UBP43 deficient mice despite the very high expression of SOCS1 at the same time point. This surprising result provides strong evidence that the inhibitory activity of SOCS1 requires the presence of USP18/UBP43.

Our results have potentially important consequences for the treatment of patients with chronic viral hepatitis with recombinant IFN α . If we assume that the human liver also becomes refractory to IFN α within hours after the first injection of recombinant IFN α and that the liver cells remain unresponsive to further IFN α stimulation, then the current practice of injecting pegIFN α with its very long half-life would lack a pharmacodynamic rationale. Clearly, the mechanisms underlying the increased efficacy of pegIFN α compared to standard IFN α remain unsolved. The results presented here should therefore motivate an in-depth analysis of the pharmacodynamic effects of the current pegIFN α treatments in the livers of patients with CHC.

5.4 Outlook: The role of miRNAs in liver disease and IFN signaling

There is an additional level of regulation involving miRNAs can be considered relevant for treatment response in HCV infected livers. MicroRNAs (miRNAs) are a large family of ~21-nt-long regulatory RNAs expressed in metazoan animals (180). Nearly all miRNAs investigated to date regulate gene expression by base-pairing to the 3'-UTR of target mRNAs and inhibiting protein synthesis at the level of translation initiation or mRNA degradation (181). The first miRNAs, lin-4 and let-7, were discovered in *Caenorhabditis elegans*, as RNAs that regulate expression of mRNAs, which control the timing of larval development (182-184). More recently, hundreds of new miRNAs have been identified through cloning, and other methods. Biological processes regulated by miRNAs include developmental timing, cell differentiation and proliferation, neuronal asymmetry, apoptosis and different metabolic reactions. Existence of numerous tissue- and developmental stage-specific miRNAs, and the evolutionary conservation of many miRNAs, argue for plentiful additional, yet unidentified, functions of miRNAs (180).

There is new evidence which links miRNAs with viruses and importantly also with the innate immune response. Some mammalian viruses such as CMV, Herpesviridae, and SV40 encode miRNAs in their own genomes, and these miRNAs may modify expression of the host genes (185). On the other hand, some of the host-encoded

miRNAs may have a profound effect on the life cycle of the infecting virus. MiR-122, expressed specifically in liver, is the most spectacular example of the latter category. The miRNA miR-122 base-pairs to the 5'-UTR of genomic RNA of HCV and positively regulates replication of HCV RNA (36). This observation raised much interest in a role of miR-122 in HCV infection and as a potential therapeutic target. Furthermore, it was reported recently that expression of miR-122 and several other miRNAs is regulated by IFN in Huh7 cells and primary mouse hepatocytes, and that miRNAs might mediate at least some effects of IFN on HCV-RNA replication *in vitro* (186). Therefore, it will be of interest to study the status of the miR-122 and other miRNAs expressed in liver during the course of HCV infection and following IFN α therapy. The availability of biopsy material collected for the studies mentioned above will allow us to study the proposed connection between miR-122 and HCV replication in a context of diseased tissue, and to test the effect of IFN α therapy on the level of miR-122 and other miRNAs in liver cells. Studies with biopsies could be accompanied by experiments with Huh7 hepatoma cultured cells expressing the HCV replicon or even using the *in vitro* HCV infectious system (both are available in our laboratory) (11-13). Importantly, IFN-induced effects on miR-122 expression could also be studied in the mouse liver samples, which had been generated for the study on refractoriness of *in vivo* IFN α signaling.

5.5 Concluding remarks

All above described experimental approaches generated important findings in the field of IFN signaling in the context of HCV infection. Most notably, our work has documented that CHC patients with pre-activation of their endogenous IFN system entirely lack a molecular response to pegIFN α . When aiming at finding better therapeutic options for this patient group, more efforts should be addressed not only to the generation of novel drugs including HCV protease and polymerase inhibitors, but also to reversing the mechanisms responsible for the observed IFN pre-activation. Most likely, the treatment of IFN-resistant patients with inhibitors of viral enzymes will lead to the development of rapid resistance, arguing for search of alternative approaches. Our finding that HCV genotypes 1 and 4 more often lead to pre-

activation in patients and that there is a possible involvement of HCV mediated targeting of viral sensory pathways provides the basis for further studies on the mechanisms leading to pre-activation.

We describe refractoriness of IFN signaling *in vivo* in the continuous presence of IFN α . Such knowledge is important for a rational design of IFN therapies, because dosing intervals shorter than the period of refractoriness would strongly reduce the efficacy of the injected IFN. This might have been the reason why classical IFN α treatment with injections every 48 hours had a limited therapeutic effect. Furthermore, it is not reasonable to administer modified IFN α with a prolonged serum half-life, i.e. pegIFN α , with the aim to achieve constant serum concentrations, if the hepatocytes as target cells remain unresponsive during most of the dosing interval. Of note, other human cells and tissues could show different response kinetics to IFN α and therefore side effects would be promoted without gaining any antiviral effects in the liver.

Further progress in the treatment of CHC most likely will depend on a better understanding of the pharmacodynamic effects of IFN α in different tissues. The work presented in this thesis provides important insights in the host-virus interaction and its influence on IFN α induced signal transduction in the liver.

References

1. Lauer GM, Walker BD. Hepatitis C virus infection. *N Engl J Med* 2001;345:41-52.
2. Williams R. Global challenges in liver disease. *Hepatology* 2006;44:521-526.
3. Choo QL, Kuo G, Weiner AJ, Overby LR, Bradley DW, Houghton M. Isolation of a cDNA clone derived from a blood-borne non-A, non-B viral hepatitis genome. *Science* 1989;244:359-362.
4. Schreiber GB, Busch MP, Kleinman SH, Korelitz JJ. The risk of transfusion-transmitted viral infections. The Retrovirus Epidemiology Donor Study. *N Engl J Med* 1996;334:1685-1690.
5. Legler TJ, Riggert J, Simson G, Wolf C, Humpe A, Munzel U, Uy A, et al. Testing of individual blood donations for HCV RNA reduces the residual risk of transfusion-transmitted HCV infection. *Transfusion* 2000;40:1192-1197.
6. Thomas DL, Villano SA, Riester KA, Hershow R, Mofenson LM, Landesman SH, Hollinger FB, et al. Perinatal transmission of hepatitis C virus from human immunodeficiency virus type 1-infected mothers. Women and Infants Transmission Study. *J Infect Dis* 1998;177:1480-1488.
7. Eyster ME, Alter HJ, Aledort LM, Quan S, Hatzakis A, Goedert JJ. Heterosexual co-transmission of hepatitis C virus (HCV) and human immunodeficiency virus (HIV). *Ann Intern Med* 1991;115:764-768.
8. Kuo G, Choo QL, Alter HJ, Gitnick GL, Redeker AG, Purcell RH, Miyamura T, et al. An assay for circulating antibodies to a major etiologic virus of human non-A, non-B hepatitis. *Science* 1989;244:362-364.
9. Kolykhalov AA, Agapov EV, Blight KJ, Mihalik K, Feinstone SM, Rice CM. Transmission of hepatitis C by intrahepatic inoculation with transcribed RNA. *Science* 1997;277:570-574.
10. Yanagi M, Purcell RH, Emerson SU, Bukh J. Transcripts from a single full-length cDNA clone of hepatitis C virus are infectious when directly transfected into the liver of a chimpanzee. *Proc Natl Acad Sci U S A* 1997;94:8738-8743.
11. Lohmann V, Korner F, Koch J, Herian U, Theilmann L, Bartenschlager R. Replication of subgenomic hepatitis C virus RNAs in a hepatoma cell line. *Science* 1999;285:110-113.
12. Lindenbach BD, Evans MJ, Syder AJ, Wolk B, Tellinghuisen TL, Liu CC, Maruyama T, et al. Complete replication of hepatitis C virus in cell culture. *Science* 2005;309:623-626.
13. Wakita T, Pietschmann T, Kato T, Date T, Miyamoto M, Zhao Z, Murthy K, et al. Production of infectious hepatitis C virus in tissue culture from a cloned viral genome. *Nat Med* 2005;11:791-796.
14. Evans MJ, von Hahn T, Tschernie DM, Syder AJ, Panis M, Wolk B, Hatzioannou T, et al. Claudin-1 is a hepatitis C virus co-receptor required for a late step in entry. *Nature* 2007;446:801-805.
15. Takamizawa A, Mori C, Fuke I, Manabe S, Murakami S, Fujita J, Onishi E, et al. Structure and organization of the hepatitis C virus genome isolated from human carriers. *J Virol* 1991;65:1105-1113.
16. Blindenbacher A, Duong FH, Hunziker L, Stutvoet ST, Wang X, Terracciano L, Moradpour D, et al. Expression of hepatitis c virus proteins inhibits

- interferon alpha signaling in the liver of transgenic mice. *Gastroenterology* 2003;124:1465-1475.
17. Mercer DF, Schiller DE, Elliott JF, Douglas DN, Hao C, Rinfret A, Addison WR, et al. Hepatitis C virus replication in mice with chimeric human livers. *Nat Med* 2001;7:927-933.
 18. Moradpour D, Penin F, Rice CM. Replication of hepatitis C virus. *Nat Rev Microbiol* 2007;5:453-463.
 19. Shimizu YK, Feinstone SM, Kohara M, Purcell RH, Yoshikura H. Hepatitis C virus: detection of intracellular virus particles by electron microscopy. *Hepatology* 1996;23:205-209.
 20. Simmonds P, Bukh J, Combet C, Deleage G, Enomoto N, Feinstone S, Halfon P, et al. Consensus proposals for a unified system of nomenclature of hepatitis C virus genotypes. *Hepatology* 2005;42:962-973.
 21. Suzuki R, Suzuki T, Ishii K, Matsuura Y, Miyamura T. Processing and functions of Hepatitis C virus proteins. *Intervirology* 1999;42:145-152.
 22. Grakoui A, Wychowski C, Lin C, Feinstone SM, Rice CM. Expression and identification of hepatitis C virus polyprotein cleavage products. *J Virol* 1993;67:1385-1395.
 23. Griffin SD, Beales LP, Clarke DS, Worsfold O, Evans SD, Jaeger J, Harris MP, et al. The p7 protein of hepatitis C virus forms an ion channel that is blocked by the antiviral drug, Amantadine. *FEBS Lett* 2003;535:34-38.
 24. Jones CT, Murray CL, Eastman DK, Tassello J, Rice CM. Hepatitis C virus p7 and NS2 proteins are essential for production of infectious virus. *J Virol* 2007;81:8374-8383.
 25. Miyamura T, Matsuura Y. Structural proteins of hepatitis C virus. *Trends Microbiol* 1993;1:229-231.
 26. Hijikata M, Mizushima H, Akagi T, Mori S, Kakiuchi N, Kato N, Tanaka T, et al. Two distinct proteinase activities required for the processing of a putative nonstructural precursor protein of hepatitis C virus. *J Virol* 1993;67:4665-4675.
 27. Kim DW, Gwack Y, Han JH, Choe J. C-terminal domain of the hepatitis C virus NS3 protein contains an RNA helicase activity. *Biochem Biophys Res Commun* 1995;215:160-166.
 28. Egger D, Wolk B, Gosert R, Bianchi L, Blum HE, Moradpour D, Bienz K. Expression of hepatitis C virus proteins induces distinct membrane alterations including a candidate viral replication complex. *J Virol* 2002;76:5974-5984.
 29. Gosert R, Egger D, Lohmann V, Bartenschlager R, Blum HE, Bienz K, Moradpour D. Identification of the hepatitis C virus RNA replication complex in Huh-7 cells harboring subgenomic replicons. *J Virol* 2003;77:5487-5492.
 30. Evans MJ, Rice CM, Goff SP. Phosphorylation of hepatitis C virus nonstructural protein 5A modulates its protein interactions and viral RNA replication. *Proc Natl Acad Sci U S A* 2004;101:13038-13043.
 31. Appel N, Pietschmann T, Bartenschlager R. Mutational analysis of hepatitis C virus nonstructural protein 5A: potential role of differential phosphorylation in RNA replication and identification of a genetically flexible domain. *J Virol* 2005;79:3187-3194.
 32. Enomoto N, Sakuma I, Asahina Y, Kurosaki M, Murakami T, Yamamoto C, Izumi N, et al. Comparison of full-length sequences of interferon-sensitive and resistant hepatitis C virus 1b. Sensitivity to interferon is conferred by amino acid substitutions in the NS5A region. *J Clin Invest* 1995;96:224-230.

33. Enomoto N, Sakuma I, Asahina Y, Kurosaki M, Murakami T, Yamamoto C, Ogura Y, et al. Mutations in the nonstructural protein 5A gene and response to interferon in patients with chronic hepatitis C virus 1b infection. *N Engl J Med* 1996;334:77-81.
34. Gale M, Jr., Blakely CM, Kwieciszewski B, Tan SL, Dossett M, Tang NM, Korth MJ, et al. Control of PKR protein kinase by hepatitis C virus nonstructural 5A protein: molecular mechanisms of kinase regulation. *Mol Cell Biol* 1998;18:5208-5218.
35. Behrens SE, Tomei L, De Francesco R. Identification and properties of the RNA-dependent RNA polymerase of hepatitis C virus. *Embo J* 1996;15:12-22.
36. Jopling CL, Yi M, Lancaster AM, Lemon SM, Sarnow P. Modulation of hepatitis C virus RNA abundance by a liver-specific MicroRNA. *Science* 2005;309:1577-1581.
37. Ishii K, Tanaka Y, Yap CC, Aizaki H, Matsuura Y, Miyamura T. Expression of hepatitis C virus NS5B protein: characterization of its RNA polymerase activity and RNA binding. *Hepatology* 1999;29:1227-1235.
38. Pileri P, Uematsu Y, Campagnoli S, Galli G, Falugi F, Petracca R, Weiner AJ, et al. Binding of hepatitis C virus to CD81. *Science* 1998;282:938-941.
39. Meola A, Sbardellati A, Bruni Ercole B, Cerretani M, Pezzanera M, Ceccacci A, Vitelli A, et al. Binding of hepatitis C virus E2 glycoprotein to CD81 does not correlate with species permissiveness to infection. *J Virol* 2000;74:5933-5938.
40. Monazahian M, Bohme I, Bonk S, Koch A, Scholz C, Grethe S, Thomssen R. Low density lipoprotein receptor as a candidate receptor for hepatitis C virus. *J Med Virol* 1999;57:223-229.
41. Scarselli E, Ansuini H, Cerino R, Roccasecca RM, Acali S, Filocamo G, Traboni C, et al. The human scavenger receptor class B type I is a novel candidate receptor for the hepatitis C virus. *Embo J* 2002;21:5017-5025.
42. Andre P, Perlemuter G, Budkowska A, Brechot C, Lotteau V. Hepatitis C virus particles and lipoprotein metabolism. *Semin Liver Dis* 2005;25:93-104.
43. Neumann AU, Lam NP, Dahari H, Gretch DR, Wiley TE, Layden TJ, Perelson AS. Hepatitis C viral dynamics in vivo and the antiviral efficacy of interferon-alpha therapy. *Science* 1998;282:103-107.
44. Cooper S, Erickson AL, Adams EJ, Kansopon J, Weiner AJ, Chien DY, Houghton M, et al. Analysis of a successful immune response against hepatitis C virus. *Immunity* 1999;10:439-449.
45. Shimotohno K. Hepatitis C virus and its pathogenesis. *Semin Cancer Biol* 2000;10:233-240.
46. Lai MM, Ware CF. Hepatitis C virus core protein: possible roles in viral pathogenesis. *Curr Top Microbiol Immunol* 2000;242:117-134.
47. Aoki H, Hayashi J, Moriyama M, Arakawa Y, Hino O. Hepatitis C virus core protein interacts with 14-3-3 protein and activates the kinase Raf-1. *J Virol* 2000;74:1736-1741.
48. Van Antwerp DJ, Martin SJ, Kafri T, Green DR, Verma IM. Suppression of TNF-alpha-induced apoptosis by NF-kappaB. *Science* 1996;274:787-789.
49. Ray RB, Lagging LM, Meyer K, Ray R. Hepatitis C virus core protein cooperates with ras and transforms primary rat embryo fibroblasts to tumorigenic phenotype. *J Virol* 1996;70:4438-4443.

50. Asselah T, Rubbia-Brandt L, Marcellin P, Negro F. Steatosis in chronic hepatitis C: why does it really matter? *Gut* 2006;55:123-130.
51. Lamarre D, Anderson PC, Bailey M, Beaulieu P, Bolger G, Bonneau P, Bos M, et al. An NS3 protease inhibitor with antiviral effects in humans infected with hepatitis C virus. *Nature* 2003;426:186-189.
52. Kwong AD, Rao BG, Jeang KT. Viral and cellular RNA helicases as antiviral targets. *Nat Rev Drug Discov* 2005;4:845-853.
53. Tsukuma H, Hiyama T, Tanaka S, Nakao M, Yabuuchi T, Kitamura T, Nakanishi K, et al. Risk factors for hepatocellular carcinoma among patients with chronic liver disease. *N Engl J Med* 1993;328:1797-1801.
54. Zarski JP, Bohn B, Bastie A, Pawlotsky JM, Baud M, Bost-Bezeaux F, Tran van Nhieu J, et al. Characteristics of patients with dual infection by hepatitis B and C viruses. *J Hepatol* 1998;28:27-33.
55. Sanchez-Quijano A, Andreu J, Gavilan F, Luque F, Abad MA, Soto B, Munoz J, et al. Influence of human immunodeficiency virus type 1 infection on the natural course of chronic parenterally acquired hepatitis C. *Eur J Clin Microbiol Infect Dis* 1995;14:949-953.
56. Vento S, Garofano T, Renzini C, Cainelli F, Casali F, Ghironzi G, Ferraro T, et al. Fulminant hepatitis associated with hepatitis A virus superinfection in patients with chronic hepatitis C. *N Engl J Med* 1998;338:286-290.
57. Horcajada JP, Garcia-Bengoechea M, Cilla G, Etxaniz P, Cuadrado E, Arenas JJ. Mixed cryoglobulinaemia in patients with chronic hepatitis C infection: prevalence, significance and relationship with different viral genotypes. *Ann Med* 1999;31:352-358.
58. Agnello V, Chung RT, Kaplan LM. A role for hepatitis C virus infection in type II cryoglobulinemia. *N Engl J Med* 1992;327:1490-1495.
59. Segerer S, Hudkins KL, Taneda S, Wen M, Cui Y, Segerer M, Farr AG, et al. Oral interferon-alpha treatment of mice with cryoglobulinemic glomerulonephritis. *Am J Kidney Dis* 2002;39:876-888.
60. Pozzato G, Mazzaro C, Crovatto M, Modolo ML, Ceselli S, Mazzi G, Sulfaro S, et al. Low-grade malignant lymphoma, hepatitis C virus infection, and mixed cryoglobulinemia. *Blood* 1994;84:3047-3053.
61. Haddad J, Deny P, Munz-Gotheil C, Ambrosini JC, Trinchet JC, Pateron D, Mal F, et al. Lymphocytic sialadenitis of Sjogren's syndrome associated with chronic hepatitis C virus liver disease. *Lancet* 1992;339:321-323.
62. Zignego AL, Brechot C. Extrahepatic manifestations of HCV infection: facts and controversies. *J Hepatol* 1999;31:369-376.
63. Marazuela M, Garcia-Buey L, Gonzalez-Fernandez B, Garcia-Monzon C, Arranz A, Borque MJ, Moreno-Otero R. Thyroid autoimmune disorders in patients with chronic hepatitis C before and during interferon-alpha therapy. *Clin Endocrinol (Oxf)* 1996;44:635-642.
64. Gerlach JT, Diepolder HM, Zachoval R, Gruener NH, Jung MC, Ulsenheimer A, Schraut WW, et al. Acute hepatitis C: high rate of both spontaneous and treatment-induced viral clearance. *Gastroenterology* 2003;125:80-88.
65. Jaeckel E, Cornberg M, Wedemeyer H, Santantonio T, Mayer J, Zankel M, Pastore G, et al. Treatment of acute hepatitis C with interferon alfa-2b. *N Engl J Med* 2001;345:1452-1457.
66. Poynard T, Marcellin P, Lee SS, Niederau C, Minuk GS, Ideo G, Bain V, et al. Randomised trial of interferon alpha2b plus ribavirin for 48 weeks or for 24 weeks versus interferon alpha2b plus placebo for 48 weeks for treatment of

- chronic infection with hepatitis C virus. International Hepatitis Interventional Therapy Group (IHIT). *Lancet* 1998;352:1426-1432.
67. Barouki FM, Witter FR, Griffin DE, Nadler PI, Woods A, Wood DL, Lietman PS. Time course of interferon levels, antiviral state, 2',5'-oligoadenylate synthetase and side effects in healthy men. *J Interferon Res* 1987;7:29-39.
 68. Wills RJ. Clinical pharmacokinetics of interferons. *Clin Pharmacokinet* 1990;19:390-399.
 69. Manns MP, McHutchison JG, Gordon SC, Rustgi VK, Shiffman M, Reindollar R, Goodman ZD, et al. Peginterferon alfa-2b plus ribavirin compared with interferon alfa-2b plus ribavirin for initial treatment of chronic hepatitis C: a randomised trial. *Lancet* 2001;358:958-965.
 70. Fried MW, Shiffman ML, Reddy KR, Smith C, Marinos G, Goncales FL, Jr., Haussinger D, et al. Peginterferon alfa-2a plus ribavirin for chronic hepatitis C virus infection. *N Engl J Med* 2002;347:975-982.
 71. Fontaine H, Pol S. Side effects of interferon-alpha in treating hepatitis C virus infection. *Transplant Proc* 2001;33:2327-2329.
 72. Terrault NA. Hepatitis C virus and liver transplantation. *Semin Gastrointest Dis* 2000;11:96-114.
 73. Farci P, Shimoda A, Wong D, Cabezon T, De Gioannis D, Strazzer A, Shimizu Y, et al. Prevention of hepatitis C virus infection in chimpanzees by hyperimmune serum against the hypervariable region 1 of the envelope 2 protein. *Proc Natl Acad Sci U S A* 1996;93:15394-15399.
 74. Houghton M, Abrignani S. Prospects for a vaccine against the hepatitis C virus. *Nature* 2005;436:961-966.
 75. McHutchison JG, Gordon SC, Schiff ER, Shiffman ML, Lee WM, Rustgi VK, Goodman ZD, et al. Interferon alfa-2b alone or in combination with ribavirin as initial treatment for chronic hepatitis C. Hepatitis Interventional Therapy Group. *N Engl J Med* 1998;339:1485-1492.
 76. Mangia A, Santoro R, Minerva N, Ricci GL, Carretta V, Persico M, Vinelli F, et al. Peginterferon alfa-2b and ribavirin for 12 vs. 24 weeks in HCV genotype 2 or 3. *N Engl J Med* 2005;352:2609-2617.
 77. Gao B, Hong F, Radaeva S. Host factors and failure of interferon-alpha treatment in hepatitis C virus. *Hepatology* 2004;39:880-890.
 78. Schiappa DA, Mittal C, Brown JA, Mika BP. Relationship of hepatitis C genotype 1 NS5A sequence mutations to early phase viral kinetics and interferon effectiveness. *J Infect Dis* 2002;185:868-877.
 79. Heim MH. Intracellular signalling and antiviral effects of interferons. *Dig Liver Dis* 2000;32:257-263.
 80. Siegal FP, Kadowaki N, Shodell M, Fitzgerald-Bocarsly PA, Shah K, Ho S, Antonenko S, et al. The nature of the principal type 1 interferon-producing cells in human blood. *Science* 1999;284:1835-1837.
 81. Dorman SE, Holland SM. Interferon-gamma and interleukin-12 pathway defects and human disease. *Cytokine Growth Factor Rev* 2000;11:321-333.
 82. Aguet M, Dembic Z, Merlin G. Molecular cloning and expression of the human interferon-gamma receptor. *Cell* 1988;55:273-280.
 83. Meurs E, Chong K, Galabru J, Thomas NS, Kerr IM, Williams BR, Hovanessian AG. Molecular cloning and characterization of the human double-stranded RNA-activated protein kinase induced by interferon. *Cell* 1990;62:379-390.

84. Taylor DR, Shi ST, Romano PR, Barber GN, Lai MM. Inhibition of the interferon-inducible protein kinase PKR by HCV E2 protein. *Science* 1999;285:107-110.
85. Carroll SS, Chen E, Viscount T, Geib J, Sardana MK, Gehman J, Kuo LC. Cleavage of oligoribonucleotides by the 2',5'-oligoadenylate- dependent ribonuclease L. *J Biol Chem* 1996;271:4988-4992.
86. Malathi K, Dong B, Gale M, Jr., Silverman RH. Small self-RNA generated by RNase L amplifies antiviral innate immunity. *Nature* 2007;448:816-819.
87. Marschall M, Zach A, Hechtfisher A, Foerst G, Meier-Ewert H, Haller O. Inhibition of influenza C viruses by human MxA protein. *Virus Res* 2000;67:179-188.
88. Nelson DR, Marousis CG, Ohno T, Davis GL, Lau JY. Intrahepatic hepatitis C virus-specific cytotoxic T lymphocyte activity and response to interferon alfa therapy in chronic hepatitis C. *Hepatology* 1998;28:225-230.
89. Biron CA. Interferons alpha and beta as immune regulators--a new look. *Immunity* 2001;14:661-664.
90. Heim MH. The Jak-STAT pathway: cytokine signalling from the receptor to the nucleus. *J Recept Signal Transduct Res* 1999;19:75-120.
91. Wang YD, Wong K, Wood WI. Intracellular tyrosine residues of the human growth hormone receptor are not required for the signaling of proliferation or Jak-STAT activation. *J Biol Chem* 1995;270:7021-7024.
92. Bernards A. Predicted tyk2 protein contains two tandem protein kinase domains. *Oncogene* 1991;6:1185-1187.
93. Hilkens CM, Is'harc H, Lillemeier BF, Strobl B, Bates PA, Behrmann I, Kerr IM. A region encompassing the FERM domain of Jak1 is necessary for binding to the cytokine receptor gp130. *FEBS Lett* 2001;505:87-91.
94. Darnell JE, Jr., Kerr IM, Stark GR. Jak-STAT pathways and transcriptional activation in response to IFNs and other extracellular signaling proteins. *Science* 1994;264:1415-1421.
95. Bhattacharya S, Eckner R, Grossman S, Oldread E, Arany Z, D'Andrea A, Livingston DM. Cooperation of Stat2 and p300/CBP in signalling induced by interferon-alpha. *Nature* 1996;383:344-347.
96. Shuai K, Horvath CM, Huang LH, Qureshi SA, Cowburn D, Darnell JE, Jr. Interferon activation of the transcription factor Stat91 involves dimerization through SH2-phosphotyrosyl peptide interactions. *Cell* 1994;76:821-828.
97. Heim MH, Kerr IM, Stark GR, Darnell JE, Jr. Contribution of STAT SH2 groups to specific interferon signaling by the Jak-STAT pathway. *Science* 1995;267:1347-1349.
98. Zhang JJ, Vinkemeier U, Gu W, Chakravarti D, Horvath CM, Darnell JE, Jr. Two contact regions between Stat1 and CBP/p300 in interferon gamma signaling. *Proc Natl Acad Sci U S A* 1996;93:15092-15096.
99. Mao X, Ren Z, Parker GN, Sondermann H, Pastorello MA, Wang W, McMurray JS, et al. Structural bases of unphosphorylated STAT1 association and receptor binding. *Mol Cell* 2005;17:761-771.
100. Shuai K, Stark GR, Kerr IM, Darnell JE, Jr. A single phosphotyrosine residue of Stat91 required for gene activation by interferon-gamma. *Science* 1993;261:1744-1746.
101. Horvath CM. STAT proteins and transcriptional responses to extracellular signals. *Trends Biochem Sci* 2000;25:496-502.

102. Horvath CM, Darnell JE. The state of the STATs: recent developments in the study of signal transduction to the nucleus. *Curr Opin Cell Biol* 1997;9:233-239.
103. Darnell JE, Jr. STATs and gene regulation. *Science* 1997;277:1630-1635.
104. Lehtonen A, Matikainen S, Julkunen I. Interferons up-regulate STAT1, STAT2, and IRF family transcription factor gene expression in human peripheral blood mononuclear cells and macrophages. *J Immunol* 1997;159:794-803.
105. Decker T, Kovarik P. Serine phosphorylation of STATs. *Oncogene* 2000;19:2628-2637.
106. Wen Z, Zhong Z, Darnell JE, Jr. Maximal activation of transcription by Stat1 and Stat3 requires both tyrosine and serine phosphorylation. *Cell* 1995;82:241-250.
107. Kovarik P, Mangold M, Ramsauer K, Heidari H, Steinborn R, Zotter A, Levy DE, et al. Specificity of signaling by STAT1 depends on SH2 and C-terminal domains that regulate Ser727 phosphorylation, differentially affecting specific target gene expression. *Embo J* 2001;20:91-100.
108. Mowen KA, Tang J, Zhu W, Schurter BT, Shuai K, Herschman HR, David M. Arginine methylation of STAT1 modulates IFN α /beta-induced transcription. *Cell* 2001;104:731-741.
109. Gouilleux-Gruart V, Gouilleux F, Desaint C, Claisse JF, Capiod JC, Delobel J, Weber-Nordt R, et al. STAT-related transcription factors are constitutively activated in peripheral blood cells from acute leukemia patients. *Blood* 1996;87:1692-1697.
110. Krebs DL, Hilton DJ. SOCS proteins: negative regulators of cytokine signaling. *Stem Cells* 2001;19:378-387.
111. Liu B, Liao J, Rao X, Kushner SA, Chung CD, Chang DD, Shuai K. Inhibition of Stat1-mediated gene activation by PIAS1. *Proc Natl Acad Sci U S A* 1998;95:10626-10631.
112. Shuai K. Modulation of STAT signaling by STAT-interacting proteins. *Oncogene* 2000;19:2638-2644.
113. ten Hoeve J, de Jesus Ibarra-Sanchez M, Fu Y, Zhu W, Tremblay M, David M, Shuai K. Identification of a nuclear Stat1 protein tyrosine phosphatase. *Mol Cell Biol* 2002;22:5662-5668.
114. ten Hoeve J, de Jesus Ibarra-Sanchez M, Fu Y, Zhu W, Tremblay M, David M, Shuai K. Identification of a nuclear Stat1 protein tyrosine phosphatase. *Mol Cell Biol* 2002;22:5662-5668.
115. Zhu W, Mustelin T, David M. Arginine methylation of STAT1 regulates its dephosphorylation by T cell protein tyrosine phosphatase. *J Biol Chem* 2002;277:35787-35790.
116. Wu TR, Hong YK, Wang XD, Ling MY, Dragoi AM, Chung AS, Campbell AG, et al. SHP-2 is a dual-specificity phosphatase involved in Stat1 dephosphorylation at both tyrosine and serine residues in nuclei. *J Biol Chem* 2002;277:47572-47580.
117. Chen Y, Wen R, Yang S, Schuman J, Zhang EE, Yi T, Feng GS, et al. Identification of Shp-2 as a Stat5A phosphatase. *J Biol Chem* 2003;278:16520-16527.
118. Duong FH, Filipowicz M, Tripodi M, La Monica N, Heim MH. Hepatitis C virus inhibits interferon signaling through up-regulation of protein phosphatase 2A. *Gastroenterology* 2004;126:263-277.

119. Chung CD, Liao J, Liu B, Rao X, Jay P, Berta P, Shuai K. Specific inhibition of Stat3 signal transduction by PIAS3. *Science* 1997;278:1803-1805.
120. Liu B, Mink S, Wong KA, Stein N, Getman C, Dempsey PW, Wu H, et al. PIAS1 selectively inhibits interferon-inducible genes and is important in innate immunity. *Nat Immunol* 2004;5:891-898.
121. Starr R, Metcalf D, Elefanty AG, Brysha M, Willson TA, Nicola NA, Hilton DJ, et al. Liver degeneration and lymphoid deficiencies in mice lacking suppressor of cytokine signaling-1. *Proc Natl Acad Sci U S A* 1998;95:14395-14399.
122. Roberts AW, Robb L, Rakar S, Hartley L, Cluse L, Nicola NA, Metcalf D, et al. Placental defects and embryonic lethality in mice lacking suppressor of cytokine signaling 3. *Proc Natl Acad Sci U S A* 2001;98:9324-9329.
123. Liu LQ, Ilaria R, Jr., Kingsley PD, Iwama A, van Etten RA, Palis J, Zhang DE. A novel ubiquitin-specific protease, UBP43, cloned from leukemia fusion protein AML1-ETO-expressing mice, functions in hematopoietic cell differentiation. *Mol Cell Biol* 1999;19:3029-3038.
124. Malakhov MP, Malakhova OA, Kim KI, Ritchie KJ, Zhang DE. UBP43 (USP18) specifically removes ISG15 from conjugated proteins. *J Biol Chem* 2002;277:9976-9981.
125. Malakhova OA, Kim KI, Luo JK, Zou W, Kumar KG, Fuchs SY, Shuai K, et al. UBP43 is a novel regulator of interferon signaling independent of its ISG15 isopeptidase activity. *Embo J* 2006;25:2358-2367.
126. Der SD, Zhou A, Williams BR, Silverman RH. Identification of genes differentially regulated by interferon alpha, beta, or gamma using oligonucleotide arrays. *Proc Natl Acad Sci U S A* 1998;95:15623-15628.
127. Malakhova O, Malakhov M, Hetherington C, Zhang DE. Lipopolysaccharide activates the expression of ISG15-specific protease UBP43 via interferon regulatory factor 3. *J Biol Chem* 2002;277:14703-14711.
128. Ritchie KJ, Malakhov MP, Hetherington CJ, Zhou L, Little MT, Malakhova OA, Sipe JC, et al. Dysregulation of protein modification by ISG15 results in brain cell injury. *Genes Dev* 2002;16:2207-2212.
129. Malakhova OA, Yan M, Malakhov MP, Yuan Y, Ritchie KJ, Kim KI, Peterson LF, et al. Protein ISGylation modulates the JAK-STAT signaling pathway. *Genes Dev* 2003;17:455-460.
130. Ritchie KJ, Hahn CS, Kim KI, Yan M, Rosario D, Li L, de la Torre JC, et al. Role of ISG15 protease UBP43 (USP18) in innate immunity to viral infection. *Nat Med* 2004;10:1374-1378.
131. Chen L, Borozan I, Feld J, Sun J, Tannis LL, Coltescu C, Heathcote J, et al. Hepatic gene expression discriminates responders and nonresponders in treatment of chronic hepatitis C viral infection. *Gastroenterology* 2005;128:1437-1444.
132. Randall G, Chen L, Panis M, Fischer AK, Lindenbach BD, Sun J, Heathcote J, et al. Silencing of USP18 potentiates the antiviral activity of interferon against hepatitis C virus infection. *Gastroenterology* 2006;131:1584-1591.
133. Yatsushashi H, Fujino T, Matsumoto T, Inoue O, Koga M, Yano M. Immunohistochemical analysis of hepatic interferon alpha-beta receptor level: relationship between receptor expression and response to interferon therapy in patients with chronic hepatitis C. *J Hepatol* 1999;30:995-1003.

134. Heim MH, Moradpour D, Blum HE. Expression of hepatitis C virus proteins inhibits signal transduction through the Jak-STAT pathway. *J Virol* 1999;73:8469-8475.
135. Pansky A, Hildebrand P, Fasler-Kan E, Baselgia L, Ketterer S, Beglinger C, Heim MH. Defective Jak-STAT signal transduction pathway in melanoma cells resistant to growth inhibition by interferon-alpha. *Int J Cancer* 2000;85:720-725.
136. Durbin JE, Hackenmiller R, Simon MC, Levy DE. Targeted disruption of the mouse Stat1 gene results in compromised innate immunity to viral disease. *Cell* 1996;84:443-450.
137. Kuhn R, Schwenk F, Aguët M, Rajewsky K. Inducible gene targeting in mice. *Science* 1995;269:1427-1429.
138. Alonzi T, Maritano D, Gorgoni B, Rizzuto G, Libert C, Poli V. Essential role of STAT3 in the control of the acute-phase response as revealed by inducible gene inactivation [correction of activation] in the liver. *Mol Cell Biol* 2001;21:1621-1632.
139. Kralovics R, Passamonti F, Buser AS, Teo SS, Tiedt R, Passweg JR, Tichelli A, et al. A gain-of-function mutation of JAK2 in myeloproliferative disorders. *N Engl J Med* 2005;352:1779-1790.
140. Duong FH, Christen V, Filipowicz M, Heim MH. S-Adenosylmethionine and betaine correct hepatitis C virus induced inhibition of interferon signaling in vitro. *Hepatology* 2006;43:796-806.
141. Yu SH, Nagayama K, Enomoto N, Izumi N, Marumo F, Sato C. Intrahepatic mRNA expression of interferon-inducible antiviral genes in liver diseases: dsRNA-dependent protein kinase overexpression and RNase L inhibitor suppression in chronic hepatitis C. *Hepatology* 2000;32:1089-1095.
142. MacQuillan GC, Mamotte C, Reed WD, Jeffrey GP, Allan JE. Upregulation of endogenous intrahepatic interferon stimulated genes during chronic hepatitis C virus infection. *J Med Virol* 2003;70:219-227.
143. Bigger CB, Guerra B, Brasky KM, Hubbard G, Beard MR, Luxon BA, Lemon SM, et al. Intrahepatic gene expression during chronic hepatitis C virus infection in chimpanzees. *J Virol* 2004;78:13779-13792.
144. Bigger CB, Brasky KM, Lanford RE. DNA microarray analysis of chimpanzee liver during acute resolving hepatitis C virus infection. *J Virol* 2001;75:7059-7066.
145. Lanford RE, Guerra B, Bigger CB, Lee H, Chavez D, Brasky KM. Lack of response to exogenous interferon-alpha in the liver of chimpanzees chronically infected with hepatitis C virus. *Hepatology* 2007;46:999-1008.
146. Lanford RE, Guerra B, Lee H, Chavez D, Brasky KM, Bigger CB. Genomic response to interferon-alpha in chimpanzees: implications of rapid downregulation for hepatitis C kinetics. *Hepatology* 2006;43:961-972.
147. Takeuchi O, Akira S. Signaling pathways activated by microorganisms. *Curr Opin Cell Biol* 2007;19:185-191.
148. Akira S, Uematsu S, Takeuchi O. Pathogen recognition and innate immunity. *Cell* 2006;124:783-801.
149. Inohara N, Nunez G. NODs: intracellular proteins involved in inflammation and apoptosis. *Nat Rev Immunol* 2003;3:371-382.
150. Yoneyama M, Kikuchi M, Natsukawa T, Shinobu N, Imaizumi T, Miyagishi M, Taira K, et al. The RNA helicase RIG-I has an essential function in double-

- stranded RNA-induced innate antiviral responses. *Nat Immunol* 2004;5:730-737.
151. Kato H, Takeuchi O, Sato S, Yoneyama M, Yamamoto M, Matsui K, Uematsu S, et al. Differential roles of MDA5 and RIG-I helicases in the recognition of RNA viruses. *Nature* 2006;441:101-105.
 152. Hornung V, Ellegast J, Kim S, Brzozka K, Jung A, Kato H, Poeck H, et al. 5'-Triphosphate RNA is the ligand for RIG-I. *Science* 2006;314:994-997.
 153. Pichlmair A, Schulz O, Tan CP, Naslund TI, Liljestrom P, Weber F, Reis e Sousa C. RIG-I-mediated antiviral responses to single-stranded RNA bearing 5'-phosphates. *Science* 2006;314:997-1001.
 154. Meylan E, Curran J, Hofmann K, Moradpour D, Binder M, Bartenschlager R, Tschopp J. Cardif is an adaptor protein in the RIG-I antiviral pathway and is targeted by hepatitis C virus. *Nature* 2005;437:1167-1172.
 155. Kawai T, Takahashi K, Sato S, Coban C, Kumar H, Kato H, Ishii KJ, et al. IPS-1, an adaptor triggering RIG-I- and Mda5-mediated type I interferon induction. *Nat Immunol* 2005;6:981-988.
 156. Xu LG, Wang YY, Han KJ, Li LY, Zhai Z, Shu HB. VISA is an adapter protein required for virus-triggered IFN-beta signaling. *Mol Cell* 2005;19:727-740.
 157. Seth RB, Sun L, Ea CK, Chen ZJ. Identification and characterization of MAVS, a mitochondrial antiviral signaling protein that activates NF-kappaB and IRF 3. *Cell* 2005;122:669-682.
 158. Kumar H, Kawai T, Kato H, Sato S, Takahashi K, Coban C, Yamamoto M, et al. Essential role of IPS-1 in innate immune responses against RNA viruses. *J Exp Med* 2006;203:1795-1803.
 159. Sun Q, Sun L, Liu HH, Chen X, Seth RB, Forman J, Chen ZJ. The specific and essential role of MAVS in antiviral innate immune responses. *Immunity* 2006;24:633-642.
 160. Sato M, Suemori H, Hata N, Asagiri M, Ogasawara K, Nakao K, Nakaya T, et al. Distinct and essential roles of transcription factors IRF-3 and IRF-7 in response to viruses for IFN-alpha/beta gene induction. *Immunity* 2000;13:539-548.
 161. Honda K, Yanai H, Negishi H, Asagiri M, Sato M, Mizutani T, Shimada N, et al. IRF-7 is the master regulator of type-I interferon-dependent immune responses. *Nature* 2005;434:772-777.
 162. Sharma S, tenOever BR, Grandvaux N, Zhou GP, Lin R, Hiscott J. Triggering the interferon antiviral response through an IKK-related pathway. *Science* 2003;300:1148-1151.
 163. Fitzgerald KA, McWhirter SM, Faia KL, Rowe DC, Latz E, Golenbock DT, Coyle AJ, et al. IKKepsilon and TBK1 are essential components of the IRF3 signaling pathway. *Nat Immunol* 2003;4:491-496.
 164. Oganessian G, Saha SK, Guo B, He JQ, Shahangian A, Zarnegar B, Perry A, et al. Critical role of TRAF3 in the Toll-like receptor-dependent and -independent antiviral response. *Nature* 2006;439:208-211.
 165. Hacker H, Redecke V, Blagojev B, Kratchmarova I, Hsu LC, Wang GG, Kamps MP, et al. Specificity in Toll-like receptor signalling through distinct effector functions of TRAF3 and TRAF6. *Nature* 2006;439:204-207.
 166. Zhao T, Yang L, Sun Q, Arguello M, Ballard DW, Hiscott J, Lin R. The NEMO adaptor bridges the nuclear factor-kappaB and interferon regulatory factor signaling pathways. *Nat Immunol* 2007;8:592-600.

167. Hashimoto C, Hudson KL, Anderson KV. The Toll gene of *Drosophila*, required for dorsal-ventral embryonic polarity, appears to encode a transmembrane protein. *Cell* 1988;52:269-279.
168. Poltorak A, He X, Smirnova I, Liu MY, Van Huffel C, Du X, Birdwell D, et al. Defective LPS signaling in C3H/HeJ and C57BL/10ScCr mice: mutations in Tlr4 gene. *Science* 1998;282:2085-2088.
169. Heil F, Hemmi H, Hochrein H, Ampenberger F, Kirschning C, Akira S, Lipford G, et al. Species-specific recognition of single-stranded RNA via toll-like receptor 7 and 8. *Science* 2004;303:1526-1529.
170. Diebold SS, Kaisho T, Hemmi H, Akira S, Reis e Sousa C. Innate antiviral responses by means of TLR7-mediated recognition of single-stranded RNA. *Science* 2004;303:1529-1531.
171. Bauer S, Kirschning CJ, Hacker H, Redecke V, Hausmann S, Akira S, Wagner H, et al. Human TLR9 confers responsiveness to bacterial DNA via species-specific CpG motif recognition. *Proc Natl Acad Sci U S A* 2001;98:9237-9242.
172. Alexopoulou L, Holt AC, Medzhitov R, Flavell RA. Recognition of double-stranded RNA and activation of NF-kappaB by Toll-like receptor 3. *Nature* 2001;413:732-738.
173. Wang T, Town T, Alexopoulou L, Anderson JF, Fikrig E, Flavell RA. Toll-like receptor 3 mediates West Nile virus entry into the brain causing lethal encephalitis. *Nat Med* 2004;10:1366-1373.
174. Conzelmann KK. Transcriptional activation of alpha/beta interferon genes: interference by nonsegmented negative-strand RNA viruses. *J Virol* 2005;79:5241-5248.
175. Foy E, Li K, Wang C, Sumpter R, Jr., Ikeda M, Lemon SM, Gale M, Jr. Regulation of interferon regulatory factor-3 by the hepatitis C virus serine protease. *Science* 2003;300:1145-1148.
176. Li K, Foy E, Ferreon JC, Nakamura M, Ferreon AC, Ikeda M, Ray SC, et al. Immune evasion by hepatitis C virus NS3/4A protease-mediated cleavage of the Toll-like receptor 3 adaptor protein TRIF. *Proc Natl Acad Sci U S A* 2005;102:2992-2997.
177. Blight KJ, Kolykhalov AA, Rice CM. Efficient initiation of HCV RNA replication in cell culture. *Science* 2000;290:1972-1974.
178. Taylor MW, Tsukahara T, Brodsky L, Schaley J, Sanda C, Stephens MJ, McClintick JN, et al. Changes in gene expression during pegylated interferon and ribavirin therapy of chronic hepatitis C virus distinguish responders from nonresponders to antiviral therapy. *J Virol* 2007;81:3391-3401.
179. Lerner AC, Chaudhuri A, Darnell JE, Jr. Transcriptional induction by interferon. New protein(s) determine the extent and length of the induction. *J Biol Chem* 1986;261:453-459.
180. Bartel DP. MicroRNAs: genomics, biogenesis, mechanism, and function. *Cell* 2004;116:281-297.
181. Pillai RS, Bhattacharyya SN, Artus CG, Zoller T, Cougot N, Basyuk E, Bertrand E, et al. Inhibition of translational initiation by Let-7 MicroRNA in human cells. *Science* 2005;309:1573-1576.
182. Lee RC, Feinbaum RL, Ambros V. The *C. elegans* heterochronic gene *lin-4* encodes small RNAs with antisense complementarity to *lin-14*. *Cell* 1993;75:843-854.

183. Wightman B, Ha I, Ruvkun G. Posttranscriptional regulation of the heterochronic gene *lin-14* by *lin-4* mediates temporal pattern formation in *C. elegans*. *Cell* 1993;75:855-862.
184. Reinhart BJ, Slack FJ, Basson M, Pasquinelli AE, Bettinger JC, Rougvie AE, Horvitz HR, et al. The 21-nucleotide *let-7* RNA regulates developmental timing in *Caenorhabditis elegans*. *Nature* 2000;403:901-906.
185. Pfeffer S, Sewer A, Lagos-Quintana M, Sheridan R, Sander C, Grasser FA, van Dyk LF, et al. Identification of microRNAs of the herpesvirus family. *Nat Methods* 2005;2:269-276.
186. Pedersen IM, Cheng G, Wieland S, Volinia S, Croce CM, Chisari FV, David M. Interferon modulation of cellular microRNAs as an antiviral mechanism. *Nature* 2007;449:919-922.

Curriculum Vitae

Magdalena Sarasin-Filipowicz

St. Alban-Vorstadt 53b, CH-4052 Basel

Magdalena.Filipowicz@unibas.ch

Tel.: +41 78 654 13 13

Date of Birth : 1st of December 1979

Place of Birth : Warsaw, Poland

Citizenship: Swiss

Marital status: Married

Education:

1986-1990 Primary school, Riehen (Switzerland)
1990-1998 Gymnasium Bäumlhof (High school), Basel
1998-2004 Medical School, University of Basel
2004 Medical state exam, University of Basel
February 2005 Doctor of Medicine (MD) degree, University of Basel
Since March 2005 MD/PhD-program of the Swiss National Science Foundation, Hepatology Laboratory, Department of Biomedicine, University Hospital Basel

Research activities:

1996-1997 Laboratory practice (6 months) during the school year at the Friedrich Miescher Institute, Basel (Laboratory of Prof. D. Monard)
Project: Use of Green Fluorescence Protein as selection marker in the analysis of gene expression
Sept. 1998 Max Planck Institute for Biophysics and Biochemistry, Department of Membrane Biology, Frankfurt, Germany (Laboratory of Dr. H. Reiländer) as award in the category "Biochemistry-Medicine" of the youth research competition "Schweizer Jugend forscht"
Project: Baculovirus expression system
Sept.-Oct. 2000 Graduate Research Assistant at the Memorial Sloan-Kettering Cancer Center, New York, USA (Laboratory of Prof. S. D. Nimer)
Project: Analysis of the Polycomb gene h-l(3)MBT in leukemic cell lines
April-July 2001 Assistant in Genetics Laboratory in the Institute of Nature and Environmental Protection, University of Basel (Laboratory of Dr. M. Haase)
Project: DNA analysis of inheritance patterns in snails
August 2001- May 2002 Medical thesis in the Laboratory of Hepatology, Department of Research, University Hospital Basel (Laboratory of Prof. Dr. M. Heim)
Dissertation title: Molecular mechanisms of Hepatitis C Virus interference with Jak/STAT signaling
Since March 2005 MD/PhD-program of the Swiss National Science Foundation: Hepatology Laboratory, Department of Research, University Hospital Basel (Laboratory of Prof. Dr. M. Heim)

Publications:

1. Duong F.H.T., Filipowicz M., Tripodi M., La Monica N. and Heim M.H.: Hepatitis C virus inhibits interferon alpha signaling through up-regulation of protein phosphatase 2A. *Gastroenterology* 2004; 126:263-277.
2. Duong F.H.T., Christen V., Filipowicz M. and Heim M.H.: S-Adenosylmethionine and Betaine correct hepatitis C virus induced inhibition of interferon signaling in vitro. *Hepatology* 2006, 43:796-806.
3. Sarasin-Filipowicz M., Oakeley E.J., Duong F.H.T., Christen V., Terracciano L., Filipowicz W. and Heim M.H.: Interferon signaling and treatment outcome in chronic hepatitis C. *Proc Natl Acad Sci USA* 2008, May 13; 105(19):7034-7039.
4. Sarasin-Filipowicz M., Wang X., Yan M., Duong F.H.T., Poli V., Hilton D.J., Zhang D.-E. and Heim M.H.: Interferon alpha induces long-lasting refractoriness of Jak-STAT signaling in the mouse liver through induction of USP18/UBP43. Manuscript in preparation 2008.

Conference contributions (oral presentations):

1. Hepatobiliary and Gastrointestinal Research Retreat 2006, Vulpera (GR), Switzerland: *S-Adenosyl-L-methionine and Betaine correct hepatitis C virus induced inhibition of interferon signaling in vitro*
2. Schauinsland Retreat 2006, Schauinsland Freiburg, Germany: *Analysis of interferon signaling in the mouse liver*
3. Hepatobiliary and Gastrointestinal Research Retreat 2007, Vulpera (GR), Switzerland: *Refractoriness of interferon alpha signaling*
4. Gastroenterology-Region-Meeting 2007, Basel (BS), Switzerland: *Interferon induced gene regulation in patients with chronic hepatitis C*
5. Schweizerische Gesellschaft für Gastroenterologie (SGG), Jahreskongress 2007, Lausanne (VD), Switzerland: *Interferon induced gene regulation in patients with chronic hepatitis C*
6. Young investigators Meeting 2007, Konolfingen (BE), Switzerland: *Refractoriness of interferon-alpha signal transduction in the mouse liver: Implications for the treatment of chronic hepatitis C*
7. Hepatobiliary and Gastrointestinal Research Retreat 2008, Vulpera (GR), Switzerland: *Interferon induced gene regulation in patients with chronic hepatitis C*
8. The European Association for the Study of the Liver (EASL), Annual Meeting 2008, Milano, Italy: *Interferon signaling and the treatment outcome in chronic hepatitis C*
9. Digestive Disease Week (DDW) 2008, San Diego, USA: *Interferon regulated gene expression in the liver determines response to treatment in chronic hepatitis C*

Awards/Stipends:

- | | |
|------|--|
| 1998 | Competition "Schweizer Jugend forscht":
Award in the category "Biochemistry-Medicine" |
| 2004 | MD/PhD stipend of the Swiss National Science Foundation (founded by the Roche Research Foundation) |
| 2005 | Faculty prize for doctoral thesis awarded by the Medical Faculty of Basel |
| 2005 | Stipend of the Swiss Society of Gastroenterology (SGGSSG) |
| 2007 | Stipend of the Swiss Society of Gastroenterology (SGGSSG) |

Clinical experience:

Oct. 2000 Outpatient Clinic at the Memorial Sloan-Kettering Cancer Center
(Hematological Oncology, Prof. S. D. Nimer), New York, USA

Practical year (5th year of Medical School):

Aug.-Oct. 2002 Internal Medicine, Regionalspital Laufenburg, Switzerland
Nov.-Dec. 2002 Pediatrics, St. Anna Children's Hospital, Vienna, Austria
January 2003 Ophthalmology, University Hospital Basel
February 2003 Pathology, Institute of Pathology, University Hospital Basel
March 2003 Surgery, Royal Hallamshire Hospital, Sheffield, England
April-May 2003 Surgery, Kantonsspital Solothurn, Olten, Switzerland
June 2003 Neurology, Centre Hospitalier Universitaire Vaudois (CHUV) Lausanne
July 2003 Gynecology, University Hospital Basel
Sept. 2003 Dermatology, University Hospital Basel

Since May 2005 Outpatient liver clinic at the University Hospital Basel, Switzerland

Temporary jobs:

1997-2000: Skiing teacher at "Jugend + Sport" skiing-camps
2000-2004: Student-job at the medical library, University of Basel
2000-2005: Student-job at the International Workshop of "Arbeitsgruppe für
Gastroenterologische Chirurgie", Davos, Switzerland

Languages: German, English, Polish, French

Hobbies: Dancing, singing, reading, guitar, piano, sports (tennis, skiing, diving)